國立臺灣大學工學院化學工程學研究所

碩士論文

Graduate Institute of Chemical Engineering

College of Engineering

National Taiwan University

Master Thesis

MIL-101 陶瓷膜之製備及其於

有機溶劑奈米過濾之應用

Synthesis of MIL-101 supported on ceramic membrane for

organic solvent nanofiltration

Minh Hien Le

指導教授：童國倫　教授

Advisor: Prof, Kuo-Lun Tung, Ph.D

中華民國 105 年 7 月

July, 2016

國立臺灣大學碩(博)士學位論文
口試委員會審定書

MIL-101 陶瓷膜之製備及其於

有機溶劑奈米過濾之應用

Synthesis of MIL-101 supported on ceramic membrane for
organic solvent nanofiltration

　　本論文係黎恆明君（R03524099）在國立臺灣大學化學工程學系、所完成之碩（博）士學位論文，於民國 105 年 7 月 4 日承下列考試委員審查通過及口試及格，特此證明

口試委員：

_____（簽名）
　　　（指導教授）

_____　　林俊德

莊清棻　　　　　　　　　黃囙哲

_____　　_____

_____　　_____

系主任、所長　王大銘　　　　（簽名）

（是否須簽章依各院系所規定）

1

ACKNOWLEDGEMENT

I would like to express my special appreciation and thanks to my supervisor, Prof. Kuo Lun Tung, you have been a tremendous mentor for me during the planning and development of this research work. I would like to thank you for encouraging my research and for allowing me to grow as a research scientist. I also want to thank him for giving me financial support, patient guidance, and useful critiques in keeping my progress on schedule. Your advice on both research as well as on my career have been priceless.

I would also like to thank Mr. Jeffery and Mr. Jarvis. They help me set up experiment, design models and guide me how to use equipment in Chemical Engineering Department. Moreover, they usually support and send me useful feedbacks to improve my experiment. Besides, my lab mates, especially Becky are very friendly and help me to approach to everything in membrane filtration lab. Thanks a lot for their helps, guidance and their sharing experiment, even at hardship.

Finally, I would like to express deepest gratitude, particularly to my Dad and mom, for the supporting and understanding. They always make me more confidence and motivation to move on the research road. If not, this project would not have been completed. I would also like to thank all of my friends who supported me in writing, and incented me to strive towards my goal. Thanks you.
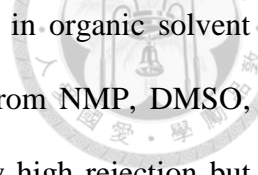
ABSTRACT

The purpose of this study is using an in-situ assisted acetic acid procedure to prepare a MIL-101 as filler in ceramic membrane. The MIL-101 membrane is firstly applied for organic solvent nanofiltration. In this study, the effects of synthetic conditions are investigated to get an invisible defect membrane and nanofiltration performance is also checked to prove the feasible application of MIL-101 membrane.
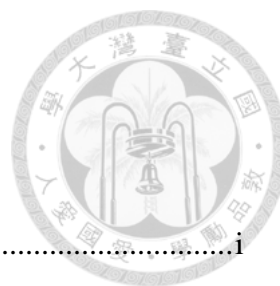
Incorporation of metal organic framework (MIL-101) as filler on ceramic membrane is firstly investigated. In-situ method assisted by acid modular is utilized to synthesize uniform and defect-free MIL-101 membrane. Effect of additives such as NaOH, HF, CH_3COOH and concentration of reactants are surveyed to find out the optimal synthetic conditions. Synthesis of MIL-101 membrane by using in-situ acetic acid-assisted method is proved as efficient way to prepare a compact and dense MIL-101 layer compared to other methods as thermal seeding method, layer by layer seeding method. The MIL-101 membranes are characterized by using a variety of different techniques, including X-ray thin film diffraction (XRD), scanning electron microscopy (SEM), energy dispersive X-ray spectroscopy EDX.

MIL-101 is chosen as material filler for membrane in nanofiltration application because of its ability to form the largest pore size in the MOFs' family and a number of its prominent properties for molecular separation applications such as high surface area and well-defined pore size. Besides, MIL-101 and ceramic substrate are inorganic materials, so they are able to be stable in harsh solvent such as N-methyl-2-pyrrolidone (NMP), dimethyl sulfoxide (DMSO), dimethylacetamide (DMAc), those usually

dissolve common polymers. The MIL-101 membranes are applied in organic solvent nanofiltration (OSN) by testing separation of Rose Bengal (RB) from NMP, DMSO, DMAc and ethanol. The MIL-101 membranes show a significantly high rejection but lower permeance compared to bare ceramic membrane. The best flux and rejection of MIL-101 membrane with RB ethanol solution are 1.65 $\text{lm}^{-2}\text{h}^{-1}\text{bar}^{-1}$ and 99.7% respectively where ratio of chromium nitrate, benzendicarboxylic acid and water is 1:1:277, respectively and 0.8 ml of CH_3COOH. The MIL-101 membranes also exhibit the stability under harsh solvent with high rejection of RB and constant flux within 3 hours.

Keywords: organic solvent nanofiltration, MIL-101, ceramic membrane, in-situ method

Contents

LIST OF FIGURES

Chapter 3

Chapter 4

LIST OF TABLE

Chapter 1 - Introduction

1.1 General overview

New and creative applications are driving the further development of NF membranes. However, the need to separate related chemicals in various production streams such as pesticides, biochemicals, nutraceuticals, flavorings, and pharmaceuticals is well understood in these industries; as a result, organic solvent nanofiltration (OSN) as a novel technique extended from aqueous nanofiltration is increasingly brought into play. Organic solvent nanofiltration is a pressure driven membrane process with enormous potential in non-aqueous environments. Solvent-stable membranes are used to gently separate larger molecules (molecular weight between 200 and 1000 Da) from organic solvents depending on their size.
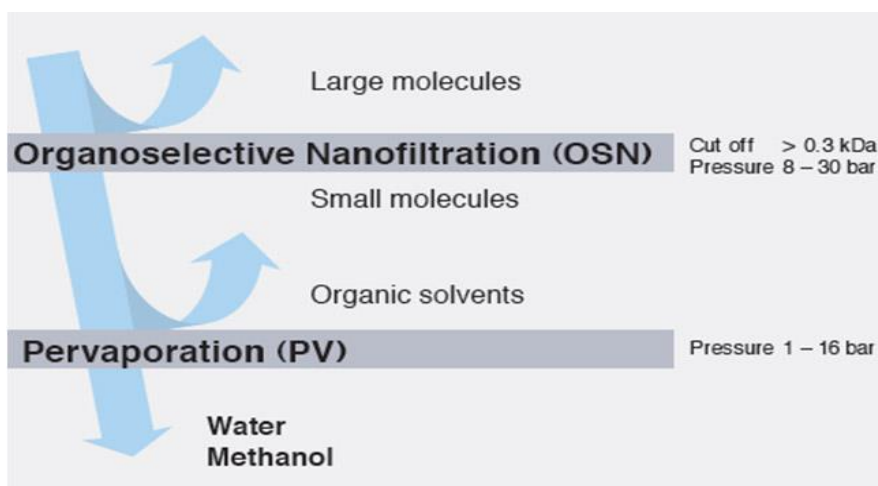
Figure 1. 1 Organic Solvent Nanofiltration
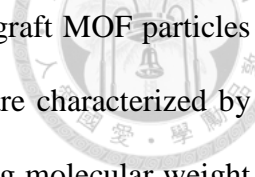
OSN could be operated as a stand-alone solution or combined with conventional separation technologies such as distillation, evaporation, chromatography, and crystallization in a hybrid solution. OSN owns lots of benefits as reduction of energy demand of separation process and improves product quality and yield. Besides, OSN is
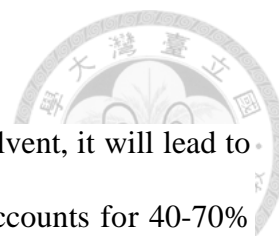
able to recover organic solvent or separate high-valued solutes in solvent, it will lead to reduce the cost of whole procedure in industry, which separation accounts for 40-70% of both capital and production expense. When OSN is combined with other traditional, the process becomes more efficient energy and achieves higher yields and better quality at comparable costs [1]. Therefore, application areas of OSN could be found in the pharmaceutical, fine chemical, and chemical industries, as well in the processing industries for natural products and oils (including flavors and fragrances) where gentle process conditions are mandatory for improved product quality. For example, several applications of OSN are non-thermal solvent recovery, solvent exchange at ambient temperature, in-situ recycling of organic solvents, purification and concentration of intermediates, monomer removal, dewaxing and product upgrading.

In the point view of materials, OSN membranes are synthesized from inorganic and polymeric materials. Polymeric membrane is widely used in OSN application because of their advantageous properties as various types of polymer, inexpensive and easy to prepare. However, polymeric membrane is not stable in harsh condition/environment, swelling phenomena and relatively short life compared to inorganic membrane. Thus, inorganic material as well as ceramic membrane is an attractive support for OSN application with excellent features as chemical – thermal stability and without swelling. The challenges for ceramic membranes are to modify pore size being suitable to NF range and increase the permeance rate.

In this study, MOF membranes as hybrid composite are researched and developed to apply in OSN application. The novel membranes utilize appreciate characteristics of MOF material for liquid separation such as well-defined pore size and large surface area.

2

The MOF membranes are simply synthesized by in-situ method to graft MOF particles on ceramic support as selective layer for OSN. MOF membranes are characterized by SEM, XRD and EDX. OSN performances are carried out by plotting molecular weight cut off (MWCO) curve and checking the stability of MOF membrane in harsh solvent as DMSO, DMAc, NMP.

1.2 Objective

This research focuses on two novel issues for MOF membranes: grafting meso-MOFs (MIL-101) on surface of ceramic membranes and apply MIL-101 membranes on organic solvent nanofiltration.

To synthesize meso-MOFs membranes, MIL-101 is selected from the MOFs' family due to its the largest pore size and excellent properties as chemical, thermal stability and large surface area. Several methods to prepare MIL-101 membranes such as thermal seeding, layer-by-layer seeding and in-situ methods are investigated to find an optimal way to fabricate a uniform and dense layer of MIL-101 on inorganic material. Typically, MIL-101 membranes are synthesized by an in-situ method assisted by additive, e.g. acetic acid combined with a defect healing step. The concentration of reactants and additives are surveyed to obtain the optimal synthetic condition.

As for organic solvent nanofiltration, applying MIL-101 membranes as inorganic material show advantageous features because of its high temperature tolerance, well mechanical strength and good anti-swelling in organic solvents. MIL-101 with meso-pore size of 2-3 nm and window cage of 1.2-1.6 nm are suitable for nanofiltration range and become potential material for OSN. Molecular weight cut off curve are plotted to demonstrate the performance of MOF membranes in OSN. Moreover, various organic

solvents that could dissolve polymers are investigated in OSN to prove the chemical stability of MIL-101 membranes.

In conclusion, MIL-101 membranes are prepared and their application of these membranes in OSN is firstly researched. All conditions of prepared MIL-101 membranes as concentration of reactants and amount of additive are investigated, and performances of OSN are surveyed to prove the prominence of MIL-101 material for MOF membranes.

4

Chapter 2 - Literature review

2.1 Nanofiltration

Nanofiltration (NF), so named because the membrane pores in the nanometer range that is around 1 nm, is one of those awkward processes that are sometimes encountered in chemical engineering. NF membranes have come a long way since it was first recognized in the late 80's in order to fill the gap in separation performance between reverse osmosis (RO) and ultrafiltration (UF) as a result of rapid development of RO and UF membranes. NF membranes are potent in the separation of inorganic salts and small organic molecules. Key distinguishing characteristics of NF membranes are low rejection of monovalent ions, high rejection of divalent ions and higher flux compared to RO membranes [2]. NF possesses many advantages compared to RO such as low operation pressure, high flux, high retention of multivalent anion salts and an organic molecular above 300 Da, relatively low investment and low operation and maintenance cost.
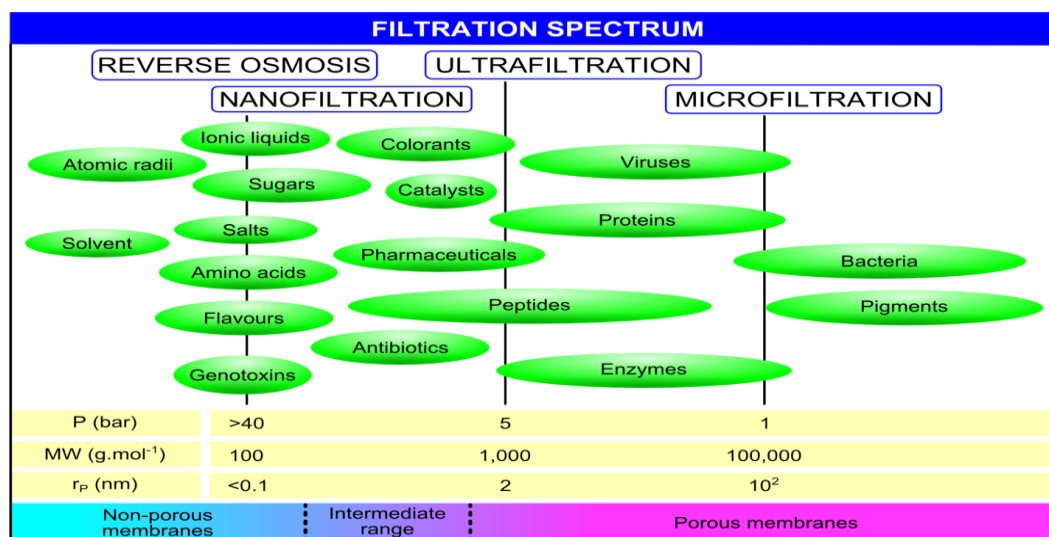
Figure 2.1 Classification of membrane processes [3]
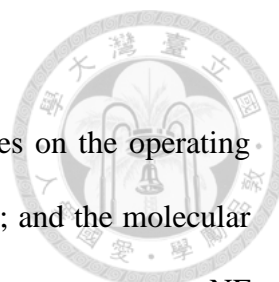
As shown in Figure 2.1, classification of filtration process bases on the operating pressure [4]; the size of the solute as well as pore size of membrane; and the molecular weight cut-off. NF process could operate at pressure from 5-20 bar, yet current NF membranes have been applied at higher pressure values, which is able to extend the pressure range for NF up to 40 bar. NF process is suitable for separation of particles in range of 1 nm to 10 nm, so the pore size of NF membranes have to appreciate to this range [5]. To match with industrial process, NF membranes are often determined by their nominal MWCO, the features of this characterization significantly depend on kind of markers, properties of solutes, solvents, and operating conditions.

These properties have allowed NF to be used in niche applications in many areas. Historically, nanofiltration and other membrane technologies used for molecular separation was applied entirely on aqueous systems. The original uses for nanofiltration were water treatment and in particular water softening. Nanofilters can "soften" water by retaining scale-forming, hydrated divalent ions (e.g. Ca^{2+}, Mg^{2+}) while passing smaller hydrated monovalent ions [6]. In recent years, the use of nanofiltration has been extended into other industries such as milk and juice productions. Research and development in solvent-stable membranes has allowed the application for nanofiltration membranes to extend into new areas such as pharmaceuticals, fine chemicals, and flavor and fragrance industries [6]. The success of NF in aqueous systems has triggered expansion to organic solvents ranging from non-polar through polar to polar aprotic as result in development in organic solvent nanofiltration technology and commercialization of membranes. In fact, in the late 1990s a new brand of NF, solvent resistant nanofiltration or organic solvent nanofiltration emerged as a new better

6

separation method [7-10]. The statement and development of NF and OSN area have described generally as well as compared like Figure 2.2 in order to support a comprehensive view.
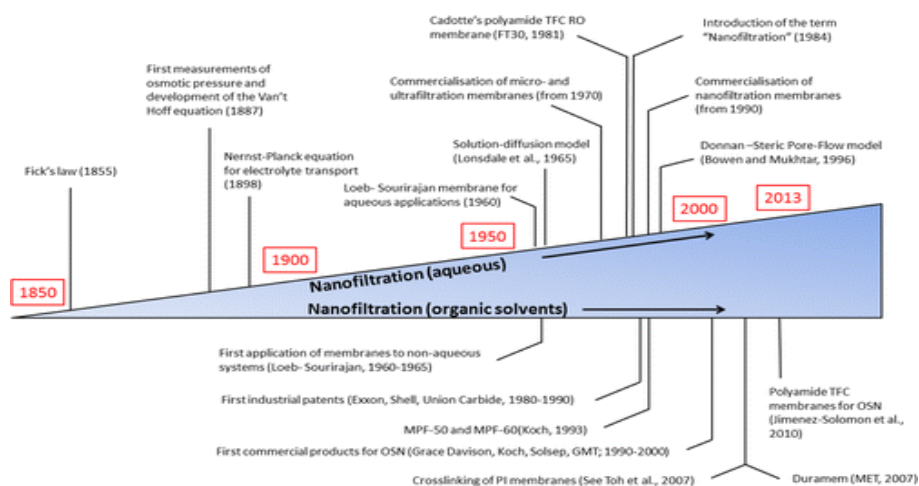
Figure 2.2 Summary of the most significant events, which have contributed to the development of NF over time [3].

Table 2. 1 Application of nanofiltration

Industry	Uses
Fine chemistry and Pharmaceuticals	Non-thermal solvent recovery and management Room temperature solvent exchange
Oil and Petroleum chemistry	Removal of tar components in feed Purification of gas condensates
Bulk Chemistry	Product polishing continuous recovery of homogeneous catalysts
Natural Essential Oils and similar products	Fractionation of crude extracts Enrichment of natural compounds Gentle Separations
Medicine	Able to extract amino acids and lipids from blood and other cell culture.

7

2.2 Organic Solvent Nanofiltration

There are a lot of papers about nanofiltration which are published through previous century. It demonstrates that separation process plays a significant role in the chemical and pharmaceutical industries [11]. However, almost all the organic synthesis in industry are frequently carried out in organic solvents or generate high valuable products that need to be separated from organic solvents. The expense for separation, recovery, or disposal of these organic solvents is considerable and made up a significant part of chemical process operating costs. From these advantages, the requirement for extension of nanofiltration process to application in organic solvents has been emerged recently as a new paradigm technology for more efficient solvent operations. This process is called "organic solvent nanofiltration" (OSN), or alternatively "solvent resistance nanofiltration" or "organophilic nanofiltration". OSN is still a novel technique and attracts more attention in this technology by both scientists and industrial producers. The number of OSN papers published until 2015 is limited and OSN needs to discovery more to development this field.
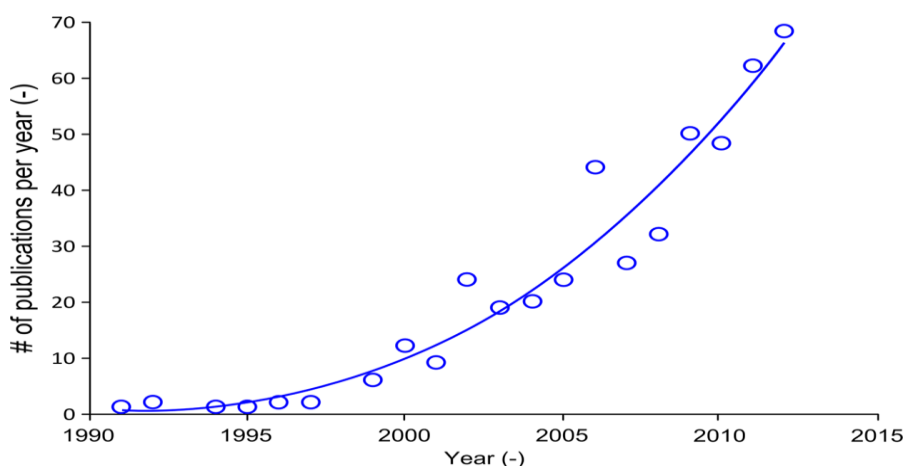
Figure 2.3 Growing interest in OSN, demonstrated by the increasing number of publications per year in the field [3].

2.2.1 Classification of organic solvent nanofiltration

OSN operations are classified into three conceptually simple operating modes for membrane processing of liquids, which are concentration, solvent exchange, and purification, which is shown in Figure 2.4 in order to figure out clearly about the defining process. Hence, OSN operations could be applied in many various processes and developed into a wide range of applications based on three simple modes.
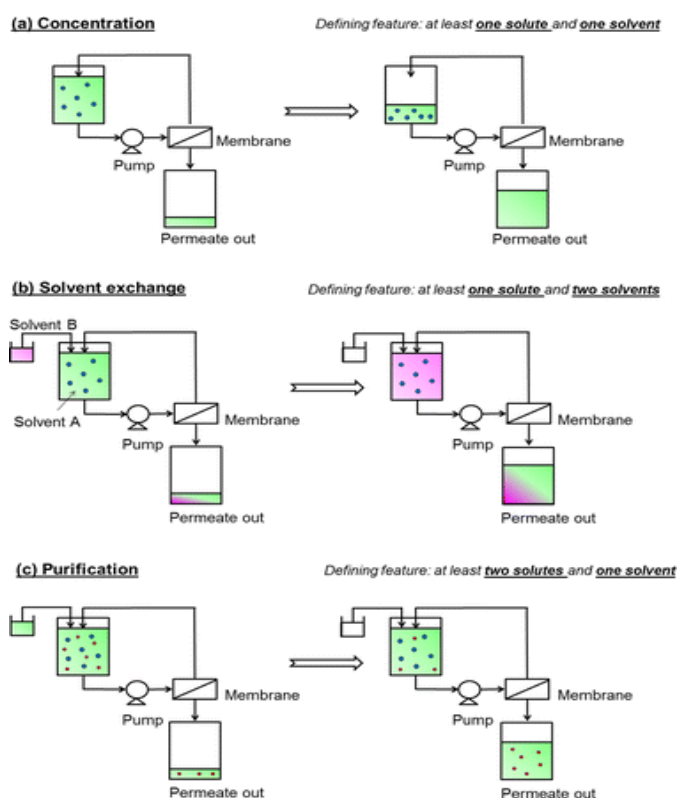
Figure 2.4 Classification of organic solvent nanofiltration [3]

According to the Figure 2.4 (a), the membrane is utilized for concentration processes by letting the solvent pass through it and reject the solute out of solution. This process consists of two cases as solute enrichment and solvent recovery. More particular, solute enrichment process is separation procedure of solute from the dilute solvent to collect a high-value solute and solvent recovery bases on removing an impurity
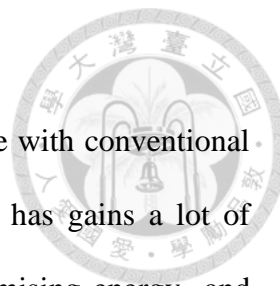
dissolved in solvent to get more concentrated solute. When compare with conventional concentration processes such as distillation and evaporation, OSN has gains a lot of attentions for industrial applications and shows high potential promising energy- and waste-efficient unit process to separate mixture down to a molecular level. Due to low energy consumption, OSN also uses low temperature for whole process and it leads to minimize thermal degradation of sensitive molecules opened up a wide range of applications in the pharmaceutical industry.

The second operation mode – solvent swap - was shown in Figure 2.4 (b). In this procedure, a green solvent (A) is replaced by pink solvent (B) by pumping solvent B into a tank containing solution of a solute and this mixture flows through membrane. Membrane in this case separates solvent A and B, in which solvent B is turned back into the tank and solvent A permeates through membrane; solute in solvent A is also rejected by membrane. Therefore, this process can be called as solvent exchange due to the changing of solution from being rich in solvent A to being rich in solvent B. The main advantage of applying membrane filtration to perform a solvent swap is that it is an athermal process, allowing, for example, solvent exchange from a high-boiling to a low-boiling solvent. Moreover, stiff membranes are very essential for both concentration and solvent exchange, they make the separation process more efficient by retaining the solutes and permeate the solvents well. The now feasible, low cost solvents recycle could contribute to decrease of hazardous chemicals discharges to the environment.

Finally, the major operation mode of membrane applied in OSN field is purification process shown in Figure 2.4 (c). This process is very important to pharmaceutical and biochemical industries; solutes as organic compounds, impurities and other
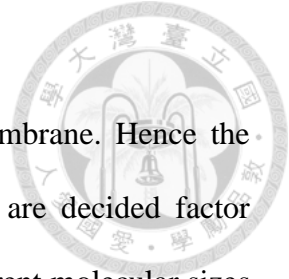
contaminants are separated from solutions by highly selective membrane. Hence the properties of membrane in this operation are really crucial, they are decided factor whether membrane are able to discriminate between solutes of different molecular sizes and/or physicochemical properties. In most cases, no additive is needed and separation do not involve any phase transition, which are advantageous for OSN.

In addition to advantages of three simple operations, OSN also shows high possibilities to install as a continuous process and just like any other membrane separations, it can be easy to cooperate with existing processes into a hybrid process compared to conventional separation techniques. Own lots of good points, nanofiltration membranes become a promising material for variety of applications and full ability to scale up into industrial process.
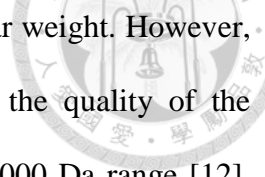
2.2.2 Membrane characterization

The performance of an OSN membrane is determined by two parameters: flux (or permeance) and rejection (or selectivity). The flux is defined as the volume liquid flowing through the membrane per unit area and per unit time, and it is usually expressed in term of $Lm^{-2}h^{-1}$, while permeation rate as $Lm^{-2}h^{-1}bar^{-1}$ is normalized to the applied pressure. Rejection (%) is mostly calculated as the function of concentration in permeate and solute concentration in the feed stream:

$$R = \left(1 - \frac{Cp}{Cf}\right) * 100 \qquad (Eq.1)$$

where: C_f and C_p denote the analyte concentration of feed and permeate, respectively.

In addition, the separation performance of a membrane can also be characterized by its 'molecular weight cut-off', which represents the smallest molecular weight (MW) that membrane could reject for 90% [12]. The MWCO can be derived from a MWCO-

11

curve as a function of rejection for analyses and increasing molecular weight. However, MWCO could not reflect all of the separation performance and the quality of the separation. NF-membranes typically display MWCOs in the 200–1000 Da range [12]. Thus, marker was used for characterization of OSN membrane that have range of 200-1000 Da as linear and branched n-alkanes [13], dyes [14-17], hexaphenyl benzene (HPB) [17, 18], polyethylene glycol (PEG) [19-21], polystyrene (PS) [22, 23] and polyisobutylene (PIB) [24, 25]. Every marker has own its advantages as well as disadvantages. For example, linear and branched n-alkanes are able to characterize MWCO at range of 100-400 g.mol^{-1} and yet they do not have enough commercial compounds for MW > 400 g.mol^{-1} [13]. Besides, the solubility of these chemicals in various solvents is still limited, and that is a reason why it is very difficult to determine and compare MWCO of membrane across different solvents. In the case, dyes used as marker is easy to analyze permeate by UV absorption and simple to check the defect of membrane by observe the color of permeate. However, a single test to determine MWCO is not feasible by using variety of dyes' sizes. Moreover, the physical properties of dyes could affect to membrane performance such as charge groups or their interactions with membrane [14-17]. Generally, oligomeric including of PIB, PEG and PS are all popular solutes to determine MWCO-curve in solvent due to coverage of a large range of MW [18-25]. Yet, the procedure to analyze the concentration of marker in permeate after NF is still complicated. Although there are a lot of authors reporting comprehensive data about OSN-membrane for specific application, it is very difficult to compare every case and arrange into suitable categories in order to screen a whole picture for OSN. In more detail, the difference properties of the solvents and solutes

12
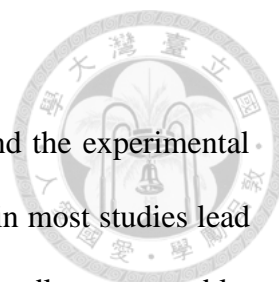
(structure, molecular size, charge, concentration, solubility, etc.), and the experimental

filtration conditions (transmembrane pressure, temperature) applied in most studies lead

filtration data and MWCO-values of different experiments hardly comparable.

Furthermore, even if filtration conditions, solvents and solutes would exactly consistent,

difference of analytical techniques to calculate rejections usually not relatively disclosed,

could vary. For this non-uniformity, the selection of a suitable membrane for a specific

application often requires the overview of many membranes and depends a lot on

literature data and manufacturer specifications. Therefore, it is urgent to develop a

consistent and general method to determine the performance of SRNF membranes.

2.2.3 System design

In laboratory, the configuration of NF process is usually dead-end filtration mode

and reported frequently in literature, while the cross-flow mode is usually applied in

industrial application. In dead-end, the feed flows perpendicularly to the membrane

surface by the pressure force, whereas in cross-flow, the feed flows tangentially to the

membrane surface, as schematically shown in Figure 2.5
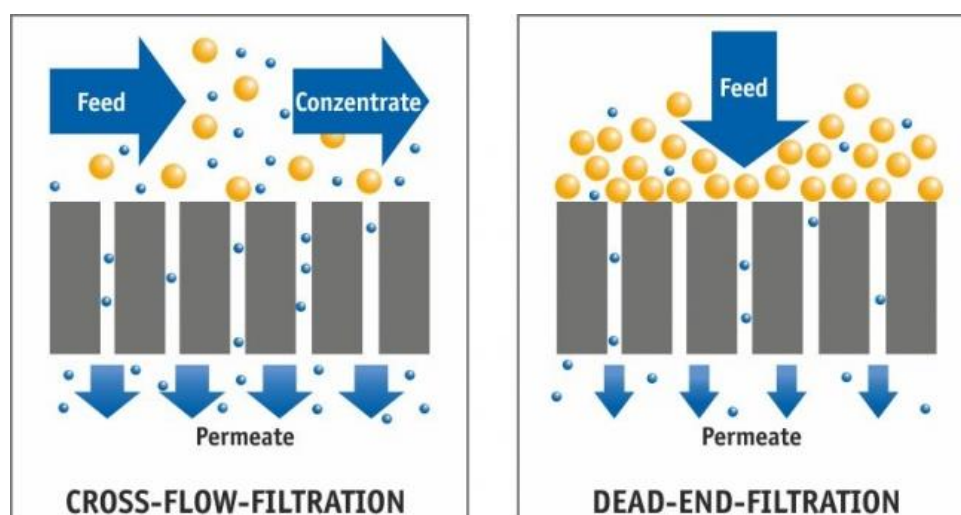
Figure 2.5 Two operating models of nanofiltration [26]

(i)   Dead-end filtration

Dead-end filtration is the most basic mode of NF operation. The complete feed flow is forced through the membrane and the filtered matter is accumulated on the surface of the membrane. The dead-end filtration is also called batch filtration due to the appearance of clogging. Typically, accumulated substances with time on the surface membrane or within the membrane increases resistance to filtration and lead to decreases the filtration capacity or permeate flux. The filtration is not sustainable forever, so the stopping of filtration in order to remove the accumulated matter is essential to carry out in a next step, or even must replace the membrane to solve this problem. Thus, this filtration mode is particularly effective when feed water carries low level of foulants.

Dead-end filtration can be a very useful technique for concentrating compounds. Furthermore, the dead-end filtration method has the following advantages: the collection rate is high (almost 100%); miniaturization is possible; the cost is low; and the filter's lifespan is extended by optimizing the materials and design. There are two kinds of filtration which can be implemented in a dead end cell unit based on flux and pressure as dead-end filtration with constant flux and dead end filtration with constant pressure drop. The dead end filtration with constant flux is conducted by positive displacement pump, it leads to keep the flux through membrane constantly. As described above about the clogging, there is a cake build-up with time on surface membrane and the pressure drop has to be increased to steady the flux. In contrast, dead end filtration with constant pressure, the permeate flux is dropped follow the time as there is no more pressure to push the feed stream to overcome the cake build-up.

14

(ii)   Cross-flow Filtration

Crossflow filtration is different from dead-end filtration in which the feed is passed through a membrane, the solutes being trapped in the filter and the filtrate being released at the other end. The feed flow travels parallel majorly the surface of membrane, rather than into the membrane, thus the process is referred to as cross-flow filtration. A proportion of the material which is smaller than the membrane pore size passes through the membrane as permeate or filtrate; everything else is retained on the feed side of the membrane as retentate. With cross-flow filtration a constant turbulent flow along the membrane surface prevents the accumulation of matter on the membrane surface. The feed flow travels tangentially to the surface by elevated pressure as driving force for the filtration process and a high flow speed to create turbulent condition. This turbulent condition makes the advantages for this mode as the filter cake is substantially washed away during the filtration process, or controls the cake layer thickness, and increases the length of time that a filter unit can be operated. Because pseudo steady-state may exist, where scouring effect and particle deposition find a balance and cake layer hardly grows. It can be a continuous process, unlike batch-wise dead-end filtration. In addition, the cross-flow method shows more beneficial properties like low filter maintenance frequency; effective when feed flow containing high level of foulants as insoluble materials, or viscous liquids as well; and ability to reuse with backwashing and chemical cleaning.

2.2.4 OSN material and ceramic membrane for OSN

OSN membranes have been fabricated from both polymeric and inorganic materials. Although polymeric membranes have a large number of advantageous properties as diverse types of polymers, relatively low cost, easy to preparation and large-scale synthesis. Polymeric membranes remain several drawbacks as lack of mechanical, physical and chemical stability, aging and compaction, so they lead to drop the separation performance. Especially, severely swell feature of polymeric membranes in organic solvents is a real problem in OSN applications. Therefore, it is crucial to develop inorganic materials to tackle the disadvantaged points of polymeric membranes. Typically, ceramic membranes are high quality materials for OSN because of their mechanical, thermal, and chemical stability; they do not compact under pressure, do not swell in organic solvents, are stable under harsh conditions and can be easily cleaned. Moreover, ceramic membranes have no pore fillers and hence there is no leaching phenomena. In spite of excellent properties of inorganic materials that polymeric membranes are deficient, ceramic membranes are still scarce in OSN application. Because fabrication of inorganic membranes is difficult to scale-up and these materials are more brittle than that of polymeric membranes. With brittle characteristic, ceramic membranes could typically operate at lower pressures compared to polymeric membranes. Furthermore, a limited number of ceramic membranes inhibit the development of these material; and metal oxide membranes have an inherently hydrophilic character due to -OH groups widely cover on their surface, thus these membranes exhibit optimal performance in NF with polar solvents and less suitable for more apolar solvents. To utilize the advantages of polymeric and inorganic membranes,
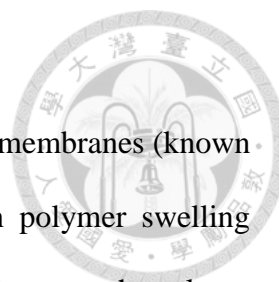
there are novel types of membranes as composite organic−inorganic membranes (known as mixed-matrix membranes). This kind of membrane could turn polymer swelling down and enhance flux rate due to compaction. Moreover, they can improve the solvent stability, rejection and flux and solve the brittle and antifouling problems of ceramic membrane membranes. The below chart will summarize and illustrate the synthesis method to prepare OSN membranes.
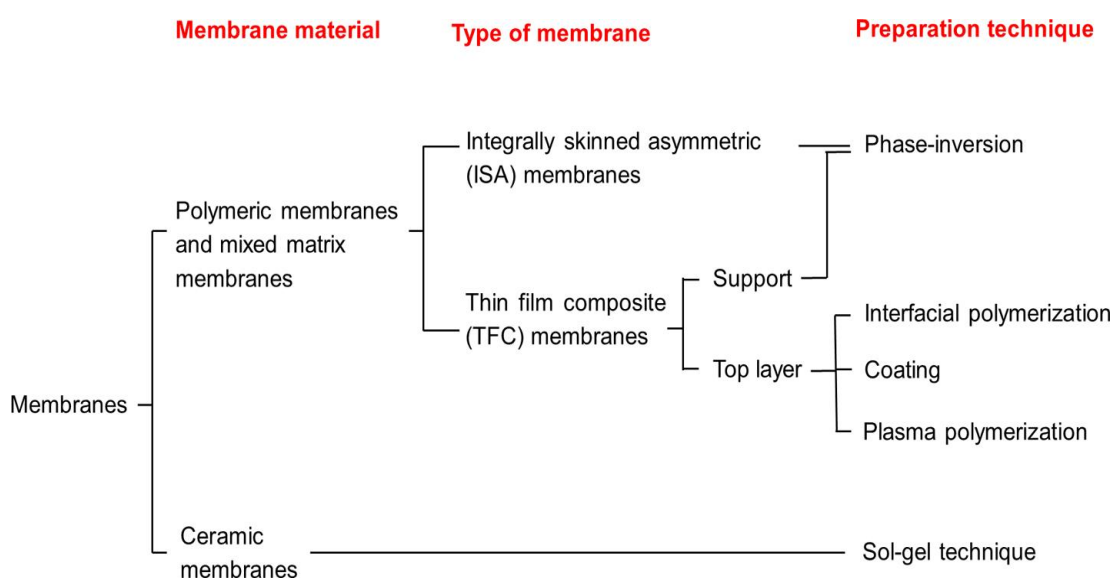
Figure 2.6 Synthesis method OSN membranes [3]

Ceramic materials including silicium carbide, Zr-, Ti-, and Al –oxides [27-29] with excellent properties are potential materials for the development of ceramic membranes for OSN applications. The ceramic membranes are often formed into an asymmetric, multi-channel element. These elements are grouped together in housings, and these membrane modules can withstand high temperatures extreme acidity or alkalinity and high operating pressures, making them suitable for many applications where polymeric and other inorganic membranes cannot be used.
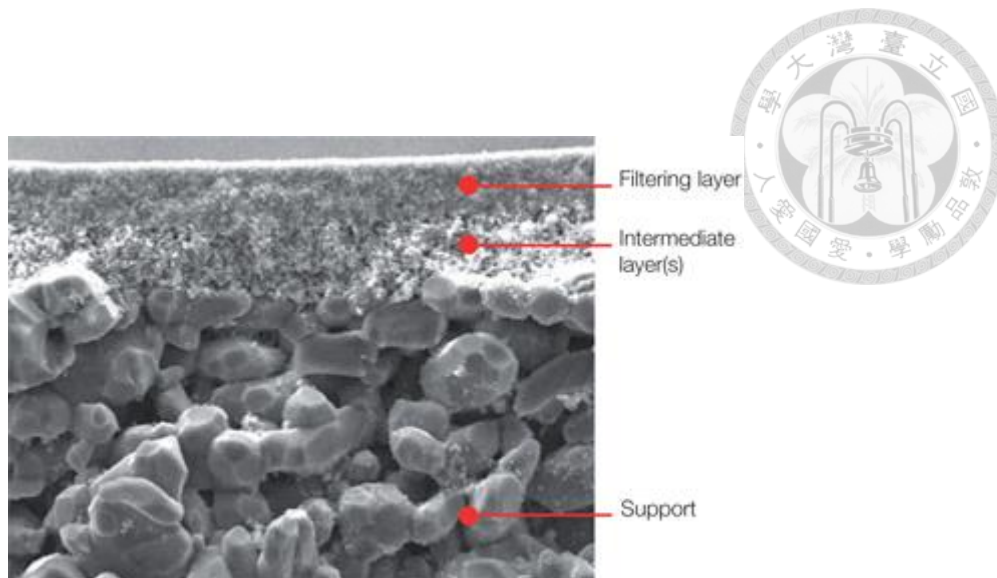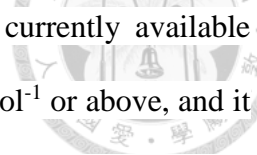
Figure 2.7 Structure of ceramic membrane [30]

According to the Figure 2.7, the structure of ceramic membrane concludes a thin layer on top and have one or more intermediate layers between top layer and support. The porous inorganic support plays a role as supply material to enhance sufficient mechanical stability and decides the external shape of the membrane.

In NF membrane synthesis method, suspension coating technique is able to be applied to prepare a thin layer with pore size of around 30 nm (upper range of UF) [31]. Besides, sol-gel process is commonly method to prepare a smaller pore size, an additional defect free layer of NF membranes. In this process, a colloidal or polymeric solution is transformed into a gel. At the first stage of the sol-gel process, the hydrolysis and poly-condensation reactions of alkoxides or salts lead to the formation of a colloidal solution, i.e. sol, of hydroxide particles whose size does not exceed several dozen nm. Suspension with several additives as viscosity modifiers or binders is deposited on the support by dip or spin coating and then gelation occurs on it. Finally, the membrane is obtained after dry process to evaporate all of solvent by calcination [4].

However, in the range of organic solvent nanofiltration, the currently available membranes do just offer a large molecular weight cut-off of 600 g.mol^{-1} or above, and it became the barrier to hind the development of OSN ceramic membrane. To approach the MWCO of NF ranges, there are some groups try to modify the pore size of ceramic membrane in order to get to grip with the challenges. In more particular, Tsuru et al. (2001) firstly reported the application of ceramic membrane for OSN. They fabricated silica-zirconia composite with various average pore size, ranging from 1-4 nm for NF in non-aqueous solution of ethanol and methanol. They demonstrated the relationship between pore sizes and various MWCO ranging from 300 to 1000 g.mol^{-1} and over 1000 g.mol^{-1} by control the pore size of NF membranes [20]. In another experiment, Tsuru's groups prepared nanoporous titania membranes with pore size ranging from 1 to sever nm for permeation of hexane [32]. Voigt et al. (2001) prepared new TiO_2-NF membrane with mean pore size of 0.9 nm and MWCO of 450 g.mol^{-1} in decoloring of textile waste water. It is also the tightest hydrophilic ceramic membrane synthesized from TiO_2 and after that prepared NF-membranes is commercialized under the name Inopor [33]. In addition to lower their MWCO challenges, the intrinsic hydrophilicity is another issues of ceramic NF membrane because of lack of compatibility to apolar solvents. Tsuru et al. (2003) modified silica-zirconia (SZ) membranes, which have the pore size of 1-3 nm, by a gas-phase reaction with trimethylclorosilane (TMS) at 200°C. They could synthesize the SZ membrane with mean pore size of 1 nm MWCO of approximately 200 g.mol^{-1}. These membranes were used to nanofiltration of ethanol solutions with solutes as alkanes and alcohol (hexanol, octanol, decanol). The permeate flux was obtained around 3 kg.m^{-2}.h[-1] at 60°C under operating pressure of 30 bar [34].

19
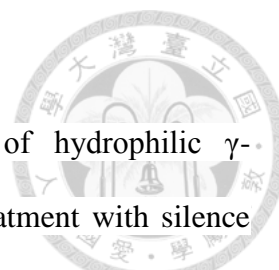
Van Gestel et al. (2003) reported the surface modification of hydrophilic γ-Al$_2$O$_3$/anatase-TiO$_2$ multilayer membranes by a silane coupling treatment with silence coupling reagents as (CH$_3$)$_2$SiCl$_2$ - C1 silane and C$_8$H$_{17}$CH$_3$SiCl$_2$- C8 silane for hexane permeation. These membranes were applicable in non-polar solvents and characterized by MWCO of 410 and a hexane permeability of 3 Lm^{-2}h^{-1}bar^{-1} (C8 silane) and a MWCO of 650 and a hexane permeability of 5 Lm^{-2}h^{-1}bar^{-1} (C1 silane) [35].
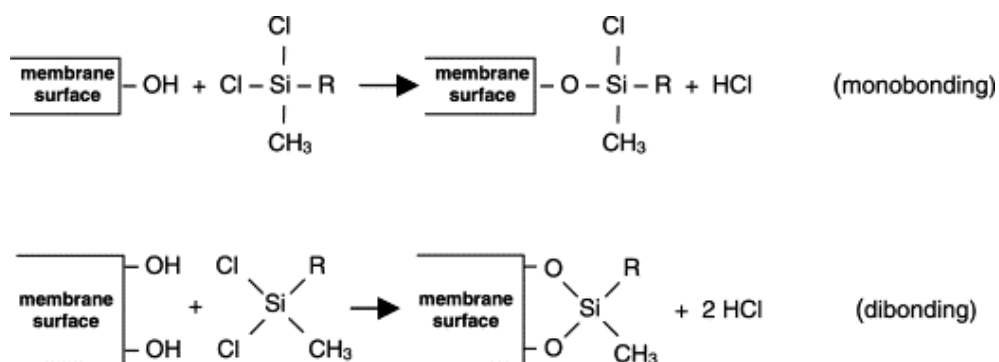
Figure 2.8 Reactions between membrane surface hydroxyl groups and silane coupling reagent [35]
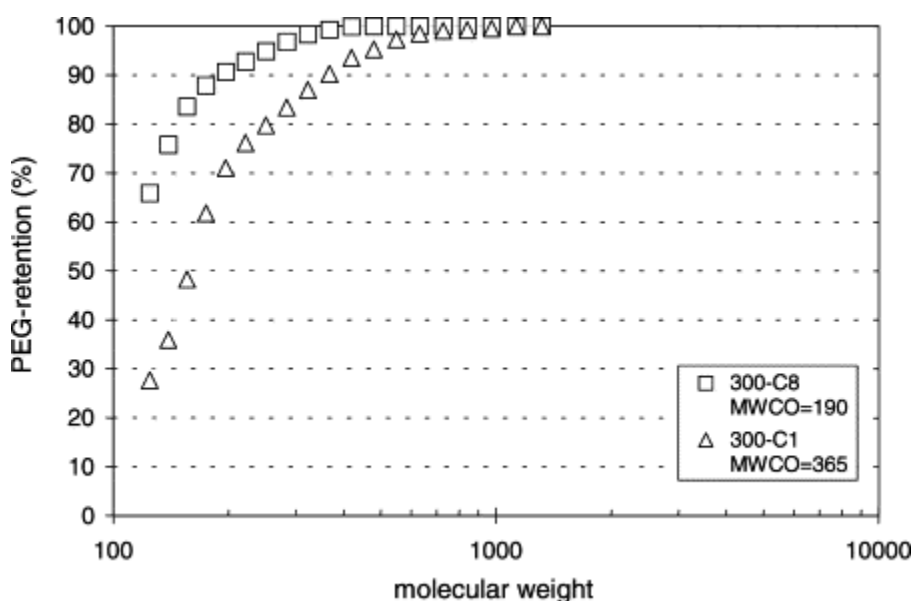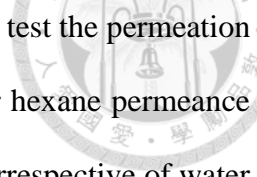
Figure 2.9 PEG-retention curves and MWCO for membranes fired at 300 ℃ and treated with a C1 and C8 silane [35]

Tsuru's group (2004) also used the TMS-modified membrane to test the permeation of hexane with presence of traces of water. They exhibited a higher hexane permeance of the modified membrane compared to the unmodified membrane, irrespective of water concentration, because the modified membrane prevented the blocking membrane by adsorption of water [36]. Duziak et al (2004) modified the pore surface by coupling silylation to make these membrane more hydrophobic [37]. Tsuru et al. (2011) continued to prepare organic/inorganic hybrid membranes with mean pore size ranging from 2 to 4 nm by coating porous substrate with methylated SiO_2 colloidal sol solutions before calcination process at 400-600°C in an inert atmosphere. Methylated SiO_2 membranes were employed for the nanofiltration of polyolefin oligomers in hexane solutions. They showed a hexane permeability of 7.2 and 27 $Lm^{-2}h^{-1}bar^{-1}$, with MWCO of 1000–2000 [38]. Hosseinabadi et al. (2014) described the use of functionalized ceramic NF membranes in solvent filtration. The membranes were grafted using a novel method for surface modification based Grignard chemistry. The Grignard reaction was carried out by metal from support (M, with M=Al, Zr, or Ti) and series of alkyl groups (R, with R= methyl, pentyl, octyl, docecyl) in order to generate covalent bonding (M-R) and make membrane surface more hydrophobic. The partial replacement of the OH- groups on the membrane surface and the consequent amphiphilic character of the modified membranes was observed. The functionalized ceramic NF membranes showed advantageous properties of both inorganic and polymeric membranes such as hydrophobic feature, absence of effects of swelling, high fluxed and the rejection of PS in acetone [39].
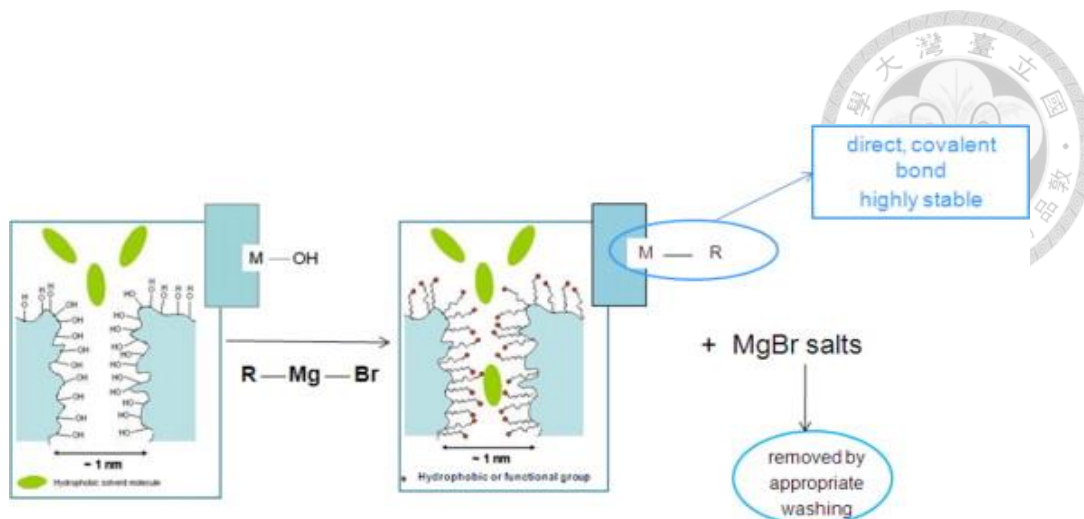
Figure 2.10 Grignard modification of ceramic membranes [39].

Even though OSN was began in the early of 1990s, ceramic membrane for OSN still encountered many challenges and required a novel types of NF membrane to keep up with growth of polymeric membrane. Generally, separation is usually based on the size and shape of the molecules to be separated, or on their interactions with the membrane material. For microporous materials, zeolites and MOFs, there are several factors, such as the limiting pore size and pore size distribution, surface diffusion, capillary condensation, shape selectivity and molecular sieving, that contribute to the separation properties. Therefore, MOF membranes as emerging inorganic membranes are very appealing for gas and liquid separations. However, the MOF membranes publish so far have been smaller than 1 nm and out range of NF. Hence, purpose of thesis is studying and preparing the mesoporous MOF membrane for OSN.
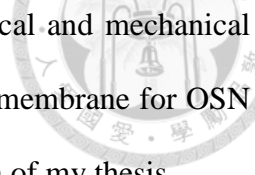
2.2.5 Challenges and future development

Although OSN have a high potential with many advantages, it has still remained some challenges to further develop membrane process for OSN:

(i) Chemical and physical stability of the membrane materials in a wide range organic solvents, in harsh acid and basic conditions, even in reactive environments with high temperature processing; high and reproducible performances in the long term.

(ii) Mechanical stability of the membrane materials toward swelling and leaching;

(iii) Versatile membranes, which may be necessary for many purposes' customers and the current membrane/module prices remain high;

(iv) The membrane selectivity or acceptable rejection are in the range between 200-1000 $g.mol^{-1}$ and solvent permeability varied depending on different organic solvents;

(v) Lack of generally accepted standard testing systems and conditions to compare and evaluate the NF performance among the various membranes – solutes – solvents.

(vi) Demand for capital investment to transfer from lab-scale to large scale OSN process.

From the drawbacks and challenges of OSN process, future researches are directed toward novel methods to tackle these issues. Synthesis of new membranes, which are stable in organic solvents, suffer harsh operating conditions, under high temperatures and extreme pH are urgent demands. Recently, thin film composites (TFCs) membranes have a potential to achieve high permeances and rejections than other types of membranes. Moreover, designing and synthesizing high-porosity TFCs membranes with the ideal nanostructure to enhance separation performance were studied and developed. Finally, the applications of inorganic membranes in OSN are less addressed till now because of the loose NF range. Inorganic membranes possess many advantages

23

compared to polymeric membrane in the aspect of chemical, physical and mechanical stability. Therefore, study and develop a new composites inorganic membrane for OSN will be an interesting topic of scientist as well as the main motivation of my thesis.

2.3 Metal organic framework – MIL-101 and MOF membranes

2.3.1 Metal organic framework

Membrane materials with a fine-tuned pore size and shape are prerequisite because a successful separation is tailored designed by size and shape of the molecules to be separated. In the last decade, there are a lot of materials used commonly for membrane fabrication such as zeolites, polymers and carbon [40-47]. In spite of their claimed potential in literature, practical applications still limited and one of the reasons is the own their bottlenecks, such as limited range of available pore sizes, limited chemical tailorability, high cost of production and others. In recent years, metal-organic frameworks (MOFs) represent a new class of crystalline porous materials with structures based on classical coordination bonds between metal moieties and poly-functional organic ligands [48]. MOFs include three series of microporous materials attractive as membrane materials: isoreticular metal-organic framework (IRMOF), zeolitic imidazolate framework (ZIF), and Material Institut Lavoisier (MIL). The wide choices of the ligand characteristics, spacer length, metal atom, and synthesis environment has made MOFs possible to make well defined size, shape, and chemical functionality of the cavities and the internal surfaces. In addition, the flexibility of the metal SBUS and organic ligands has led to thousands of compounds being prepared and studied each year [49]. Besides, the ordered porous constructions with high surface
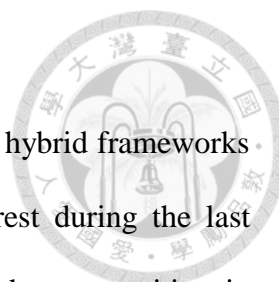
areas and porosities together with the possibility to functionalize the hybrid frameworks are the main reasons why MOFs have gained a tremendous interest during the last decade [50]. This unique structural feature offers unprecedented opportunities in membrane material for gas separation, pervaporation and nanofiltration [51].
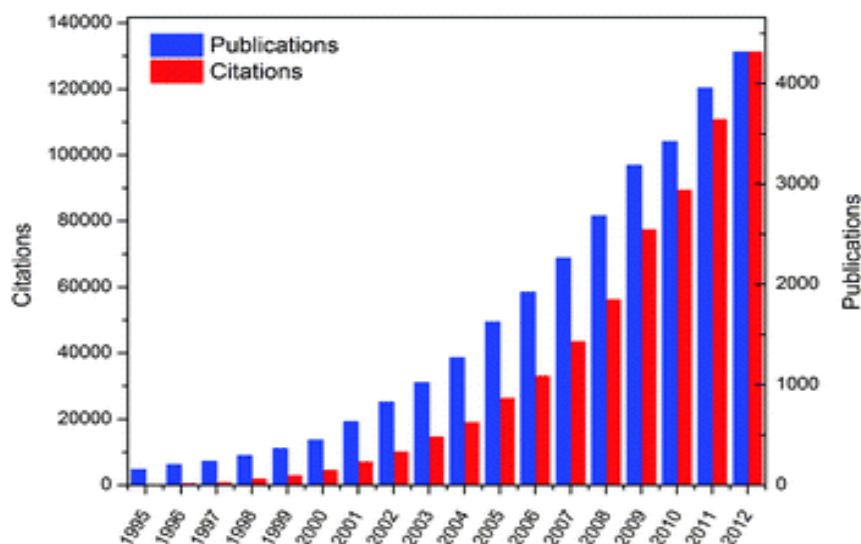
Figure 2.11 Number of publications on MOFs over past decade [52]
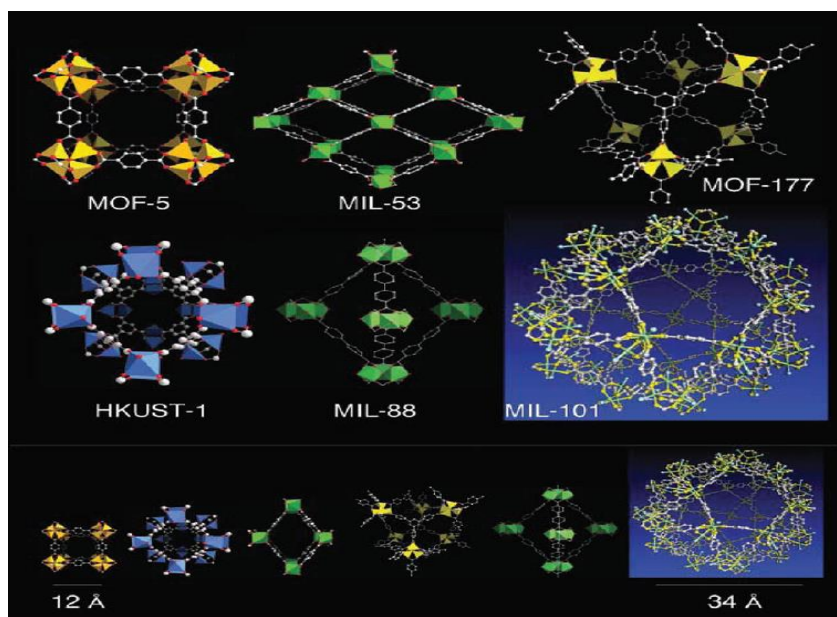
Figure. 2.12 Various reported MOF structures. Structures are arranged according to effective pore size along the bottom [53]

25

2.3.2 MIL-101

Férey et al. (2005) prepared MIL-101 by a hydrothermal method with the aid of computer simulations and targeted chemistry [54]. The robust framework of MIL-101 was composed of trimeric chromium(III) interconnected by 1,4- benzendicarboxylate (BDC) anion (Figure 2.13) - $\{Cr_3F(H_2O)_2O(BDC)_3.nH_2O\}$ (n ~ 25) and superior physicochemical properties emerged soon after. This structure was comprised of two types of mesoporous cages with diameters of ~29 and 34 Å accessible through two types of microporous windows (the smaller cages have pentagonal windows with a free opening of ~12 Å, while the larger cages possess both pentagonal and hexagonal windows with a ~14.7 Å by 16 Å free aperture).
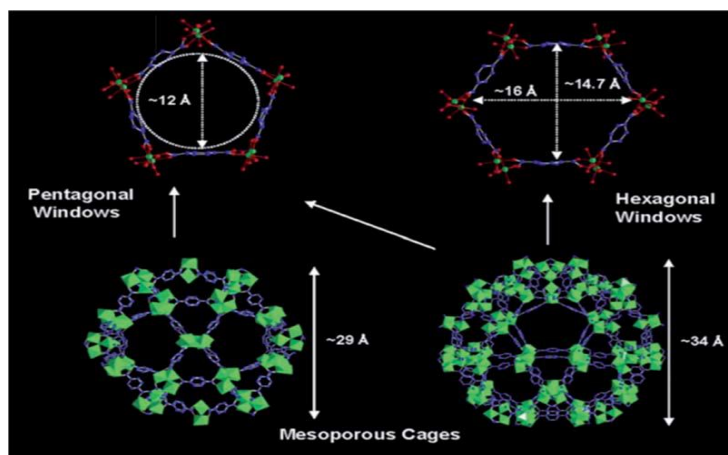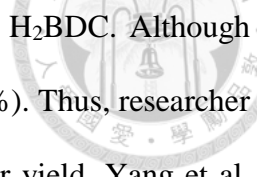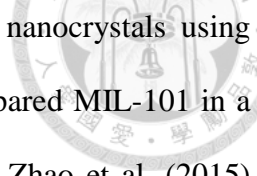
Figure 2.13 Structure and shape of MIL-101's pore size [54]

However, synthesized MIL-101 from the first report were a mixture of MIL-101 powder and huge amount of needle-like (2-10cm) crystals of recrystallized H_2BDC [54]. Generally, to collect the pure resulting products separated huge amount of H_2BDC are required with a complicated post-treatment as filtration with double fritted glass filter, then washing with mixture of hot ethanol and water (around 70°C), and finally washing
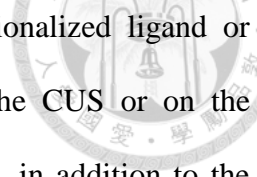
with ammonium fluoride (NH_4F) to remove completely remaining H_2BDC. Although there are post-treatment steps, the yields obtained were still low (50%). Thus, researcher improved these original multiple synthesis steps to achieve a higher yield. Yang et al. (2010) chose tetramethyl ammonium hydroxide (TMAOH) as an alkaline media to synthesize successfully MIL-101 and obtain pure product [55]. Kim et al. (2013) reported another novel method namely dry-gel conversion synthesis of Cr-MIL-101 aided by grinding. The prepared MIL-101 with surface areas greater than 4100 m^2/g was collected with yields approaching 90% without the extensive post-synthesis washing [56]. Moreover, preparation of MIL-101 also encountered with the problem of using hazardous hydrofluoric acid (HF) according to the traditional method, and control the nano-size of MIL-101 is an attractive issue. Therefore, there are several groups to find new ways to synthesize MIL-101 in order to avoid using HF as a harmful mineralizing agent and control the desired size of MIL-101. Liang et al. (2013) published a comparison of conventional and HF-free-synthesized MIL-101. They indicated that both MIL-101 without HF and MIL-101 assisted with HF showed good crystallinity, although there is a little difference in crystallinity, but it is not significant [57]. Khan et al. (2010) suggested a facile method to synthesize nano-sized MIL-101 by optimizing the reaction conditions like pH by and water concentration combining with microwave without HF. The particles of MIL-101 were collected with size of around 50 nm by MW irradiation in 15 min from diluted reagent mixtures containing a base [58]. Zhou et al. (2013) reported a facile synthetic approach of high-quality MIL-101 by acetate-assisted method in the absence of toxic HF. In this research, they could obtain the MIL-101 without trace of H_2BDC and nano-size of MIL-101 around 80 nm [59]. Yang et al.

27
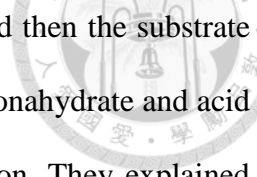
(2013) demonstrated a rapid hydrothermal synthesis of MIL-101 nanocrystals using expanded graphite (EG) as a structure-directing template. They prepared MIL-101 in a much shorter reaction time (2h) and energy-efficient manner [60]. Zhao et al. (2015) surveyed the effect of organic (mineral) and organic acid modifiers in the synthesis of MIL-101(Cr). They showed that HNO_3 could raise the purity to over 80% of a product with average $S_{BET} > 3200$ $m^2.g^{-1}$ in small-scale laboratory and $S_{BET} \sim 4000$ $m^2.g^{-1}$ in large scale (>100g). Besides, acetic acid (CH_3COOH) were added as additive replaced for HF, and combining with seeding could drop the reaction temperature to the lowest temperature 160℃ (from typically 220℃ in traditional method), with high yield and large surface area compared to conventional way. They also investigated the effect of other acids as hydrofluoric acid, trifluoroacetic acid, sulfuric acid, hydrochloric acid, phenylphosphonic acid, benzoic acid, formic acid, fumaric acid, citric acid and succinic acid as modifiers to synthesize MIL-101, yet yields of MIL-101 were low and decrease the porosity of the material [61].

Among the MOFs family, MIL-101 is one of the most appreciating porous material for future energy and environmental applications for its own several unprecedented properties [62]. In more detail, MIL-101 is composed by mesoporous zeotype architecture with mesoporous cages and microporous windows, a giant cell volume, huge surface area, and numerous unsaturated chromium sites. Moreover, MIL-101 owns several excellent stabilities against moisture and other chemicals, and it can generate two coordinatively unsaturated open metal sites (CUS) per trimetric Cr (III) octahedral cluster to interact more with molecular in separation process by removing terminal water molecular under vacuum at 423K. In addition to its highly porous nature, MIL-

28

101 has functional modification by either directly using a functionalized ligand or indirectly via the diverse post-synthesis chemical treatment on the CUS or on the organic linker so it attracted considerable attention. These features, in addition to the potential for generation of unsaturated Chromium(III) sites in the framework on activation, make MIL-101(Cr) particularly attractive for practical applications involving selective gas adsorption, storage, separation and heterogeneous catalysis [63]. In addition, MIL-101 could be integrated with other particles or embedded into polymer and onto inorganic materials for separation and catalyst. Typically, Pan et al. (2010) worked on deposition of palladium nanoparticles on chromium terephthalate MIL-101 by a simple impregnation method as a highly efficient multifunctional catalyst for one-step synthesis of methyl isobutyl ketone with a dramatically high activity compared to palladium on metal oxide or zeolites [64]. In technology of analysis area, Yang et al. (2011) reported a high performance separation of fullerenes on MIL-101 as stationary phase for HPLC with excellent selective and high throughput due to high surface area and large pore sizes [65]. Fernandez el al. (2011) synthesized MIL-101 immobilized on a monoliths for the selective oxidation of tetralin in the liquid phase, and an easy recovery of the material is essential for catalyst study because of long-term stability, chemical and thermal stability of MIL-101 [66]. Anbia et al. (2012) prepared a hybrid composite of multi walled carbon nanotubes (MWCNTS) and MIL-101 to enhance adsorption capacity for carbon dioxide due to the increase in micropore volume, and thermal stability of MIL-101 is also increase after combining with MWCNT [67]. Jiang et al. (2012) reported a facial synthesis of MIL-101 film via in situ seeding of nanoparticles on alumina support by use of dimethylacetamide (DMA). In this research,

29

they pre-treated alumina substrate by DMA first at 220ºC for 8h and then the substrate was transferred into Teflon autoclave containing chromium nitrate nonahydrate and acid terephthalic at the same condition to carry out hydrothermal reaction. They explained that DMA could be hydrolysis under acid condition to produce acetic acid in order to promote the formation of MIL-101 particles [68]. Qing et al. (2012) synthesized and characterized MIL-101/graphene oxide composites for adsorption, and they investigated the various ratio of two components through in-situ method. The study also showed the influence of GO on formation MIL-101 units, the size of crystals and the porosities of composites [69]. Sorribas et al (2013) reported a thin film nanocomposite membrane containing MOF nanoparticles (MIL-101) in a polyamide (PA) thin film layer synthesized via in situ interfacial polymerization on top of cross-linked polyimide support. Membrane performance in OSN was investigated on the basic of methanol and tetrahydrofuran permeance and rejection of styrene oligomers (PS). The incorporation of nanosized MIL-101(Cr), with the largest pore size of 3.4 nm, led to an exceptional permeance. 3.9 $Lm^{-2}h^{-1}bar^{-1}$ for MeOH/PS [70]. Rallapalli et al. (2013) prepared activated carbon (AC) incorporated with MIL-101 (Cr) to enhance hydrogen storage by reduce the unutilized voids in MIL-101 and thereby increase its volumetric hydrogen storage. The hybrid composite was synthesized successfully by mixing AC into the precursor solution of MIL-101 in various ratio under hydrothermal conditions and this research open up a novel approach for development hydrogen storage application due to a great growth in hydrogen adsorption capacity [71]. Ahmed et al. (2013) illustrated detailed synthesis of graphite oxide (GO)/MIL-101 composites and its application for liquid-phase adsorption, typically sulfur-containing compounds and nitrogen-containing
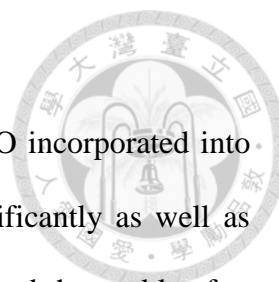
compounds from fossil fuels. Because of the suitable amount of GO incorporated into MIL-101, the porosity and surface area of MIL-101 enhance significantly as well as increase the adsorption capacity. Besides, this material was also found that stable after several times using without degradation in performance and it opened a broad horizon for application in adsorption, catalyst, separation, drug delivery [72]. Sun et al. (2014) prepared GO/MIL-101 to test n-hexane adsorption performance and the result of characterization material indicated the larger Langmuir surface area of the composites than that of pure MIL-101 as well as the higher adsorption capacities of n-hexane on the hybrid material than parent MIL-101, and around 2-11 times higher than that of traditional activated carbons and zeolite [73].
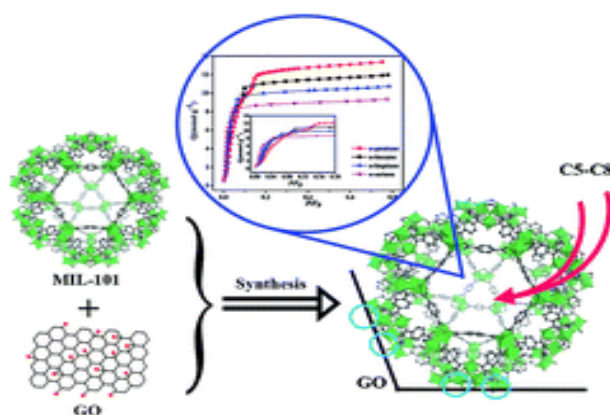
Figure 2.14 Structure of composite GO/MIL-101 [73]

Zhou et al. (2014) described a novel composite material graphene GrO@MIL-101 by using solvothermal synthesis reaction to increase adsorption capacity for acetone. The well-defined GrO@MIL-101 was formed with higher surface area and pore volume, and the results indicated that the crystal sizes of MIL-101 in composite smaller than that of the fresh MIL-101. The reason for improve of acetone adsorption could be explained by the larger surface area of composite than that of MIL-101 and dispersive forces

31

presenting in GrO sheets. The fast adsorption and desorption features of GrO@MIL-101 made it become a potential candidate for adsorption of VOCs such as acetone [74]. Xing et al. (2015) reported mixed matrix membrane (MMM) by using MIL-101 as fillers based polyethylenimine (PEI), which was applied in CO_2 separation. The MMM was synthesized by integrating MIL-101 into PEI via a facile vacuum-assisted method and then incorporated into sulfonated poly (ether ether keton) (SPEEK), and authors could achieve the high loading, uniform dispersion and improvement of interface compatibility of MIL-101 in PEI because of the electrostatic interaction and hydrogen bond between sulfonic acid group and PEI. MMM was also characterized and got the impressive results for the gas separation performance, thermal stability and mechanical stability [75]. Lin et al. (2014) investigated the particles size of MIL-101 and the molecular-weight of PEI in the CO_2 capture ability for MMM (PEI/MIL-101). They demonstrated that shrinking the MOF particle size could increase the loading of PEI in MIL-101, yet decrease surface area and pore volume; and lower molecular-weight PEI could readily diffuse into the inner pores, while larger PEI can be only partly loaded into the pores and the rest would remain on the MOF surface [76]. Alentiev et al. (2014) synthesized a hybrid composite membrane material base on PIM-1 polymer of intrinsic microporosity and MIL-101 nanoparticles of meso porous material. They showed that the present of MIL-101 in polymer tending to enhance the permeability and diffusion coefficients of gasses (He,O_2, N_2, CO_2) compared to the original polymer [77]. Lin et al. (2015) worked on preparation of mix matrix membrane with MIL-101 decorated carbon nanotubes (CNTs) fillers for efficient CO_2 separation. MMM was formed by the growth of NH_2-MIL-101(Al) on the surface CNTs as fillers before embedding into polyimide.

32
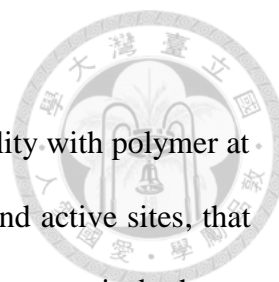
The well-defined CNT-MIL fillers showed good interface compatibility with polymer at high loading and the introduction of extra amino functional group and active sites, that are efficient for CO_2 separation through present of dramatic enhancement in both gas permeability and selectivity of CO_2 compared to original polymer. From this study, they recommended the novel strategy to improve the gas separation of MMM by modification of MOFs on available fillers to increase the compatibility or selective with specific gases and open up a new path toward the promising applications for this material [78].
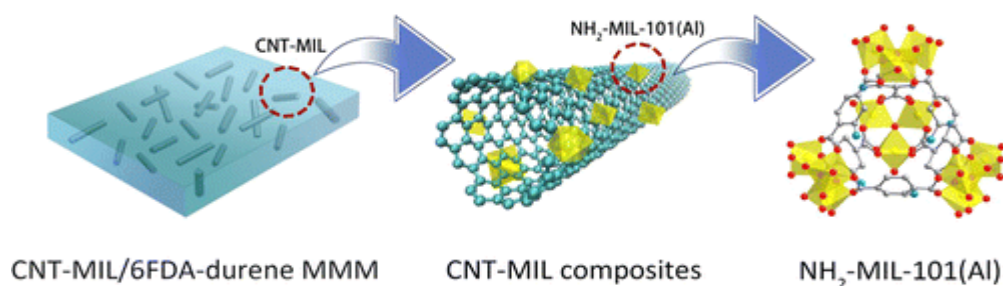
Figure 2.15 Structure of NH_2-MIL-101(Al)/CNT composites [78]

Naseri et al. (2015) synthesized mixed matrix membranes with MIL-101 immobilized into matrimid 5218 polymer. This composite was used for gas separation as CO_2, CH_4 and N_2, in which MIL-101 showed the significant adsorption of CO_2 compared with two other gases at difference pressure. They achieved 30% loading of MIL-101 in polymer and showed good adhesion to and dispersion into polymeric MMM, but 10% loading of MIL-101 in polymer led to the best gas performance [79]. Iglesia et al. (2016) published the new application of MIL-101 based MMM for esterification of ethanol and acetic acid in a membrane reactor. They prepared successfully MMMs based on commercial matrimid 5218, and using MIL-101 as filler. MMM displayed a better reactor performance than the pare PI membrane due to the excellent properties of MIL-101

33
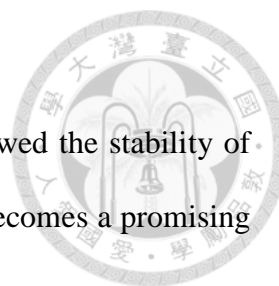
fillers such as its large surface area and active sites. They also showed the stability of membrane after esterification by leaching experiment that made it becomes a promising material as catalyst for esterification [80].
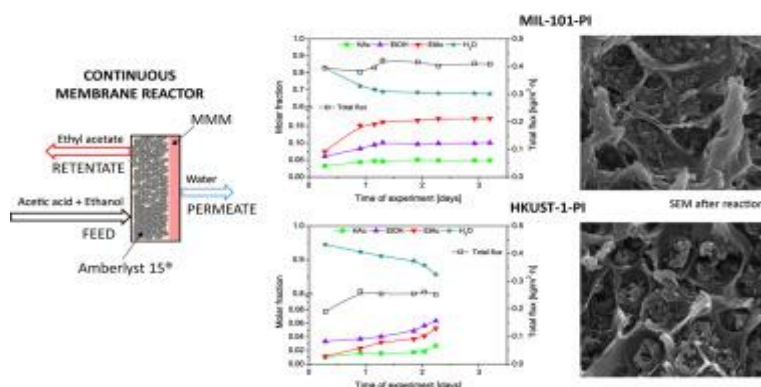
Figure 2.16 Application of MIL-101-PI and HKUST-1-PI for esterification

Overall, MIL-101 owns lots of excellent properties such as large surface area, high porosity, thermal and chemical stability, so it could be used in a wide range of applications. MIL-101 can be combined with polymer as matrimid, polyimide to form mixed matrix membrane for major gas separation application. Moreover, there are several groups that concentrated on synthesis of composite GO/MIL-101 and GrO/MIL-101 in 2013-2014 for gas adsorption and separation with impressive results. Because MIL-101 is inorganic material, so use MIL-101 to graft on the surface of inorganic substrates forming a continuous thin film still has limited so far due to the poor interaction with the substrates. However, the potential of MIL-101 in separation area is a real and be demonstrated. Therefore, this research will study and investigate how to fabricate the smooth and dense layer of MIL-101 on inorganic substrate like ceramic membrane for liquid separation.

2.3.3 Metal organic framework composite membranes

MOFs possess well-defined, regular pore structure and high porosity, besides they are high thermal and chemical stability materials compared to other inorganic materials like zeolite, activated carbon and graphene oxide. In addition, pore size of MOFs can be easily controlled by the combination of difference metal ions or cluster and organic linker, and the MOFs can be functionalized with typical groups to enhance the compatibility with solutes or gases. From there, MOFs materials become striking compounds for separation applications under severe conditions like high temperatures and organic solvent environments [40-51]. Similarly, membranes made from MOFs are expected to offer unique opportunities with a potential to achieve superior performance. The fabrication of thin and continuous MOFs layer on porous supports has been an attractive topic due to the fact that membrane-based devices are of interest in separations, membrane reactors, and other advanced applications such as optical, electronic, and magnetic applications [81-85].
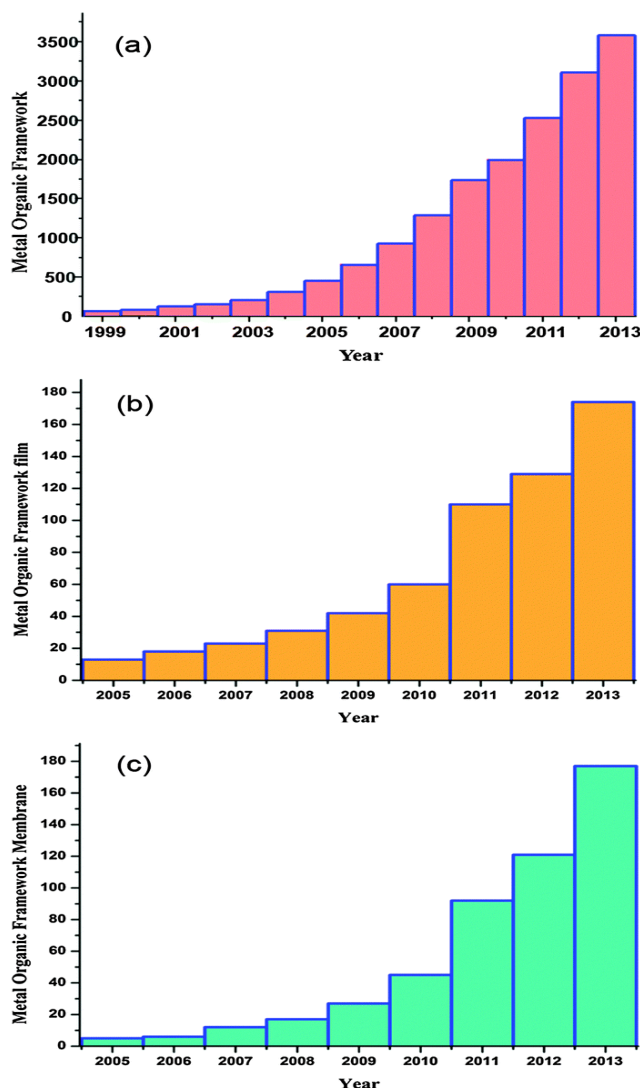
Figure 2.17 The number of publications per year (a) metal organic framework, (b) metal organic framework film and (c) metal organic framework membrane [86]

The synthesis methods for both inorganic and polymeric substrates are divided into three broad categories based on diffusion direction of metal ion and linker in crystallization process:

1. Solvothermal/hydrothermal method

2. Interfacial (contra-diffusion) synthesis method

3. Liquid epitaxy (step-by-step or layer by layer) method
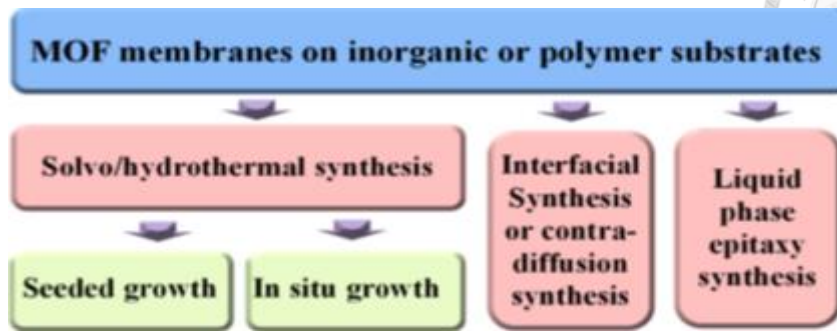
Figure 2.18 Synthesis method of MOF-based membranes [87]
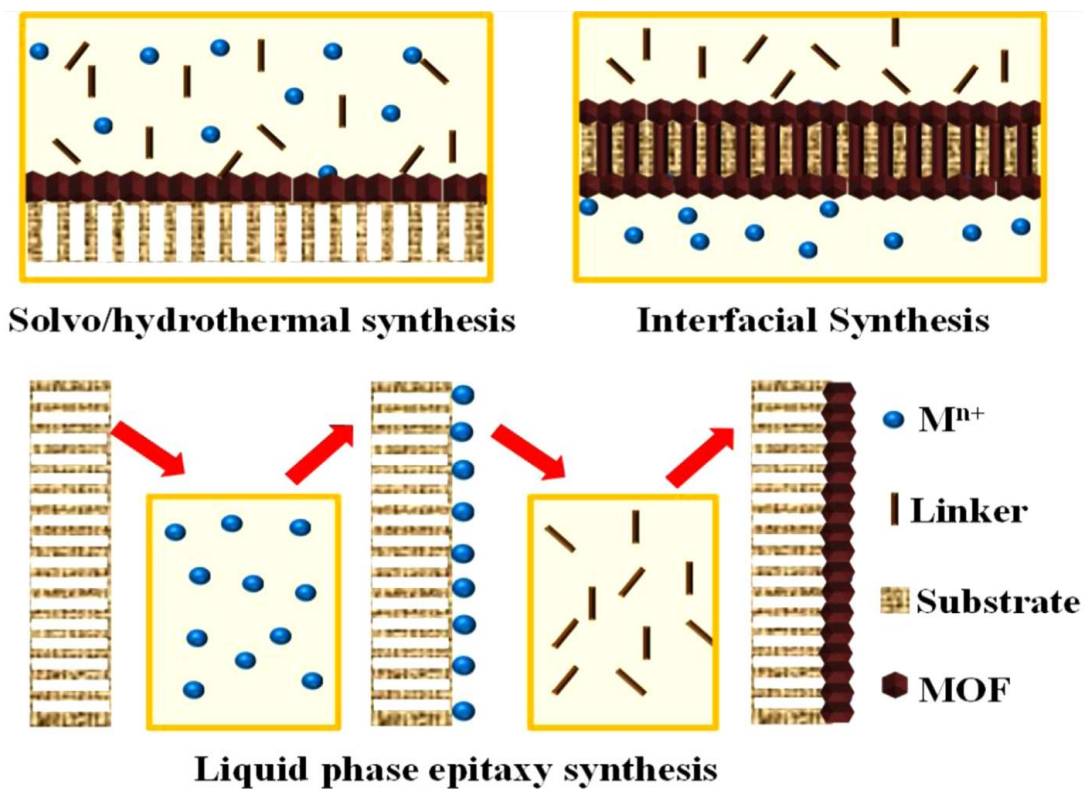
Figure 2.19 Scheme of the synthesis methods for continuous membranes [87]

In solvothermal or hydrothermal method, the substrates are immerged in the mixture of solution of metal ion and organic ligand to growth the crystal directly. Thus, the metal ion and organic linker are diffused follow one direction from bulk solution to the surface substrate to generate the MOF layer. In interfacial method, MOF layer is formed at the liquid-liquid interface of solution of organic linker and metal ion by their

37
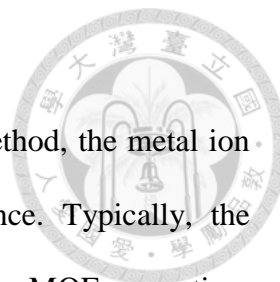
diffusion in opposite direction. In liquid phase epitaxy synthesis method, the metal ion and organic linker are contacted to substrate follow the sequence. Typically, the substrate is immerged alternatively in metal ion and organic ligand for MOF generation, and the substrate also needs to wash before forwarding to the second solution. The advantages as well as disadvantages will be discussed more in next section.

Base on equipment and condition to synthesize MOF membranes, the methods were divided into five categories: hydro/solvothermal method [88], plasma spray method [89], counter diffusion method [90], interfacial method [90], and microwave method [91]. In general, all of five above methods follows one of two approaches like inorganic membranes: in-situ growth or seeded assisted (secondary) growth [92-95]. Typically, the surface is coating with a seed layer initially, and a relatively diluted solution is used to reduce bulk crystallization and favor formation of a continuous layer in secondary step. Seeded growth is an important step, which has been commonly used in synthesis MOF membrane by fabrication of layer of seeds on a support surface, facilitate more rapid growth of heterogeneous nucleation on the substrate in the secondary growth step. Other membrane features such as membrane thickness and grain boundary structure can be optimized by secondary growth step. Hence, seeded growth is a key factor for the secondary growth and led to generate better membrane performance [96]. Besides, the secondary growth method can decouple the nucleation and growth steps, which offer better control over membrane microstructure and easily crystallographic orientation of nucleation on the surface. By this way, the fabrication of high quality MOF membranes can be achieved with a compact, smooth, dense and continuous layer of MOFs covered on the support.
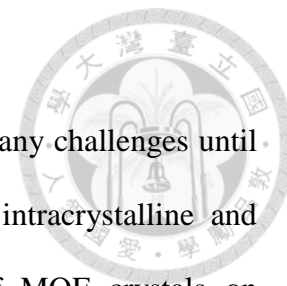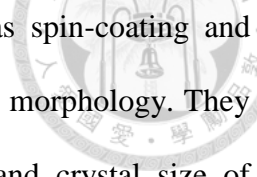
Generally, preparation of MOF membranes has encountered many challenges until now. The presence of pinhole defects, grain boundary defects, intracrystalline and intercrystalline cracks, low heterogeneous nucleation density of MOF crystals on support can great ruin the separation performance of the membrane formation. Unlike ZIFs, it turns out rather challenging to fabricate MOF films since the organic linkers typically do not provide labile linkage groups that can form covalent bonds with linkage groups on the surface of the supports to growth a compact membrane. Therefore, it is extremely difficult to prepare high quality MOF membranes through the in situ solvothermal or hydrothermal methods, and heterogeneous nucleation sites on the surface of the inorganic substrates are very important for the preparation of well-intergrowth MOF membranes. Overall, the efficient and reasonable classification of synthesis method of MOFs on inorganic substrate base on physical-chemical properties of the substrates. This classification facilitates access easy, simple, and general; and arrange towards the better way to solve these above challenges.
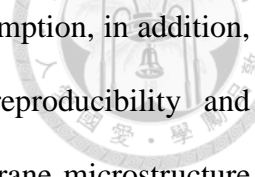
(i) MOF membrane on unmodified inorganic substrates

(ii) MOF membrane on physically modified inorganic substrates

(iii) MOF membrane on chemically modified inorganic substrate

(i)   MOF membrane on unmodified inorganic substrates

In the early time of preparation of MOFs on inorganic substrates (2005-2008), MOF-5, $Cu_3(BTC)_2$ and $Zn_2(bdc)_2(dabco)$ crystals were attached to 'Terminated Self-Assembled Monolayers' on alumina and silica supports [81, 84, 85], while $Mn(HCO_2)_2$ crystals were deposited on graphite disks modified with formate [97]. Dense, uniform coatings, however, were not achieved in these studies. Garson et al. (2008) produced a

39

dense coating of HKUST-1 on α-alumina by seeding approach as spin-coating and amorphous MOF precursors, with coordination polymer of different morphology. They surveyed the effect of synthesis conditions on the morphology and crystal size of HKUST-1 to optimize the strategies for the preparation of continuous layers. They also demonstrated that crystallization of MOF on support just occurs by incorporation seeding methods with low concentration mother liquors. However, they still not had enough data to confirm high quality of MOF membrane and tried to figure out its application [98]. After that, Liu et al. (2009) firstly reported the synthesis of continuous MOF-5 membrane for gas separation. MOF-5 layer was grown on an unmodified porous alumina by placing the substrate into the Teflon autoclave containing MOF mother solution through solvothermal reaction at 105°C (in-situ technique). The continuous film showed the strong adhesion to the porous α-alumina support due to the covalent bonds between the carbonyl groups of linkers and the hydroxyl groups at the surface of alumina substrate and it is appreciated for gas permeation experiment [88]. Bux et al. (2009) fabricated ZIF-8 by microwave-assisted solvothermal reaction in order to shorten the synthesis process. Besides, Bux's group synthesized a crack-free, dense polycrystalline layer of ZIF-8 on a porous titania support by using microwave-assisted heating and they could significantly reduce process time to 4h. With the trade-off between flux and selectivity of gas, especially for H_2, they demonstrated that it is generally possible to synthesize highly gas-selective MOF membrane on ceramic substrates via in-situ crystallization [99]. Shah et al. (2013) produced continuous well-intergrown membranes of prototypical MOFs, HKUST-1 and ZIF-8 by rapid thermal deposition (RTD), slip-coating substrate in MOF mother solution. By new technique,

40

they could save the synthesis time (tens of min) and precursor consumption, in addition, this technique displayed several advantages like scalability, reproducibility and commercialized cost. The enhanced crystal morphology and membrane microstructure membrane showed better gas separation performances than that of membrane from conventional solvothermal methods [100].

Shekkah et al. (2014) reported a novel efficient methods named the liquid – phase epitaxy (LPE) to fabricate ultrathin (0.5-1 µm) continuous and defect-free ZIF-8 membranes. In the experiment, α-alumina substrate was immerged in metal ion solution and then washed with methanol. The procedure was done in the same way in linker solution instead of metal ion solution. Whole process was repeated for further growth cycles. With new method they could control over film growth thickness. However, gas permeance of ultrathin membrane generated from LPE method was 100 times lower than that of the paper reported previously due to the difference in internal structure of the ZIF membrane [101].

Counter diffusion or interfacial method was concerned as synthesis MOF membranes on bare substrates. Ameloot et al. (2011) firstly reported this method and they succeeded to prepare HKUST-1 membrane by interfacial method. They demonstrated how the difference in solubility characteristic of the organic and inorganic MOF precursors could be used in a synthetic approach that enables the synthesis of uniform thin MOF layers through a self-completing growth mechanism according to the below figure [102].
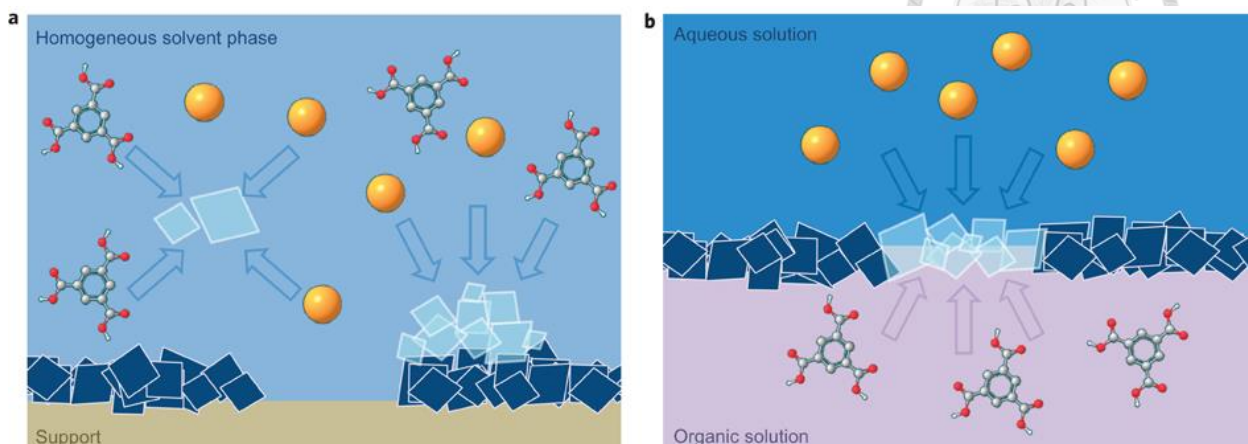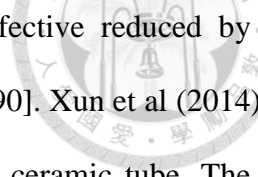
Figure 2.20 Different concepts in the synthesis of MOF films[102]

Kwon et al. (2013) reported a simple one step in situ method based on counter-diffusion concept to prepare well-defined ZIF-8 membrane with significantly enhance microstructure for propylene/propane separation. In more detail, the substrate was immerged in the solution of metal ion first to get saturated support and then transferred into Teflon containing solution of organic ligand to carry out interfacial procedure. Finally, the substrate was placed in again in Teflon with precursor solutions to heal a defect membrane. They indicated that the advantages of counter-diffusion method are an ability to healing the poorly intergrown membranes and saving the costly precursor solutions due to its recycling after synthesis process. They also expected this method can become a general method for almost MOFs by successful synthesis of ZIF-7 and SIM-1 membrane via interfacial method. This success will open up the attractive path to prepare the high-quality MOF membrane for potential large scale practical application [103]. Hara et al (2013) prepared a MOF - CuBTC layer within the porous support by counter-diffusion method for gas separation. A solution of linker was poured into inner side of hollow fibers, while a solution of metal ion was contacted to outside of hollow fiber to diffuse through membrane and met linker within the membrane. They

42
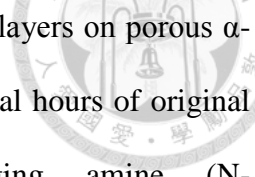
successfully demonstrated that inter-crystalline defects can be effective reduced by appearance of molecular-sieve effect via counter-diffusion method [90]. Xun et al (2014) fabricated tubular MOF membranes on the inner surface of Al_2O_3 ceramic tube. The experiment was carried out follow two steps: a self-modified fabrication of homogenous ZIF-8 nanocrystals inner side of tube by efficient counter-diffusion and secondary growth for forming continuous ZIF-8 thin films. They discovered that ZIF-8 nano-particles was fully plugged into the pore size of ceramic membrane under the solvent evaporation forces, and ligand modification, which facilitate the growth of the membrane [104]. Huang et al. (2015) synthesized ZIF-71 hollow fiber membranes by modified counter-diffusion for separation of ethanol-water mixtures with a good performance. As the same experiment with other counter-diffusion method, the sequence of steps is similar and they also got high integrity and thin film membrane. This is one of the limited application of ZIF-membrane for liquid separation, it promised a potential material ethanol – water separation [105]. Hara et al. (2015) again prepared ZIF-8 membrane by counter-diffusion method, yet they formed ZIF-8 thin film at miscible and immiscible liquid-liquid interfaces. Typically, ZIF-8 membrane synthesized from the immiscible pair of water and 1-octanol and applied in propylene/propane separation with a good permeance of $5.2x10^{-9}$ $molm^{-2}s^{-1}Pa^{-1}$ and permselective of 7.2 at 25°C. Compare to their previous report in 2013, the interface of two liquids was fabricated on the outer surface of hollow fiber instead of inner surface. They explained that the inner part and the substrate were initially filled with zinc nitrate solution and ratio of linker/metal ion was 2, which lead to form ZIF-8 on the outermost part of substrate. Finally, they could get the free-defect membrane in immiscible pair of

solvents as advantageous step before successive reaction in miscible pair of solvents in order to prepare high quality ZIF-membrane, and high performance for propylene/propane separation [106].

(ii) MOF membrane on physically modified inorganic substrates

Due to the poor heterogeneous nuclei, the preparation of MOF membrane on bare support are relatively fewer. Thus, physically modified inorganic substrates is the better way to tackle this problem and this way is carried out by the coverage of nanosize MOF crystals as primitive nuclei on the substrate for promoting the heterogeneous nucleation. Ranjan et al. (2009) synthesized microporous MOF membrane on porous support using the seeded growth method. The polish α-alumina substrate was modified using polyethyleneimine (PEI) and do twice to ensure the coverage of the support in order to increase adhesion of seed via H-bonding and free hydroxyl group of the support surface. Moreover, PEI could form Zn-N coordination bond to zinc cations on the surface of the nanocrystals. After that, the pretreated membrane was coated by seed layers through the manual assembly method before process of secondary growth. Nevertheless, permeance values are relatively low and decrease further with raise temperature; the orientation and thickness of membrane were still not clear and need to investigate more [107]. In the same way, Cu_3BTC_2 membranes was fabricated by secondary growth approach on pre-seeded α-alumina hollow ceramic fibers (HCFs) modified with chitosan, that reported by Zhou et al. (2012) [108]. This method was applied to synthesize ZIF-7, ZIF-8 membranes by Li's group (2010) [109] and Bux's group (2011) [110], respectively. There was a little difference compared to previous report, ZIF-7 and ZIF-8 nanocrystals was mixed with PEI to collect a viscous seeding solution and then coated on the support

surface. Yoo's group (2009) prepared densely packed MOF-5 seed layers on porous α-alumina substrate by microwave for 1-2 minutes compared to several hours of original methods. Furthermore, they also used proton scavenging amine (N-ethyldiisopropylamine – EDIPA) in precursor solution during secondary growth steps to avoid dissolving of seed crystal and form a continuous membrane. This was also the first time there was a group that prepared about preferentially oriented MOF-5 films by growing oriented MOF-5 crystals seeded on thick graphite-coated substrates [91]. Guerrero et al. (2010) prepared HKUST-1 membranes on porous support using secondary growth with using new seeding technique called "thermal seeding". They synthesized the HKUST-1 seed crystal first and stored the mother liquor to apply for thermal seeding step. The mother liquor after synthesis of HUKUST-1 containing un-reacted ligands and copper species was dropped on surface of hot support (200°C) and acted as binder to increase adhesion of HKUST-1 and membrane. Consequently, the seeded support was immerged in solution of precursors of HKUST-1 to implement the secondary growth. The key point of this experiment is the presence of both unreacted metal ion and linker in seed solution at elevated temperature. They also controlled the cooling and drying temperature process to avoid the formation of crack [111]. Tao et al (2012) reported a continuous well-intergrown ZIF-8 membrane on hollow ceramic fiber by novel crystallizing-rubbing seed deposition. In this study, they synthesized ZIF-8 membrane via in-situ method under solvothermal condition. Following first step, the surface of support was rubbed with an average diameter of about 60 nm of ZIF-8 on entire support by sand paper to obtain a dense seed layer before seeded support was continued to growth into a defect-free ZIF -8 membrane by secondary growth method.

The membrane obtained from this method exhibited a high permeance of H_2 and good permeation selectivity for H_2 over CH_4, N_2 and CO_2 [112].
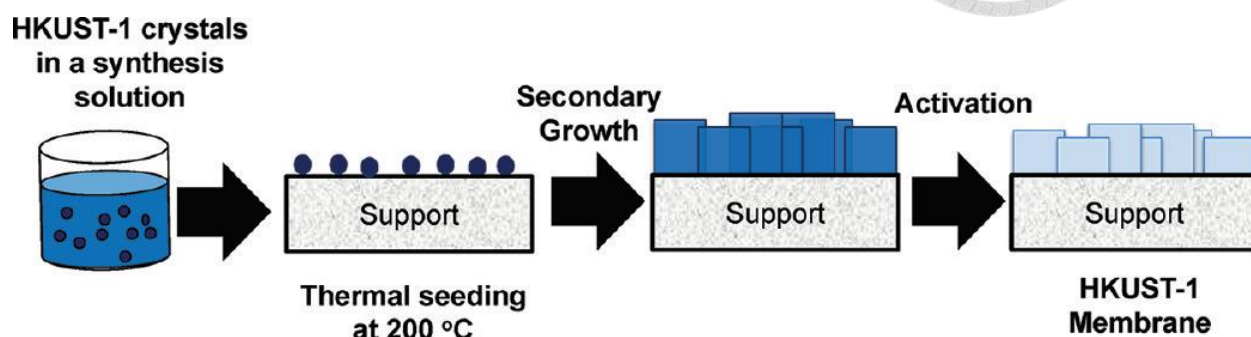

Figure 2.21 Illustration of HKUST-1 membrane fabrication using thermal seeding and secondary growth [111]
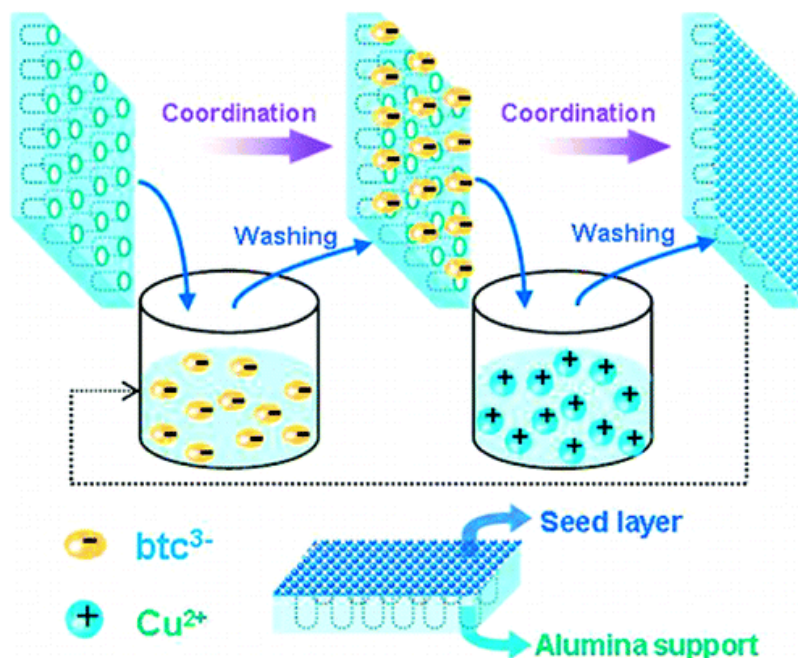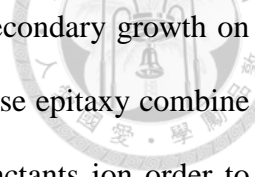
Figure 2.22 Schematic diagram of step-by-step deposition of btc^{3-} and Cu^{2+} on alumina support [113]

Nan et al. (2012) reported a step-by step seeding procedure for preparing HKUST-1 membrane on porous α-alumina. This is novel seeding method to form HKUST-1

46

membranes and high quality membrane could be obtained by the secondary growth on the seeded support. This method was relatively similar to liquid phase epitaxy combine with secondary growth. They could adjust the concentration of reactants ion order to regulate the continuity and integrity of membrane layer. However, HKUST-1 membrane in this situation had no good results for H_2 separation due to larger pore size than that of kinetic diameter of gases as H_2, N_2, CO_2 and CH_4; it offered a potential composite for separation of larger compounds [113]. Finally, the seeding method by dip coating and spin coating is a common way to synthesize MOF membranes. For example, ZIF-69 membranes was prepared via dip-coating seeding method integrated with secondary growth by Liu's groups (2011) [114], and spin-coating seeding method was applied in synthesis of ZIF-8 membranes reported by Pan et al. (2012) [115].

(ii)   MOF membranes on chemically modified inorganic substrates

Because of the poor adhesion between seed layer or MOF layer and substrate, chemically modified inorganic substrate is necessary to improve the bonding of metal source or linker with the substrate. By this method, the substrate is functionalized by some special groups as $-NH_2$, -COOH, - OH to increase the heterogeneous nucleation sites for MOF layer growth and significantly enhance the adhesion of MOF layer and support. Guo et al. (2009) reported the copper net supported $Cu_3(BTC)_2$ membrane by new technique named "twin copper source". Through this method, they heated the copper net (400 mesh) and oxidized the surface copper net to provide homogeneous nucleation sites or metal source to support a continuous MOF film growth. Hence, they solved the problem of heterogeneous nucleation problems, and showed an excellent permeation selective for gas separation and high permeance because of the high porosity

47
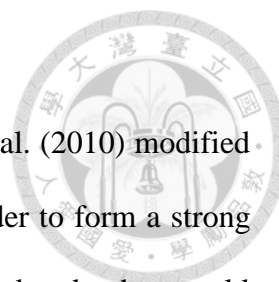
of CuBTC and the copper nets [116]. By another way, McCarthy et al. (2010) modified

the surface by reaction of organic linker and α-Al$_2$O$_3$ support in order to form a strong

covalent bonds between ZIF layer and substrate. With the covalent bonds, they could

facilitate the heterogeneous nucleation and growth of ZIF membrane. The procedure

was described as below figure, the hot support will react directly with organic linker to

fabricate the covalent bonding and then the modified support will let in precursor

solution to implement secondary growth method. To demonstrate the efficient

application of this method, ZIF-7 was also used to test and get the successful result

[117].
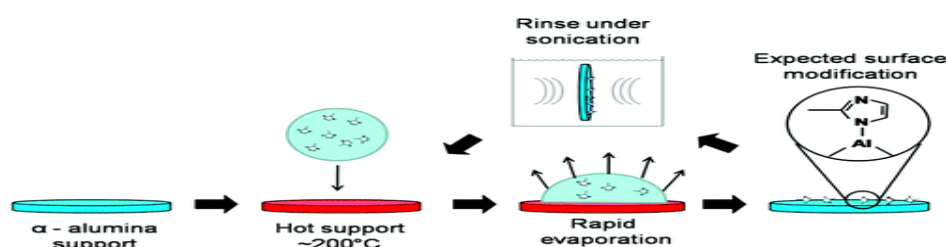
Figure 2.23 Illustration of the substrate modification process [117]

However, not all organic linker could react with the substrate due to appearance of

functional group on α-Al$_2$O$_3$ support as –OH or physically surface structure. Thus,

Zhang et al. (2013) prepared a low-defect ZIF-8 tubular membrane by substrate

modification with ultrathin ZnO layer followed by surface activation to promote

homogeneous surface for gas separation with dramatically high gas permeation and

selectivity. They deposited ZnO layer by slip casting on hollow fiber, afterward ZnO

layer was activated by linker for ZIF-8 growth [118]. By the same way, Zhang et al.

(2014) prepared ZIF-8 membrane supported on vertically aligned ZnO nanorods for gas

permeation and separation. They indicated that the role of strut-like structure could

compensate for the mismatch in the expansion coefficient of the membrane and support

48

due to great vertical and lateral movements. The nanorods act as organic linker for the growth of a defect-free membrane [119].
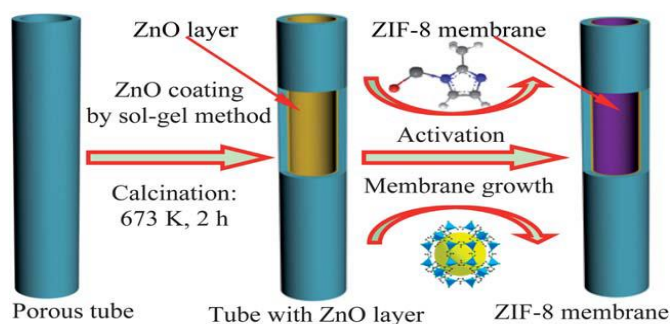
Figure 2.24 New membrane preparation procedure [118].
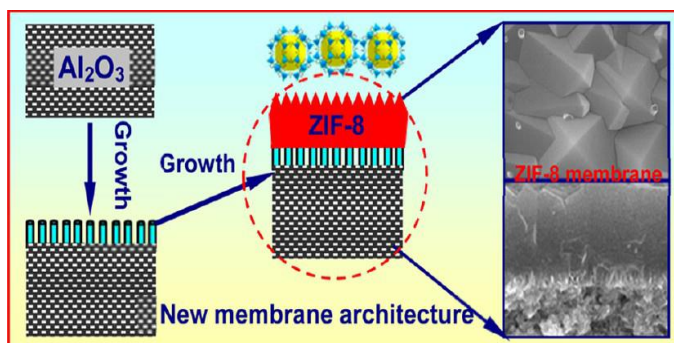
Figure 2.25 Preparation scheme for ZnO nanorod supported ZIF-8 membrane [119]

Compare to the modified treatment of substrate by reaction between linker and substrate or coverage of ZnO layer/nanorods on substrate as a support to growth MOF crystal. Hu et al (2011) fabricated MOF-membrane via reactive seeding by linking the seed layer and chemical support by chemical interaction, that means the support sever as metal source reacting with organic ligand to generate the seed layer. By this method, a strong adhesive and uniform seeding layer could promote the preparation of well-intergrowth MOF membranes in the secondary steps. This is advantageous method due to combining both seed synthesis and seeding method into one step. They also demonstrate the general application of this method by successful applying to synthesize

49

continuous and high integrity MIL-96 membrane. Application of prepared MIL-53 membrane for dehydration of azeotrope of ethyl acetate (EAC) aqueous solution by pervaporation opened up a new path for MOF membrane in liquid separation [120]. Dong and Lin et al. (2012-2013) group also applied this method to synthesize ZIF-71 and ZIF-78 membrane [121, 122]. Beside these membranes were used to separation ethanol/water and dimethyl carbonate (DMC)/methanol mixture by pervaporation.
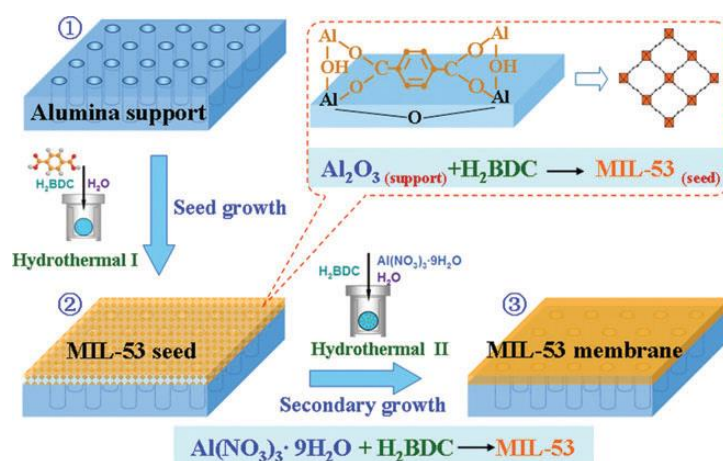
Figure 2.26 Schematic diagram of preparation of the MIL-53 membrane on alumina support via the RS method [120].

Finally, they used a third party bridging the MOF layer and substrate by some functionalized groups such as $-NH_2$ and $-COOH$ via covalent bonding. Huang et al (2010) recommended a novel covalent functionalization strategy to prepare ZIF-90 molecular sieve membranes by using 3-aminopropyltriethoxysilane as a covalent linker between the ZIF-90 layers and Al_2O_3 support via imines condensation. Typically, the ethoxy group of APTES reacted with hydroxyl group on the substrate to fix these molecular, then another head of APTES is amino group reacting with aldehyde group of imidazole-2-carboxylate via imine condensation. After, the nucleation and crystal growth of the ZIF-90 generate at these fixed sites on the surface of ceramic support. The

50
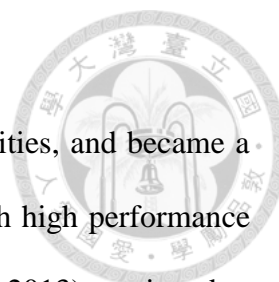
prepared membrane exhibited high thermal and hydrothermal stabilities, and became a promise material for both hydrogen production and purification with high performance [123]. Because of the general and useful method, Huang et al. (2010-2013) continued to make ZIF-7, ZIF-8, ZIF-22, ZIF-90 and ZIF-95 membranes by this method and all of prepared membranes were applied for gas separation [124-127].
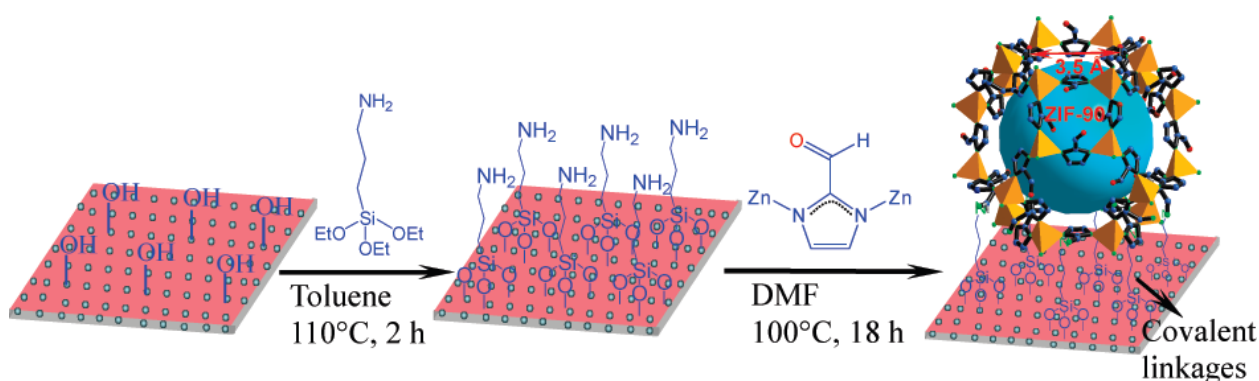
Figure 2.27 Scheme of preparation of ZIF-90 membranes by using APTES as a covalent linker between ZIF-90 membrane and Al_2O_3 support via an imine condensation reaction [123].

In conclusion, synthesis MOF-base membranes have achieved great development in recent year. There are various inorganic substrates as alumina, titania, porous ZnO, that can be exploited to support the MOF membranes. For MOF membranes on inorganic substrates, the well-intergrown and complete defect-free MOFs on the substrates for separations can be generated by enhancing the heterogeneous nucleation sites on the interfaces or reducing the homogeneous nucleation sites in the bulk. In addition, MOF membranes have been used for a variety of separation process, such as gas separation, pervaporation and listed in Table 2-1. Compared to gas separation, far fewer studies have been reported on separation of liquid mixture by MOF membranes. Exploring

51
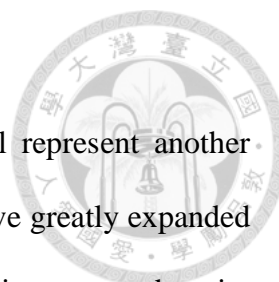
liquid separation properties and stability of MOF in solvents will represent another important area of research of MOF membranes. Although MOFs have greatly expanded the scope of porous materials, they are still largely restricted to the microporous domain, which limits their applications in a wide range of fields. Therefore, synthesized mesoporous MOF membranes will provide extraordinary advantages over microporous MOF membranes and these MOF membranes could be applied in liquid separation as organic solvent nanofiltration.

Table 2. 2 Application of inorganic MOF membranes

Membrane	Application	Ref
ZIF-7/ alumina disc	Gas separation	[128], [129], [109]
ZIF-8/ alumina tube	Gas separation	[118], [130]
ZIF-8/titania	Gas separation	[99]
ZIF-8/ alumina disc	Gas separation	[131], [132], [133], [100], [115], [134]
ZIF-22/ alumina disc	Gas separation	[124]
ZIF-78/ porous ZnO	Gas separation	[121]
ZIF-90/ alumina disc	Gas separation	[123]
ZIF-90 post/ alumina disc	Gas separation	[135],[125]
ZIF-95/ alumina disc	Gas separation	[126]
MIL-53-NH_2/ glass frit disc	Gas separation	[136]
MOF-5/ alumina disc	Gas separation	[88], [91], [137]
CuBTC/ copper net	Gas separation	[116]
CuBTC/ alumina disc	Gas separation	[111], [113]
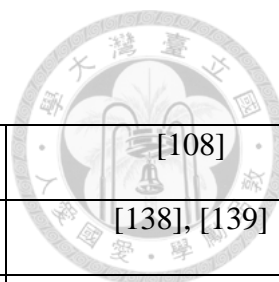
CuBTC/ alumina fiber	Gas separation	[108]
CuBTC/ AAO disc	Gas separation	[138], [139]
ZIF-69/ alumina disc	Gas separation	[140]
SIM-1/ alumina tube	Gas separation	[141]
ZIF-9-67/ alumina disc	Gas separation	[142]
Bio-MOF-13/ alumina disc	Gas separation	[143]
$Co_3(HCOO)_6$/ glass frit disc	Gas separation	[144]
CAU-1/alumina disc	Gas separation	[145]
ZIF-8/ alumina disc	Pervaporation	[146]
ZIF-71/ porous ZnO	Pervaporation	[122]
ZIF-78/silica	Pervaporation	[147]
Zn-BLD/ZnO	Enantioselective separation	[148]
MIL-53/ alumina	Pervaporation	[120]

Chapter 3 - Experimental methods and equipment
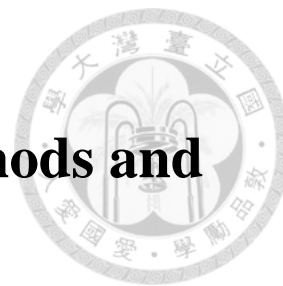
In this study, MIL-101 membranes were synthesized by grafting MIL-101 particles on the on aluminum ceramic membrane via in-situ seeding assisted by acid modulator. $Cr(NO_3)_3.9H_2O/H_2BDC/H_2O$ molar ratio, the concentration of acid modulator were the main parameters on synthesis MIL-101 membranes process. Besides, the effect of solvent and synthesis method to experiment were also surveyed. The performance of the MIL-101 membranes for organic solvent nanofiltration were shown in this study. Therefore, the materials, apparatus, chemicals, the technology of MIL-101 membranes and the flowchart of organic solvent nanofiltration will be introduced in this chapter.

3.1 Experimental materials

3.1.1 Supports

The supports used in experiments are α-Al_2O_3 ceramic membranes. They are produced from Fraunhofer IKTS company. Ceramic membranes have a round shape with diameter of 30 mm and thickness of 1mm. The ceramic substrates are comprised of two layers: support with pore size around 2.5 μm and top side with pore size about 200 nm. The morphology of ceramic membrane was observed in Figure 3.1
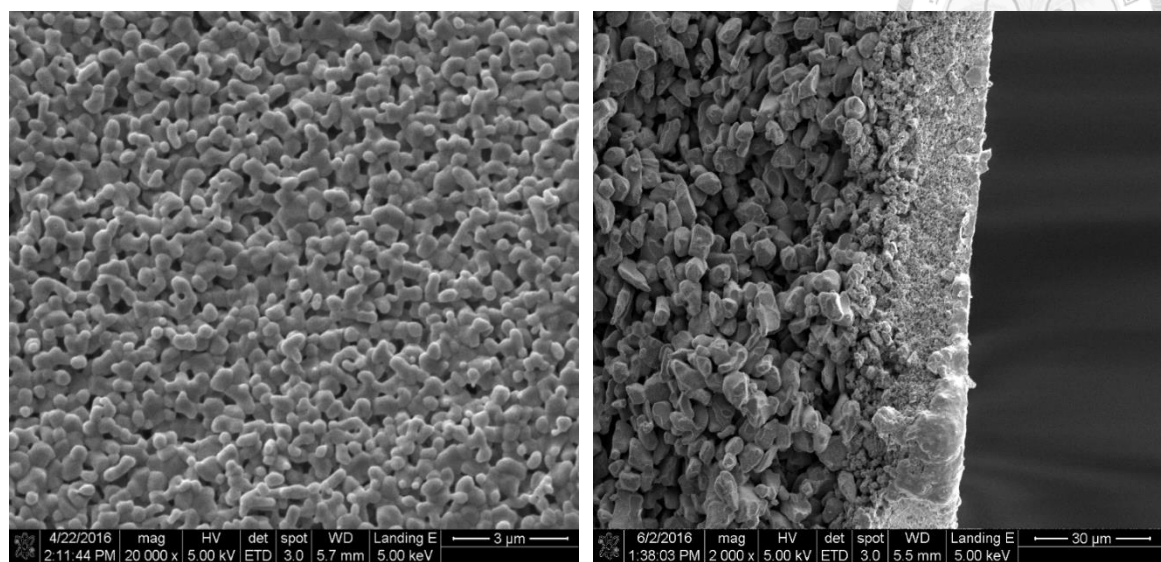
Figure 3.1 SEM image of alumina substrate (left-top view and right-cross section view)

3.1.2 Chemicals for MIL-101 particles and MIL-101 membranes

Chromium nitrate nonahydrate ($Cr(NO_3)_3.9H_2O$) was kindly provided from Sigma-Aldrich. Terephthalic acid or benzendicarboxylic acid (H_2BDC) was purchased from Alfa Aesar – A Johnson Matthey Acetic acid (CH_3COOH) was purchased from J. T. Baker. Ethanol (C_2H_5OH) and dimethylformamide (DMF) used for washing and exchange solvent was purchased from Echo chemical Co. ltd.

3.1.3 Chemical for OSN performance

Table 3. 1 Chemical for OSN performance

Chemical	Company
Ethanol (C_2H_5OH)	Echo chemical Co. ltd
NMP (C_5H_9NO)	Macron fine chemical
DMSO (C_2H_6SO)	Alfa Aesar – A Johnson Matthey
DMAc (C_4H_9NO)	J. T. Baker Co. ltd
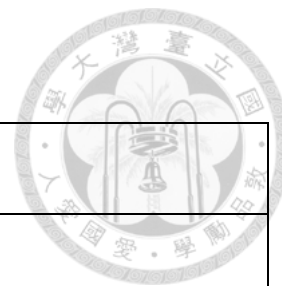
Rose bengal (RB)	Acros
Acid fuschin (ACF)	Acros
Brilliant blue (BB)	TCI Co. ltd
SAFRANIN O.	Acros

Table 3. 2 Characteristic of dyes
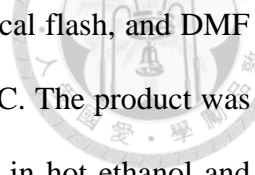
Dyes	Mw (g/mol)	wavelength (nm)
Rose bengal (RB)	1017	544
Acid fuschin (ACF)	585.53	551.5
Brilliant blue (BB)	825.97	587
SAFRANIN O.	350.85	520

3.2 Experiment

3.2.1 Synthesis of MIL-101 particles

(i)   Original method

The synthesis of MIL-101 nanoparticles was prepared according to method of the Ferey 's group [54]. Firstly, 0.4g (1mmol) of $Cr(NO_3)_3.9H_2O$ was dissolved in 2 ml of deionized water and 0.1667 g of H_2BDC was distributed in 3 g of deionized water. Then, these two solutions were mixed together at room temperature for 10 minutes after adding 0.1 ml HF. Mixture of two reactants was transferred into Teflon-lined stainless steel reactor and sealed. The reactor was placed inside a hot air oven at 220°C and held for 8h. After reaction time, the reactor was cooled down to room temperature. In order to remove the unreacted H_2BDC out of the fine green powder MIL-101 as main

56

products, the mother solution was completely transferred into a conical flash, and DMF was added incrementally with continuous shaking to dissolve H_2BDC. The product was dried at 120^oC overnight. Then, MIL-101 particles were immerged in hot ethanol and placed in an oven at 70^oC for 20h. After cooling, the resulting product was double filtered by glass filter and washed with mixture of ethanol and H_2O with ratio 95:5 wt%. The final product was dried at 120^oC overnight.

(ii)   Effect of additives

MIL-101 was prepared follow Ferey's process. Other additives as CH_3COOH, NaOH and free-additive were used instead of HF to promote the growth of MIL-101 crystal. All of ratio of reactants and post treatments were keeps as similar to previous experiments.

3.3 Characterization of MIL-101 and MIL-101 membrane

3.2.2 Synthesis MIL-101 membranes

(i)   In-situ method assisted by acid modulator

The precursor solution was prepared by mixing the reactants concluding of $Cr(NO_3)_3$, H_2BDC and H_2O. The amount of $Cr(NO_3)_3$, H_2BDC and water were changed follow these ratio 0.5 mmol – 0.5 mmol – 10 ml H_2O, 1 mmol – 1 mmol – 10 ml H_2O and 1mmol – 1 mmol – 5 ml H_2O, respectively. After that, additives as 0.1 ml of NaOH, CH_3COOH, HF or free-additive was added into precursor solutions and then a mixture was poured into Teflon auto clave. A ceramic membrane was horizontally placed in Teflon autoclave and synthesis reaction was take place at 220^oC for 8h. After reaction, the ceramic membrane was cooled to room temperature and wash with hot ethanol
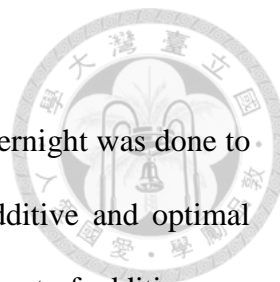
(70°C) overnight. Then, drying at 120°C under vacuum condition overnight was done to active the MIL-101 membranes. Subsequently, finding the best additive and optimal volume of additive were essential steps and need to survey. The amount of additive was varied from 0.1 ml to 1.2 ml to get the appreciate value.

(ii)   Defect healing step

The precursor solution was prepared by mixing the reactants concluding of $Cr(NO_3)_3$, H_2BDC and H_2O. The amount of $Cr(NO_3)_3$, H_2BDC and water were investigated like to prior experiment. The amount and kind of additive was an optimal result collected from in-situ step. The in-situ prepared ceramic membrane was horizontally placed in Teflon autoclave and synthesis reaction was carried out at 220°C for 8h. After reaction, ceramic membrane was cooled to room temperature and wash with hot ethanol overnight. Beside, effect of concentrations of reactants to defect healing procedure also was surveyed by changing the amount of reactants as in-situ process.

(iii)   Layer by layer seeding method

In a typical synthesis, 0.4 g of $Cr(NO_3)_3$ was dissolved in 20 ml of H_2O (solution A), and 0.1667 g of terephthalic acid was dissolved in 5 ml of H_2O (solution B). The ceramic membrane was soaked in the solution A for 30 min under vacuum condition. The disk saturated with the chromium salt solution was positioned horizontally in a Teflon-lined autoclave containing the solution B. Then, the autoclave was subjected to solvothermal synthesis for 8h at 220 °C. After seeding steps, the seeded membrane was cooled to room temperature and washed simply with water. Then, the membrane was transferred into autoclave containing 0.4g $Cr(NO_3)$ and 0.1667g H_2BDC in 5ml H_2O to
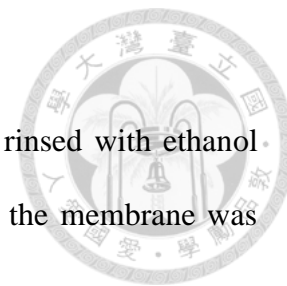
take place 2nd growth. After synthesis, the membrane sample was rinsed with ethanol several times and immersed in ethanol at 70°C overnight. Finally, the membrane was dried at 120°C overnight to collect the final product.

(iv) Hydrothermal seeding method

MIL-101 seed crystals were synthesized follow the previous procedure and CH_3COOH was used as additive. In a typical synthesis, 0.4g of $Cr(NO_3)_3$ was dissolved in 2.5 ml of DI water and 0.1667 g of terephthalic acid in 2.5 ml of DI water. Both solutions were mixed and stirred for about 10 min. The precursor solution was then poured in a Teflon-lined autoclave and heated at 220°C for 8h in a convective oven. The autoclave was naturally cooled down to room temperature. The resulting solution containing MIL-101 crystals (solution C) was stored for seeding. Prior to seeding, the bare a-alumina supports were heated in a convective oven at 80°C for 15 min. While the supports were still inside the oven, the solution C containing MIL-101 crystals, un-reacted ligands and chromium species was dropped using a disposable pipette on the surface of the hot supports until the support surface was completely covered. To make sure the solvent evaporated completely, the supports were kept inside the oven for about 15 min. This ''thermal seeding'' process was repeated three times to completely cover the support surface with seed crystals. The seeded supports were then thoroughly washed with a copious amount of ethanol to remove crystals loosely attached to the supports. The entire process (i.e., three times dropping of the solution C and washing and sonication) was repeated until the supports were uniformly coated with MIL-101 crystals.

3.3.1 Field-emission scanning electron microscope (FESEM)

The morphology of the samples was observed by FESEM (Novaᴛᴍ NanoSEM). The MIL-101 nanoparticles and the top surfaces of membranes were stick onto carbon conductive tape. The clear cross-section of the membranes was made by bending the membranes and not cut by knife or scissors. Before observation, all of the samples were kept vacuum condition for 15 minutes and subjected to Pt coating for 120 seconds by sputter at a current of 20 mA. The element distribution in a membrane was analyzed by elemental mapping.

3.3.2 X-ray diffracatometer for particles (XRD)

Wide-angle patterns of powder X-ray diffraction were measured on Rigaku Ultima IV with Cu Kα radiation (λ=1.5418 Å) to check the crystalline. All of the setting conditions are listed in Table 3-4.

Table 3. 3 The setting conditions of XRD powder

X-ray	Cu Kα
Wavelength（λ）	1.5418 Å
Voltage	40kV
Current	40mA
Angle range（2θ）	3º-20º
Scanning per step	0.02º/step
Scanning rate	20º/min

60

3.3.3 X-ray diffractometer for thin film(XRD)

Wide-angle patterns of membrane X-ray diffraction (XPert) were measured on XPERT with Cu Kα radiation (λ=1.5418 Å) to check the crystalline. All of the setting conditions are listed in Table 3-5.

Table 3. 4 The setting conditions of XRD thin film

X-ray	Cu Kα
Wavelength (λ)	1.5418 Å
Voltage	45kV
Current	40mA
Angle range （2θ）	5º-40º
Scanning per step	0.02º/step
Scanning rate	20º/min

3.3.4 Specific surface area analyzer

The nitrogen adsorption/desorption isotherm was measured with Micromeritics ASAP2020. The specific surface area was evaluated correspondingly. Samples were dewatered at 100ºC to remove all of the impurities. After cooling to room temperature, samples were kept at 77K during the measurement.

3.3.5 UV/VIS Spectrophotometer

The Cary 300 is a versatile UV-visible spectrophotometer with a versatile set of accessories and a large photometric range for use in research laboratories. The instrument is shipped with liquid sample holders and can be fitted with a wide range of accessories to provide extra capabilities. The wavelength range is between 200-900 nm.

3.4 Nanofiltration performance

The filtration experiments were carried out using a stainless steel dead-end filtration cell described follow below figure with 19.6 cm^2 active membrane area. All the experiments were carried out with a feed solution concentration of solute of 0.01% weight. The solute was distributed well in solution by sonication before pouring into the tank. The feed solution was in the tank and pressurized (feed pressure of 4 bar) with nitrogen to the desired pressure at room temperature. Permeate was collected under atmospheric pressure. The solute was change alternatively with RB, BB, ACF and SFN to build MWCO curve. The stability of MIL-101 membranes was also investigated by using various organic solvent such as DMSO, DMAc, and NMP. Permeance was calculated using Eq.2. The measurement was performed by collecting and weighing samples in closed vials as a function of time.

$$F = \frac{Vp}{A * t * P} \qquad\qquad \text{Eq.2}$$

where, Vp: the permeate volume (l),

      A: the membrane surface area (m^2),

      t: the permeation time (h)

      P: the pressure (bar).

Rejection were defined as in Eq. (3):

$$R\ (\%) = \left(1 - \frac{Cp}{Cf}\right) * 100 \qquad\qquad \text{Eq.3}$$

where, Cf and Cp the solute concentrations in the feed and in permeate, respectively. The dye concentrations were measured by an ultraviolet-visible spectrophotometer at the maximal absorption wavelength of the dye.
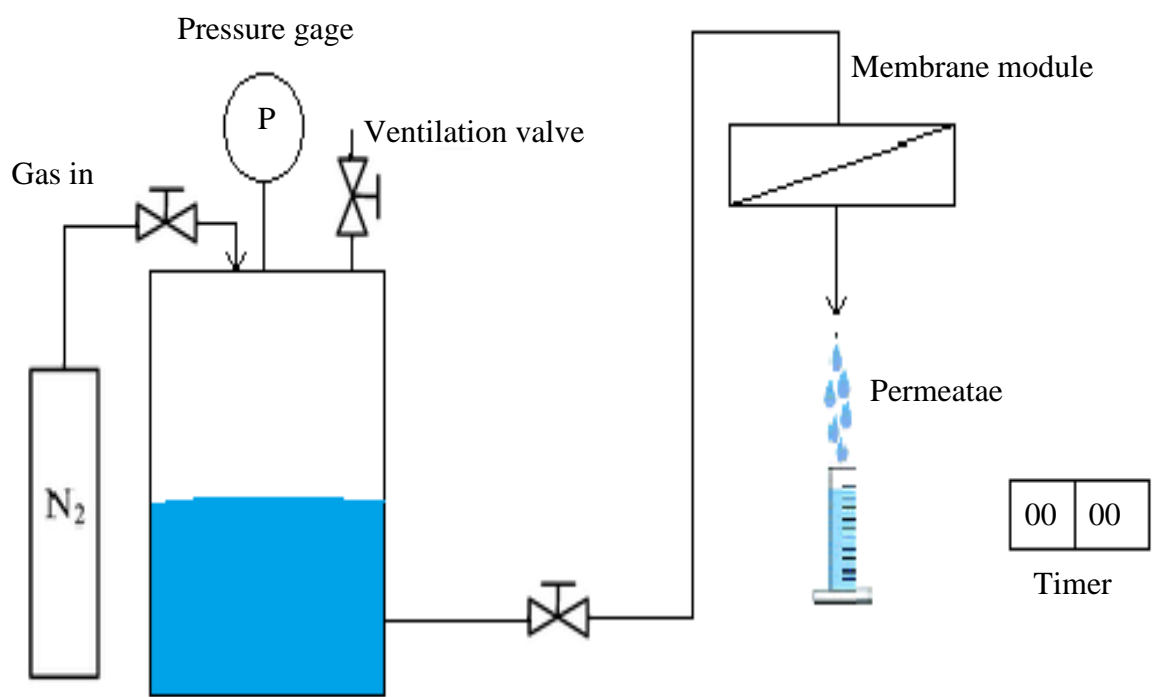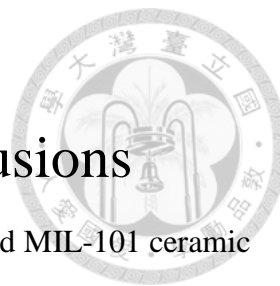
**Figure 3.1** Schematic of nanofiltration testing set-up

Chapter 4 - Results and conclusions

In this section, the characterization of MIL-101 nanoparticles and MIL-101 ceramic membrane will be discussed. Furthermore, we will focus on the effect of the concentration of reactants and amount of acetic acid on the synthesis of MIL-101 membranes. Finally, the OSN performance of the MIL-101 membranes on organic solvents and dyes will be tested.

4.1 Characterization of MIL-101 nanoparticles

The synthetic reaction of MIL-101 was synthesized in water by solvothermal method according to Feréy group [54]. The simple form of this reaction is described below:

$$3Cr(NO_3)_3 \xrightarrow{H2BDC,H2O,HF,8h,220oC} Cr_3F(H_2O)_2O(BDC)_3.nH_2O$$
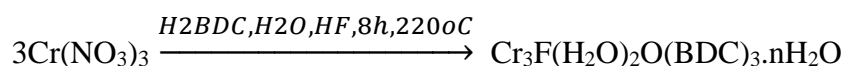
In this work, from reaction mixture of chromium nitrate (0.4g, 1 mmol), benzendicarboxylic acid (0.1667 g, 1 mmol), 0.1 ml of acid fluoric and 5 ml of H_2O, MIL-101 particles are obtained in the form of light green crystals. The yield of the product is 53% based on chromium. The product is stable in air and insoluble in water, and in common solvents such as ethanol, acetone, n-hexane, DMF, NMP and DMSO.

The XRD patterns of MIL-101 particles are shown in Figure 4.1. In Figure 4.1, the XRD of prepared MIL-101 is consistent with the simulated one. Besides, the MIL-101 particles are highly crystallized according the strong peaks in the XRD pattern. The specific of surface area of MIL-101 particles can be measured by BET equation and nitrogen adsorption/desorption isotherm curve is show in Figure 4.2. The specific surface area of MIL-101 particles is about 3132.54 m^2/g and the isotherm curve belongs

to type II adsorption/desorption isotherm curve, which is the behavior of mesoporous

materials. According to literatures, the pore size of MIL-101 nanoparticles is 2.9-3.4 nm

with size of window cage of 1.2-1.6 nm which is suitable for the range of NF [54].
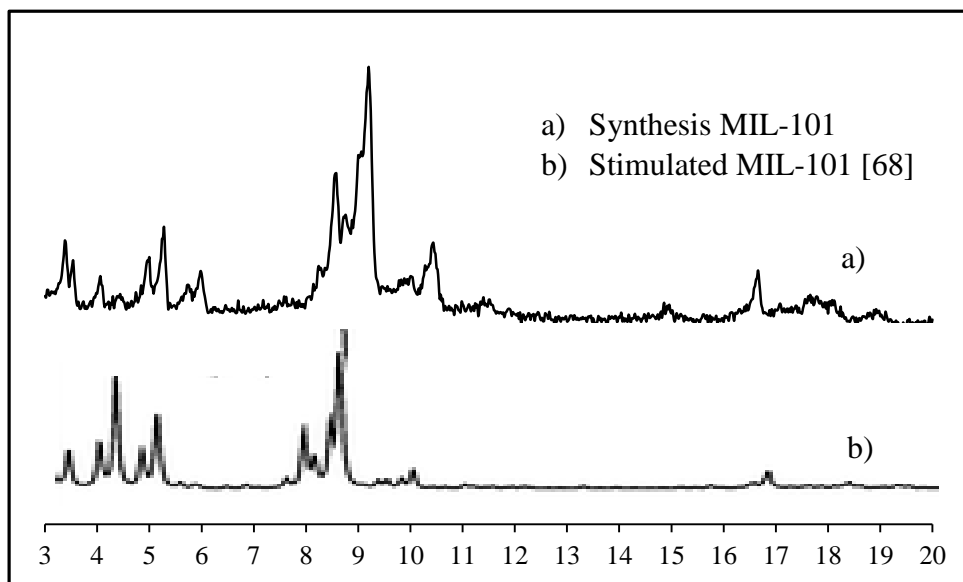
Figure 4. 1 XRD patterns of MIL-101 nanoparticle
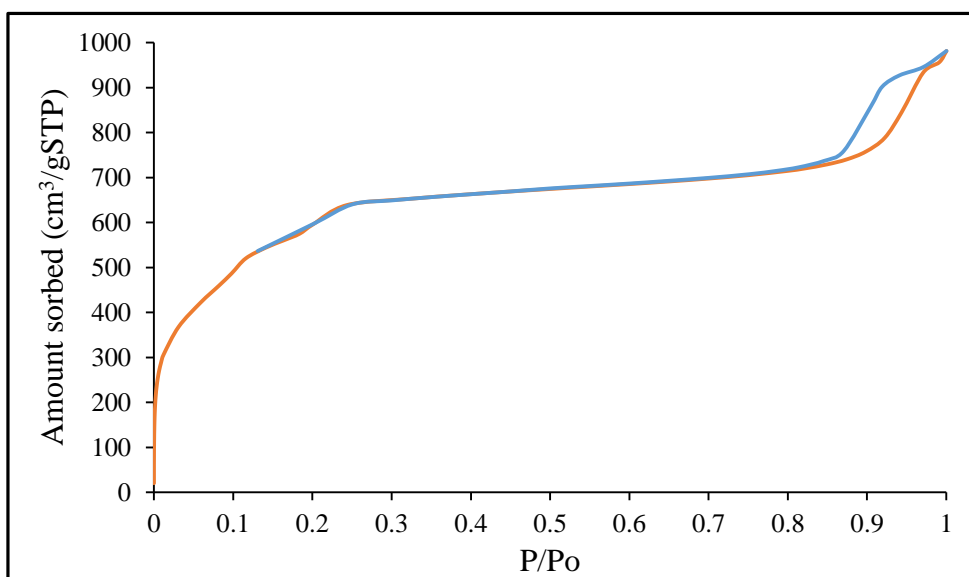
Figure 4. 2 Nitrogen adsorption/desorption isotherm curve of MIL-101 nanoparticles.

65
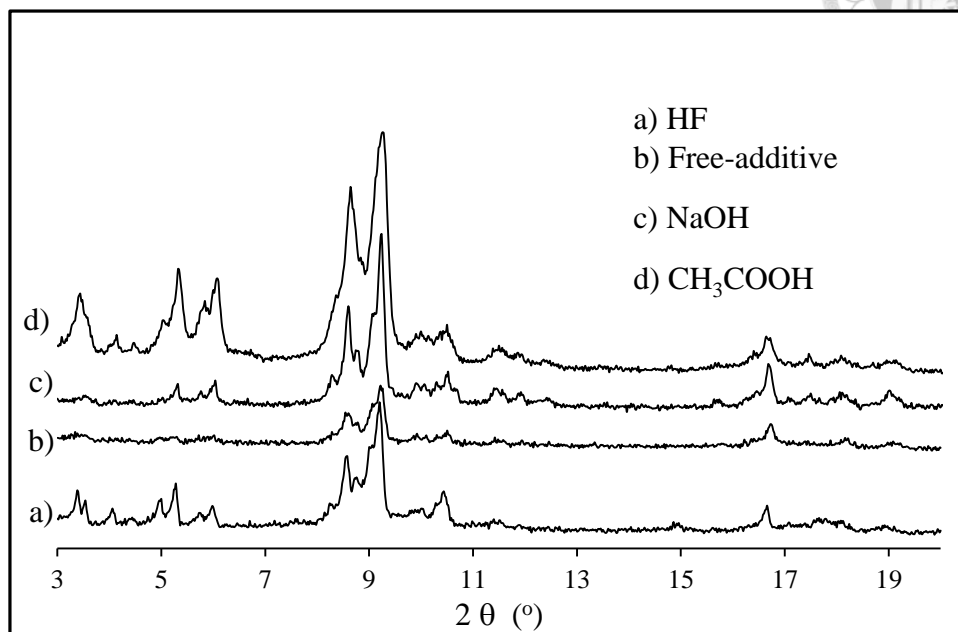
Figure 4. 3 XRD patterns of MIL-101 particle synthesized from different additives

Figure 4.3 shows XRD patterns of MIL-101 particles synthesized from HF (4.3-a), free-HF (4.3-b), NaOH (4.3-c) and CH3COOH (4.3-d) to indicate the effect of additives to crystallization of particles. The XRD patterns of (a) and (b) (Figure 4.3) agree well with literature demonstrating formation of the MIL-101 structure [57]. Liang et at (2013) indicated that the XRD pattern of free-HF prepared MIL-101 lacked the first peak, due to widely-spaced planes likely to disappear if crystallinity was reduced. HF synthesized MIL-101 pattern (Figure 4.4-b) exhibits stronger peaks than (a) and shows the first peak. Both of them show the good crystallinity of MIL-101.
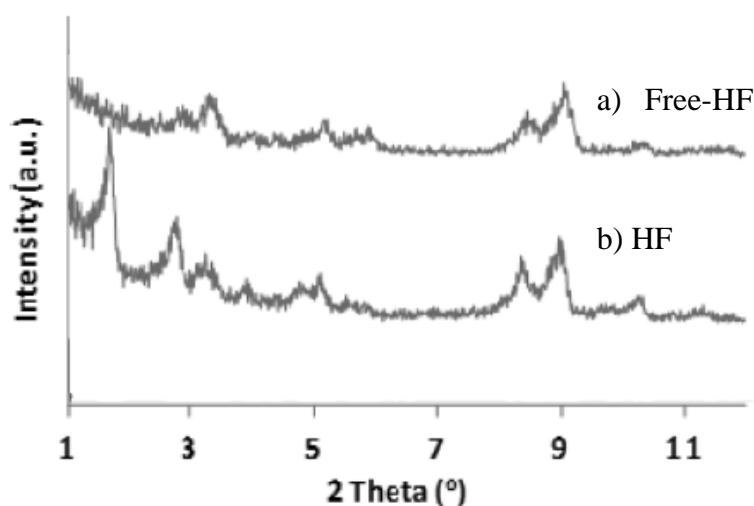
Figure 4. 4 Powder XRD patterns of free HF and HF synthesis MIL-101 [57]

Besides, NaOH is selected as additive follow the procedure of Khan's group because control pH by NaOH could lead to increase selectivity to MIL-101 than MIL-53 [149]. And MIL-101 gets a high yield at higher pH around 3.5. XRD pattern of MIL-101 assisted with NaOH shows the same shape and peak position with that of free-additive synthesized MIL-101, and it illustrates the stronger and sharper peak than (b) pattern in Figure 4.3. Even though it is not easy to explain the effect of pH on the synthesis of Cr-BDCs, it can be noted that a chromium trimer or super tetrahedron (ST) is necessary to build up the MIL-101 structure [54]. Furthermore, CH_3COOH is chosen as additive according to the way of Zhao et al. [61]. Follow the collected result, the XRD pattern of prepared MIL-101 particles assisted by CH_3COOH exhibits the sharp peaks appeared at 3°, 5° and 9°; and indicates higher crystalline of MIL-101 than the others by strong signals. Moreover, acetic acid could reduce the synthesis temperature without significant influence on the porosity of the material, and it's essential for viewpoint of energy and setup costs [61]. Overall, acetic acid as additive shows the best crystalline of MIL-101 and it is efficient modifier for preparation of MIL-101.

67

4.2 Characterization of MIL-101 membranes

4.2.1 Effect of additives
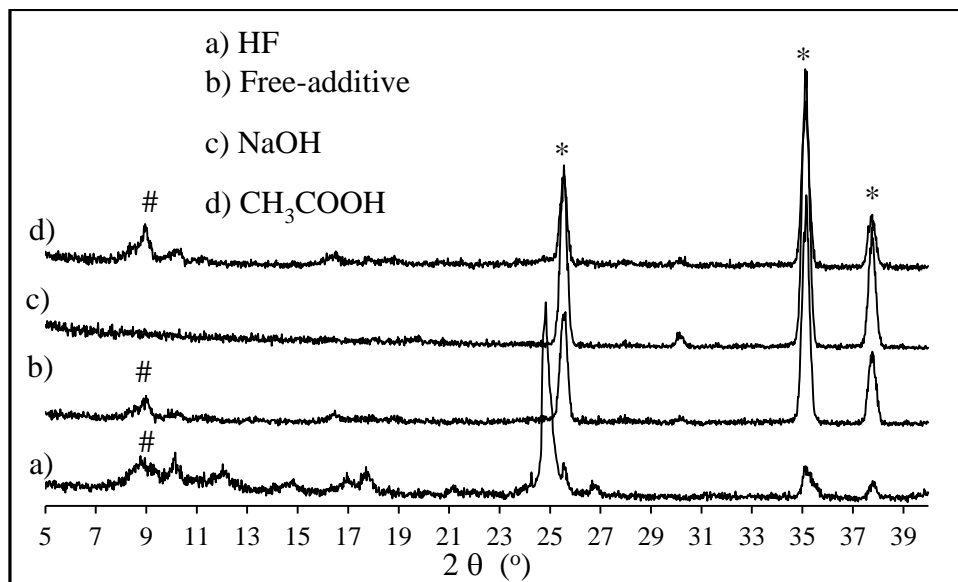
Figure 4. 5 XRD patterns of MIL-101 membranes synthesized from different additives

(* peak of alumina, # peak of MIL-101)

The XRD patterns of the MIL-101 membranes prepared from different additives are shown in Figure 4.5 to determine the crystalline structure of MIL-101 nanoparticles and ceramic membranes. All of XRD patterns in Figure 4.5 show three peaks of ceramic membrane at 25.5^o, 35° and 38° as signals of alumina oxide. Low peaks of XRD patterns at around $9-10^o$ are matched with MIL-101 particles as shown in Figure 4.1. The intensities of MIL-101 signals are much weaker than those of ceramic membrane because MIL-101 is embedded into the top layer of ceramic membrane instead of cover on the top side, and MIL-101 layer is very thin compare to ceramic layer. This will be demonstrated through cross-section images. Because of weak MIL-101 signals on ceramic membrane, next XRD patterns are spread from $5-14^o$ to observe clearly the signal of MIL-101. It can also be observed that use HF as additive would damage the

68
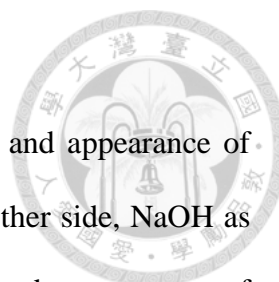
substrate by decreasing significantly signals of ceramic membrane and appearance of high peak at 25° because of reaction between HF and Al_2O_3. In another side, NaOH as additive could not graft the MIL-101 particles on ceramic membrane by no present of MIL-101 signals. It can be explained that NaOH increase the solubility of H_2BDC in solution, that leads to increase the homogeneous reaction rate and MIL-101 particles prefer to grow in bulk solution to the surface of substrate. Synthesized MIL-101 without additive could form MIL-101 on ceramic membrane, yet the signal is lower than that of prepared MIL-101 assisted by acetic acid. Therefore, XRD patterns in Figure 4.5 provide the evidence of MIL-101 grafted successfully in ceramic membrane by use of acetic acid as additive.

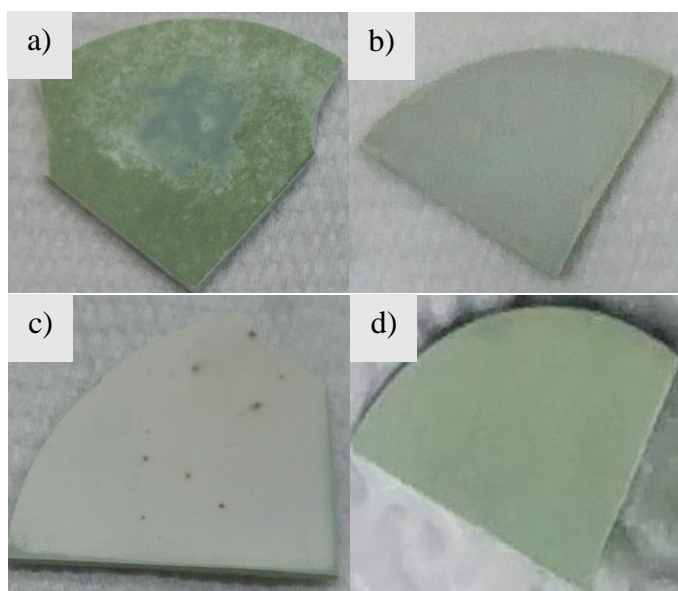**Figure 4. 6** Digital photos of MIL-101 membranes synthesized from different additives

(a) - HF, (b) – free additive, (c) - NaOH, (d) - CH_3COOH

Distribution of MIL-101 could be observed through digital photos shown in Figure 4.6. A dark green and dissimilarity color derived from chromium salts is displayed on the ceramic membrane using HF as additive in Figure 4.6-a. On using free-additive,

only very poor coverage with MIL-101(Cr) is observed, as determined by the pale green color of the plates follow the Figure 4.6-b. Only a very pale green color is exhibited on the ceramic substrate by support of NaOH follow the Figure 4.6-c, suggesting that the MIL-101particles does not form on ceramic membrane. Finally, Figure 4.6-d shows the uniform green color of MIL-101, and it indicates the well distribution of MIL-101 particles in ceramic membrane.
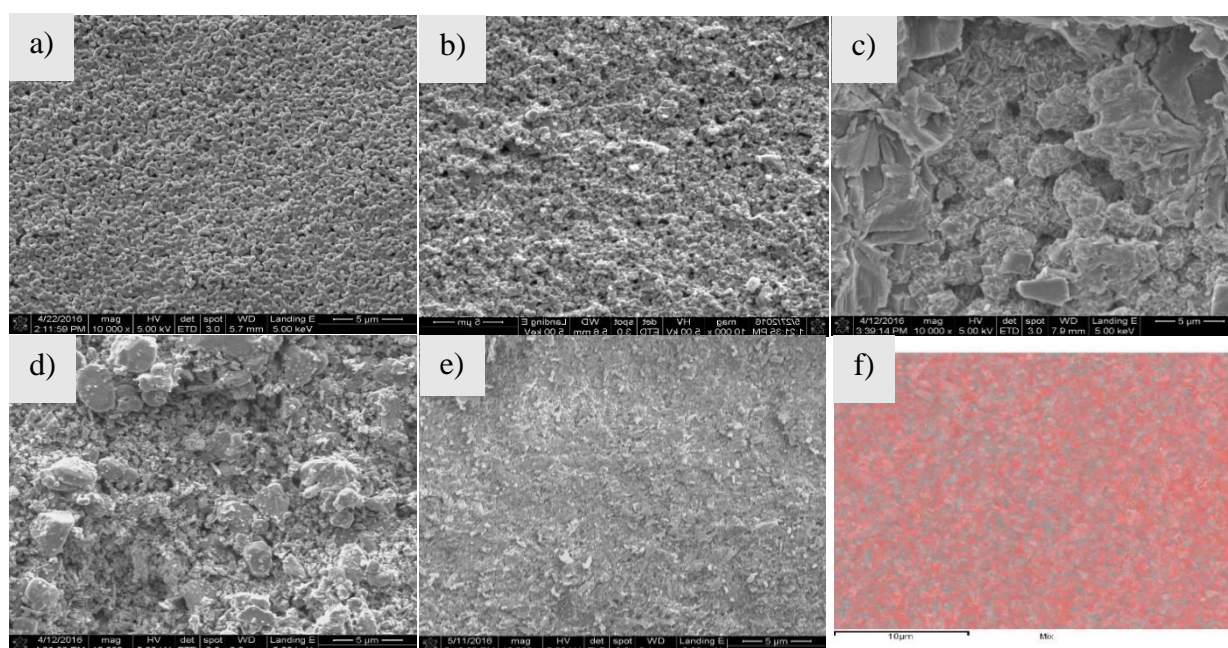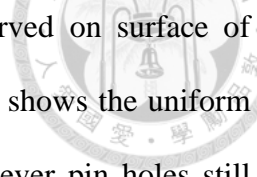
Figure 4.7 SEM of top surface of MIL-101 membranes synthesized from different additives (a)-bare ceramic membrane; (b)-free-additive; (c)-HF; (d)-NaOH; (e)-CH$_3$COOH, (f)-elemental mapping

The morphology of in-situ membranes prepared from various additives and bare ceramic membrane has been observed through SEM images. From the top view, pin holes are appeared on MIL-101 membrane without using additives showed in Figure 4.7-b. The morphology of MIL-101 membrane in Figure 4.7-b is not different from the bare ceramic membrane, and it proves that there is less coverage of MIL-101 on ceramic

substrate. In the Figure 4.7-c/d, unknown large crystals are observed on surface of ceramic membrane with a lot of pin holes and defects. Figure 4.7-e shows the uniform distribution of MIL-101 nanoparticles on ceramic membrane, however pin holes still exit on the top side of membranes. Jiang et at demonstrated that nanoparticles of MIL-101 (Cr) can be prepared hydrothermally and their particle size can be adjusted through judicious choice of a monocarboxylic acid modulator [150]. Therefore, acetic acid as a simple monocarboxylic could control the size of MIL-101 particles in nano-size and make MIL-101 size fit closely into the 200nm pore of ceramic membrane. Due to the lack chemical bonding between MIL-101 particles and substrate, MIL-101 is embedded and fastened into the pore of ceramic; forming a physical attach with inorganic material is an appreciate way to generate MIL-101 membrane. By this way, the MIL-101 layer could be stable under high pressure of nanofiltration experiment because of reinforcement of ceramic framework. Besides, generation a dense and uniform MIL-101 on ceramic membrane need to be improved and discussed more in the later section. Because the coordination element of MIL-101 is chromium, from the chromium elemental mapping, the uniform distribution of MIL-101 on ceramic membranes can also be observed.

4.2.2 Effect of concentration of reactants on in situ method

Figure 4.8 shows the XRD patterns for MIL-101 membranes synthesized from different concentration of reactants with ratio of $Cr(NO_3)_3$-H_2BDC-H_2O (mmol) as 0.5-0.5-555 (10ml) (a); 1-1-555mmol (10ml) (b); 1-1-277 (5ml) (c); respectively. MIL-101 membrane could not form in diluted solution with no present of peak MIL-101 in Figure 4.8-a. As shown in Figure 4.8-b, the XRD pattern is similar to stimulated MIL-101 in

71
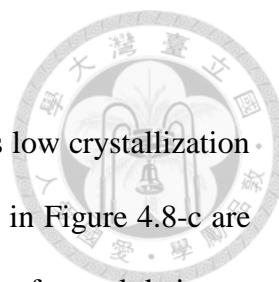
term of peaks position, however, peaks are not quite sharp as well as low crystallization of MIL-101. In the case of concentrated solution, peaks of MIL-101 in Figure 4.8-c are sharper than that of in Figure 4.8-b. Besides, there is an appearance of a peak being at 10.2º as a peak position of MIL-53 and the effect of acetic acid to generation of mixture MIL-53 and MIL-101 will be discussed later.
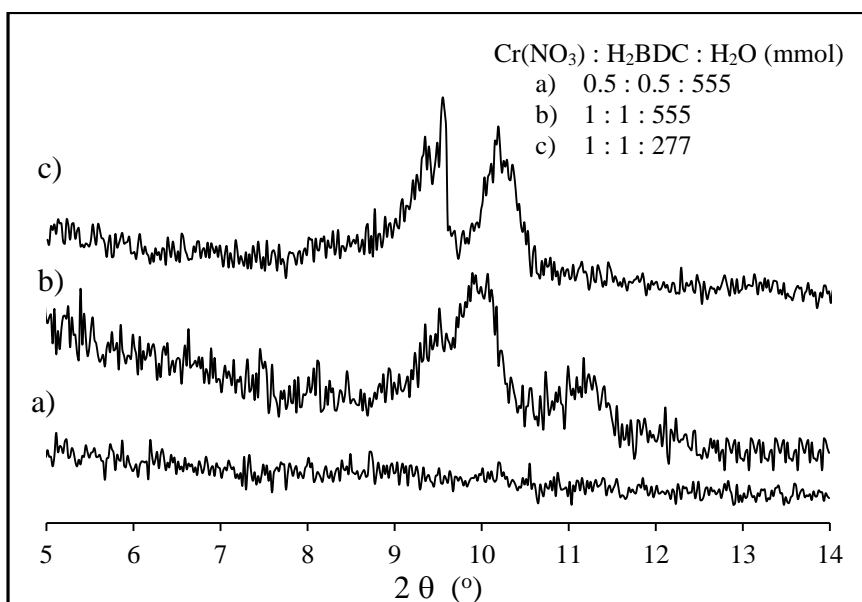

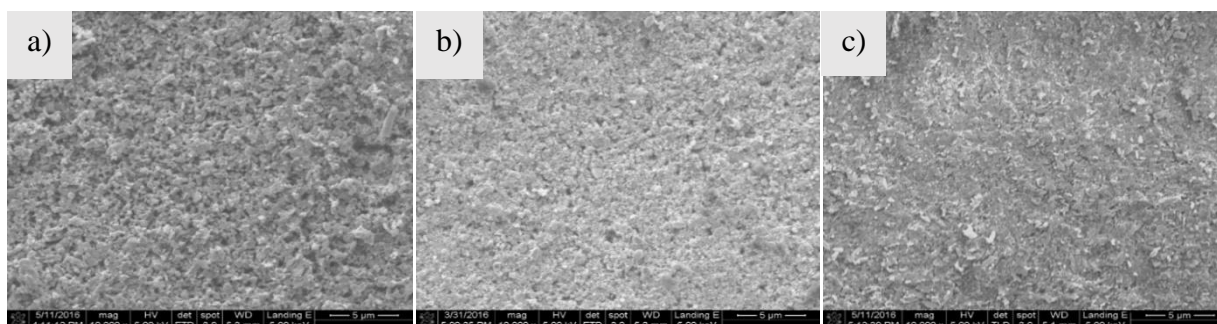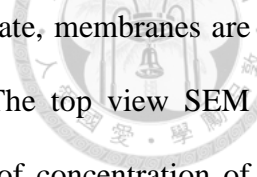**Figure 4.8** XRD patterns of MIL-101 membranes synthesized from different concentration

Figure 4. 9 SEM of MIL-101 membranes synthesized from different concentration Ratio of $Cr(NO_3)_3 : H_2BDC : H_2O$ (mmol) as (a) 0.5 : 0.5 : 555 , (b) 1 : 1 : 555, (c) 1 : 1 : 277

72

To compare the coverage of MIL-101 on top of ceramic substrate, membranes are thoroughly inspected by using SEM images follow Figure 4.9. The top view SEM images show that coverage of MIL-101 rises follow the increase of concentration of reactants. The concentration is limited in this range because MIL-101 and MIL-53 are selectively obtained when the H_2O/Cr molar ratio is greater than or equal to 500 and less than or equal to 200, respectively [149]. Results in my experiments are consistent with results reported by Xu et al. about the preparation of ZIF-8 membrane from a concentrated synthesis gel [151]. They indicated that the concentrated gel is very viscous and easily deposited on the surface of substrate; during solvothermal treatment, ZIF-8 nucleation and growth occur rapidly in the concentrated gel, leading to intergrowth of the crystals. On the other hand, Jiang et al proved that acetic acid acts an important role in reaction with high concentration of reactants. Because, high concentrations of metal ions and ligands required to form the films are not compatible with nanoparticle formation. It has, however, been reported that the MOF nanoparticles can be formed by supplying chemical additives such as monocarboxylic acids or functional polymers into the reaction mixture [150, 152]. By this method, high concentrations of MOF nanoparticles could be induced, in situ, on the surface of the support during the synthesis of the MOF membranes. Moreover, synthesis MIL-101 nanoparticles aided by acetic acid on the support is a simple method without complex pre-modifications of the support or using the alkaline solvent to control the size of MIL-101.

73

4.2.3 Effect of amount of acetic acid

Figure 4.10 show the XRD patterns of MIL-101 membrane synthesized from different from 0.1 ml (a), 0.4 ml (b), 0.8ml (c) and 1.2 ml (d) of acetic acid, respectively. In Figure a-b-c, the XRD patterns of MIL-101 membrane prepared with volume of acetic acid under 1.2 ml match well with stimulated XRD patterns in spite of a little shift in peak position, but no significant. The signal of peak at 10.2^o decrease when increase the amount of acetic acid and it could be explained that acetic acid could effect to the yield of Cr-BDC (MIL-53 or MIL-101).
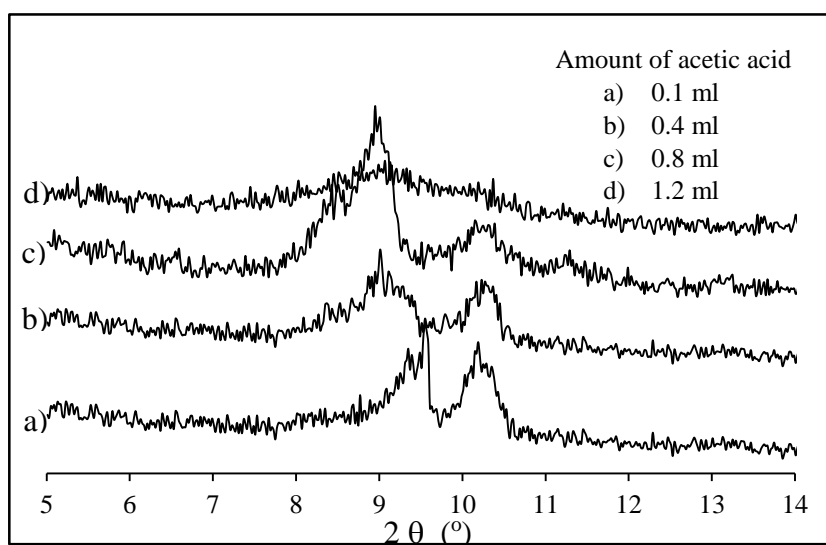
Figure 4. 10 XRD patterns of MIL-101 membranes synthesized from different amount of acetic acid

There are no papers proving this effect, yet the result of Khan's groups showed effect of water content to yield of Cr-BDC that had the same trend with our result as shown in Figure 4.11 [149]. More particular, the peak at around 10.5^o decrease with increasing yield of MIL-101 and decreasing of formation of MIL-53. Nevertheless, XRD pattern of MIL-101 membrane synthesized from 1.2 ml of acetic acid does not show the peak of

MIL-101 crystal due to the low solubility of H₂BDC in high acidic media that results in no reaction between chromium salts and acid benzene dicarboxylic.
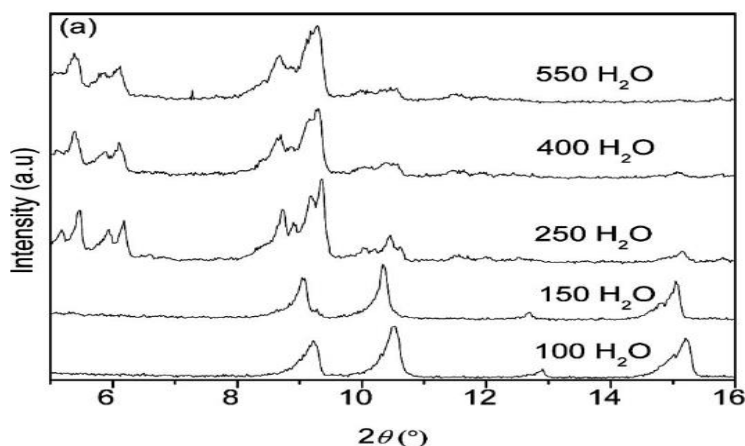
Figure 4. 11 XRD patterns of the Cr-BDCs depending on the water concentration [149].

SEM images of MIL-101 grown on an alumina support using different amount of acetic acid from 0.1 to 1.2 ml are shown in Figure 4.12, respectively. The MIL-101 particles are evenly distributed on the surface of support and the membrane surface is homogeneous and free of defect when increase the volume of acetic acid from 0.1 to 0.8 ml. Moreover, the crystal of H₂BDC is observed clearly in Figure 4.12-c by using 1.2 ml of acetic acid and it agrees well with XRD pattern of MIL-101 with no generation of MIL-101 crystal. Cross-section SEM images in Figure 4.13 show the membranes are well intergrow with a uniform distribution of MIL-101 in 200nm pore size layer of ceramic membrane when using 0.1-0.8 ml of acetic acid. The dense and compact layer of MIL-101 could be observed obviously in the top side when increase the amount of acetic acid from 0.1 ml to 0.8 ml. Besides, MIL-101 particles are distributed in the 2.5 μm pore size of ceramic membrane when use under 0.8 ml of acetic acid. Moreover, element mapping by EDXS of cross section reveals distribute well of MIL-101 in the top layer and have a clear boundary with the substrate at 0.8 ml of acetic acid.
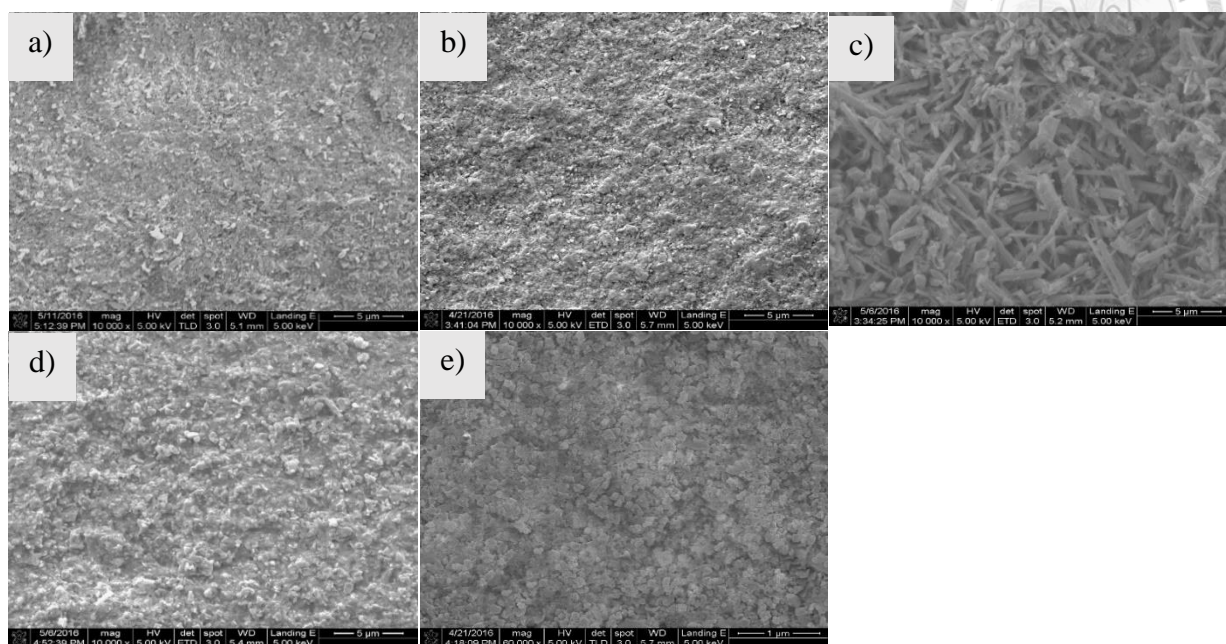
Figure 4. 12 SEM of MIL-101 membranes synthesized from different amount of acetic

acid (a) - 0.1 ml, (b) - 0.4 ml, (c) - 1.2 ml, (d)-(e)- 0.8 ml
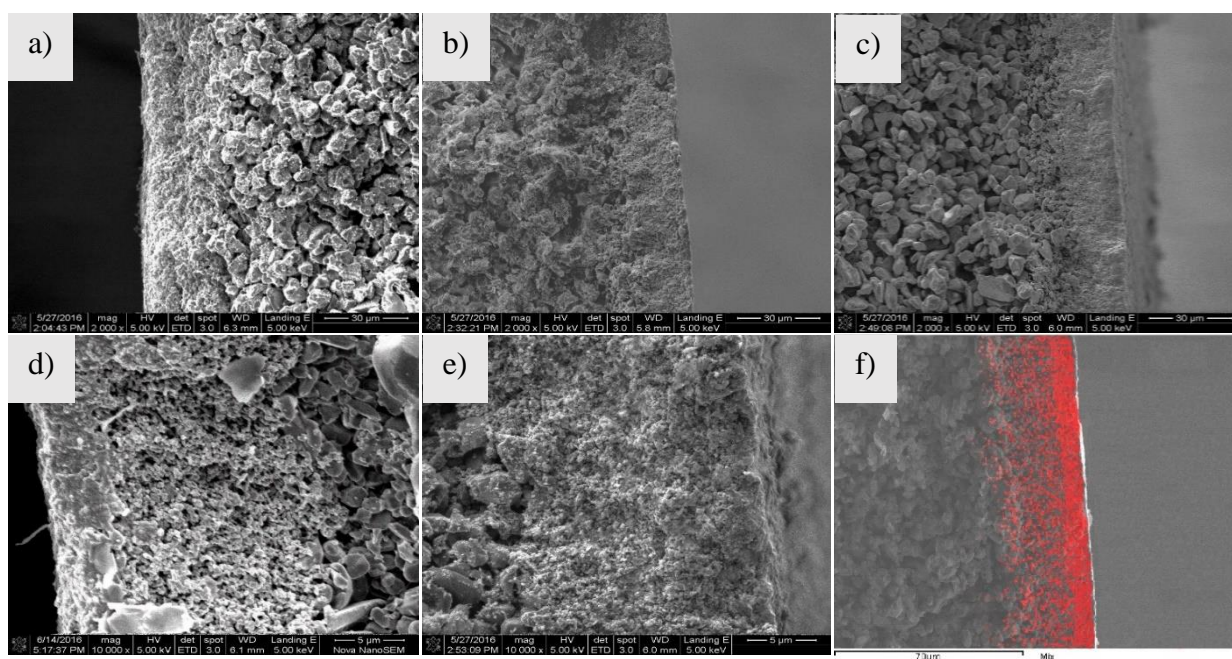
Figure 4. 13 SEM of cross section of MIL-101 membranes prepared from various

amount of CH_3COOH: (a)-0.1 ml, (b)-0.4 ml, (c)-(e)-(f)-0.8 ml, (d)-ceramic membrane

76
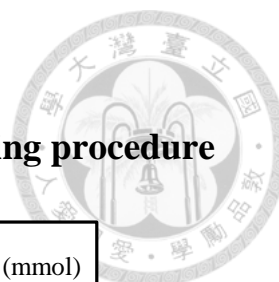
4.2.4 Effect of concentration of reactants in defect healing procedure
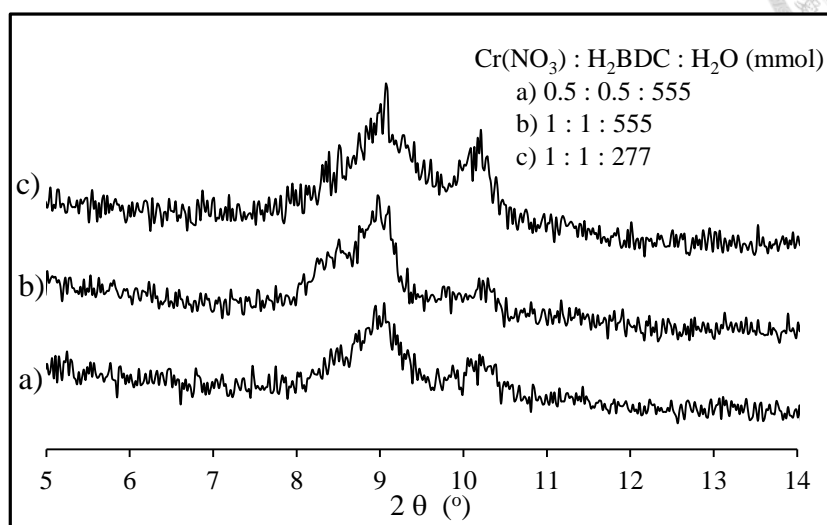
Figure 4. 14 XRD patterns of MIL-101 membranes synthesized from different concentration in defect healing procedure
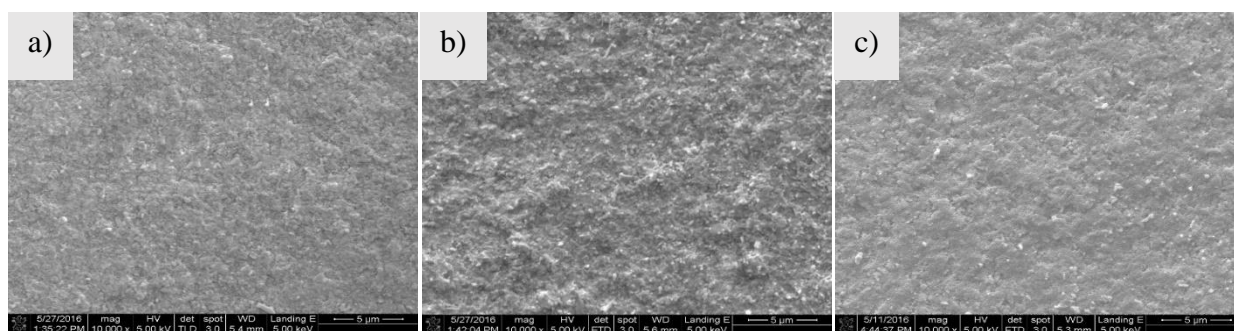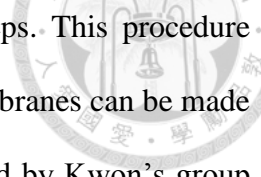
Figure 4. 15 SEM of MIL-101 membranes synthesized from different concentration in defect healing procedure. Ratio of $Cr(NO_3)_3 : H_2BDC : H_2O$ (mmol) as 0.5 : 0.5 : 555 (a), 1 : 1 : 555 (b), 1 : 1 : 277 (c)

By comparing the XRD patterns and surface morphology of MIL-101 membranes obtained from defect healing procedure with different concentration of reactants as shown in Figure 4.14-15, it is evident that there is no significant change belong them. In more detail, the MIL-101 particles do not grow as heterogeneous nucleation on the

77

substrate in the secondary growth from MIL-101 layer in-situ steps. This procedure plays a role as healing defective step and the poorly intergrown membranes can be made into well intergrown membranes by healing the membranes reported by Kwon's group [103]. However, XRD pattern of MIL-101 membranes in Figure 4.14-c shows the high peak of MIL-53 at 10.2° compared to Figure (a) and (b), it proves that mixture of Cr-BDC as MIL-101 and MIL-53 could be synthesized at high concentration in a long time. Yield of formation MIL-101 particles greatly depends on reaction time, temperature and concentration of reactants, kind of solvents. Remarkably, the overall concentration of the reaction mixture can be a decisive factor for product formation [153]. In the field of metal carboxylate, the combination of linear organic linkers, especially terephthalic acid, with trivalent metal cations such as Al^{3+}, Cr^{3+}, Fe^{3+}, V^{3+}, Sc^{3+}, and In^{3+} under solvothermal synthesis conditions results in the formation of at least eight crystalline phases with very close chemical formulas but different structures: MIL-53 ($M(OH)BDC \cdot guest$), MIL-68 ($M(OH)BDC \cdot guest$), MIL-71 ($M_2(OH)_2F_2BDC \cdot guest$), MIL-85 ($Fe_2O(O_2C\text{-}CH_3)_2BDC \cdot guest$), MIL-88B ($M_3O\text{-}(BDC)_3 \cdot X \cdot guest$), MIL-101 ($Cr_3O(BDC)_3 \cdot X \cdot guest$), $Sc_2(BDC)_3$, and $In_2(OH)_3(BDC)_{1.5}$. Moreover, Carson's groups (2013) surveyed the synthesis parameters to MIL-47(V), MIL-88(V), MIL-101 (V) built by trinuclear transition metal (TM) clusters, and identified the key synthesis parameters that control the formation of those MOFs: temperature, time and pH as show in Figure 4.16. Therefore, MIL-101 is a kinetic product and it is easy to transform into other type of MOFs. That is reason why synthesis condition of MIL-101 membrane need to control thoroughly to ensure the higher yield of MIL-101 than that of other MOFs.
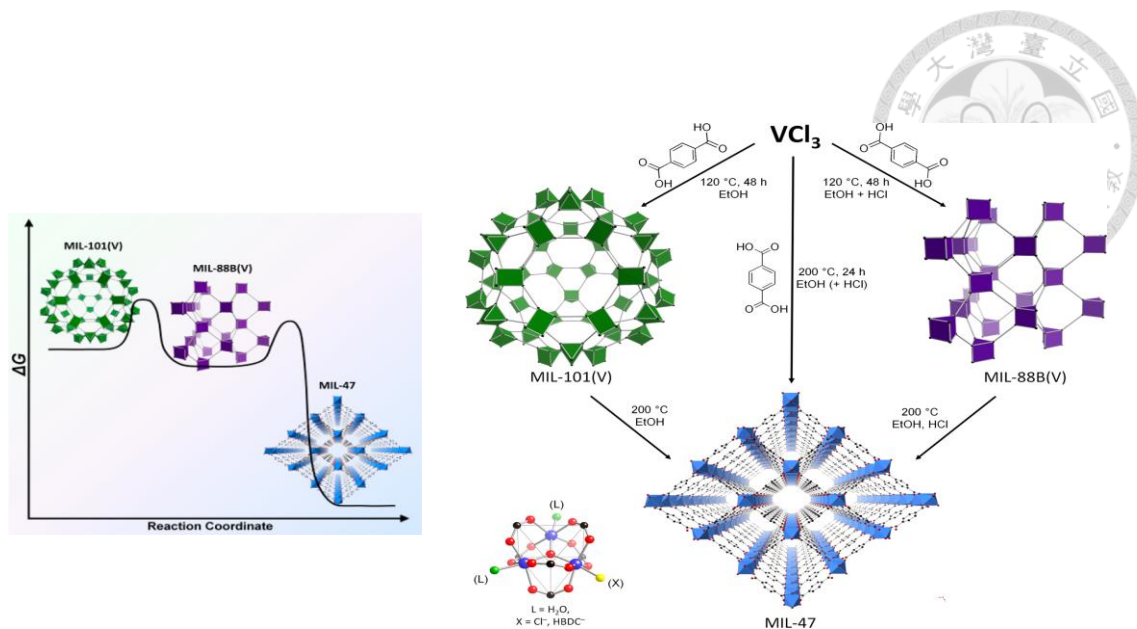
Figure 4. 16 Synthesis scheme for MIL-88B(V), MIL-101(V), and MIL-47

4.2.5 Compare to other methods
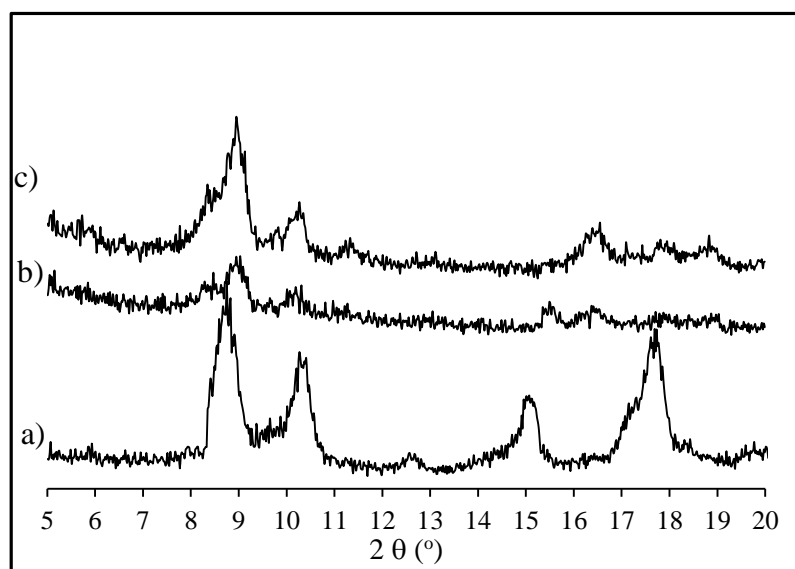
Figure 4. 17 XRD of MIL-101 membranes synthesized from (a) layer by layer seeding method, (b) thermal seeding method and (c) in-situ method assisted by acid modulator

As shown in Figure 4.17-a, XRD pattern of MIL-101 membrane synthesized using layer by layer seeding method indicates high and sharp peaks of MIL-53 and MIL-101 crystal at 8.9 and 10.2°, besides peaks of H_2BDC is observed clearly at 15° and 18°. Through SEM images in Figure 4.18-a, the crystal of H_2BDC exhibited obviously and
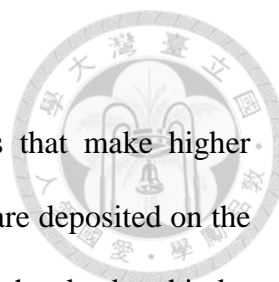
the particles of MIL-101 and MIL-53 attach on H_2BDC crystals that make higher intensity of XRD signals than the others. Because, H_2BDC crystals are deposited on the top side of substrate and seal the pore size of ceramic membrane, that lead to hinder MIL-101 particles embedded into 200nm layer. However, the morphology of MIL-101 membrane from this method is not uniform and have a lot of visible defect.

MIL-101 membrane prepared by thermal seeding method show the low intensity of signal in XRD pattern as Figure 4.17-b. Pin holes and visible defects are observed in SEM images (Figure 4.18-b) that demonstrate this method is not effective way to synthesize MIL-101 membrane. And again, MIL-101 is a kinetic product, so the procedure of synthesis MIL-101 membrane need to make as simple as possible in order to control the formation of MIL-101.
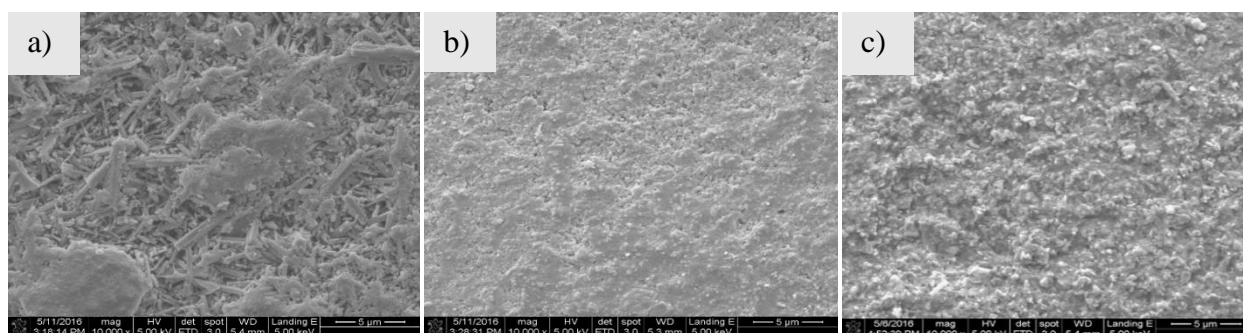
Figure 4. 18 SEM of MIL-101 membranes synthesized from a) layer by layer seeding method, b) thermal seeding method and c) in-situ method assisted by acid modulator

4.3 OSN performance

Although the vast majority of MOF-based hybrid membranes have been tested in gas separation [154], few have been studied for separation by nanofiltration in liquid systems [155]. We evaluated the separation performance of the membrane for the removal of dyes from organic solvent. The effect of introducing the MIL-101 in a ceramic membrane is studied by carrying out OSN experiments. Firstly, MIL-101 membranes synthesized from 1mmol $Cr(NO_3)_3$: 1mmol H_2BDC : 277 mmol H_2O and assisted by 0.8 ml of acid are used to test OSN experiments. Rose Bengal dye as marker in ethanol solvent is used for flux and rejection comparison between bare substrate and MIL-101 membrane. Figure 4.19 and 4.20 clearly shows that ethanol flux of pure ceramic membrane (409 $Lm^{-2}h^{-1}bar^{-1}$) considerably increased compared to that of MIL-101 membrane (1.6 $Lm^{-2}h^{-1}bar^{-1}$). The flux and rejection of bare ceramic membrane are tested for 10 minutes because the flux is very high, and 10 minutes is enough to observe the constant flux. However, the RB retention of these pure ceramic membrane (4-5%) significantly decreases with respect MIL-101 membranes (99.7%), as observed in Figure 4.20-21. Figure 4.21 also shows that MIL-101 membrane is stable within 3 hours through the constant flux and rejection. The excellent compatibility between the ceramic and the MOF particles eliminates the formation of nonselective voids. This result indicates that MOF particles are distributed uniformly in ceramic membrane and MIL-101 membrane could be obtained with no defect.
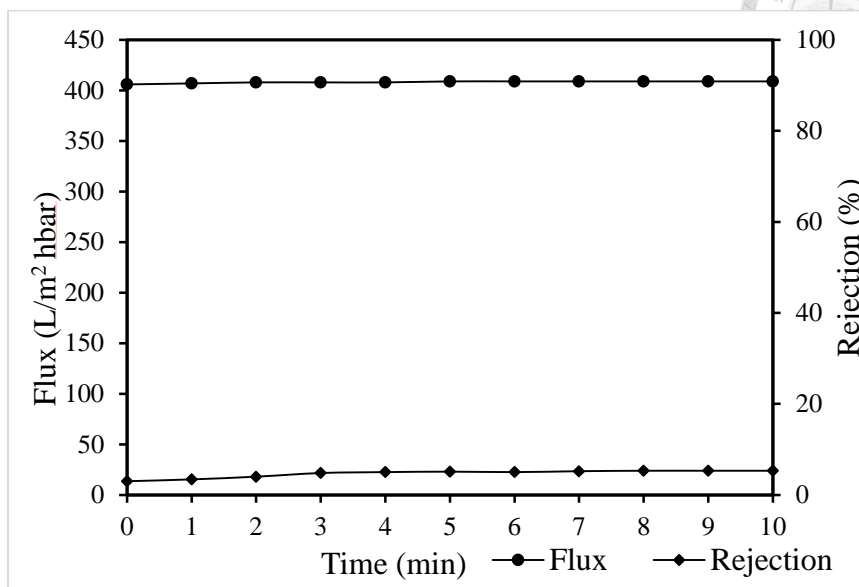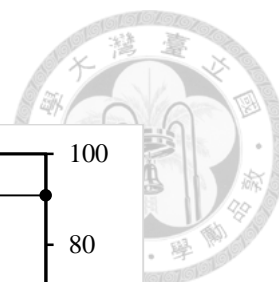
Figure 4. 19 OSN performance of 00.1% RB ethanol solution with pure ceramic substrate
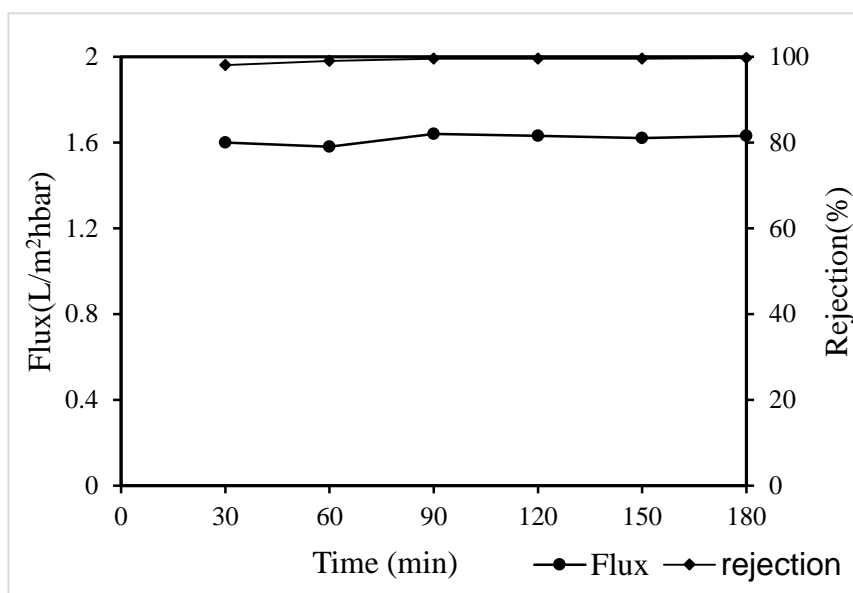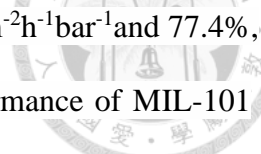
Figure 4. 20 OSN performance of 0.01% RB ethanol solution

The nanofiltration experiments of other dye molecules from ethanol with the MIL-101 membrane are also explored. Figure 4.21 shows a flux of around BB ethanol solution around 1.64 Lm⁻¹h⁻¹bar⁻¹ at 4 bar and rejection about 94.3% after 3 hours. The

82

flux and rejection of ACF ethanol solution is approximately 1.74 $Lm^{-2}h^{-1}bar^{-1}$ and 77.4%, as shown in Figure 4.22. SO ethanol solution is used to test performance of MIL-101 membrane with flux and rejection of 1.75 $Lm^{-2}h^{-1}bar^{-1}$, 14.2% respectively in Figure 2.23. The flux and rejection of all experiment keep constant within 3 hours and achieve equilibrium in this period time. Overall, the flux of dyes ethanol solution keep stable around 1.64-1.75 $Lm^{-2}h^{-1}bar^{-1}$ in Figure 4.24, the results indicate that when the molecular size of the dye decreased, the flux of the membrane increased a little. Because these fluxes are still low, so difference along the fluxes is not significant. Whereas the retention decreased dramatically, thus indicating a different removal profile towards different dyes. In detail, the Safranin (MW 350 g/mol) and Acid Fuschin (MW 585g/mol) are rejected to 14.2% and 77.4%, respectively; and the higher molecular weight dyes Brilliant blue (MW 825 g/mol) and Rose Bengal (MW 1017 g/mol) are rejected over 90%. MWCO of membrane is interpolated from Figure 4.25 and the MWCO value is about 760 g/mol. The hybrid membrane can thus be used in the separation of dye molecules with MWCO higher than 760 g/mol. And the MWCO is equivalent to membrane with pore size of 1.5 nm, that is matched with the window cage of MIL-101 (1.2-1.6 nm) follow the Donnan steric pore-flow model [156]. This indicates that the solution just passes through the pore of MIL-101 material and there are no voids or pin holes that let the solvent passes through.

83
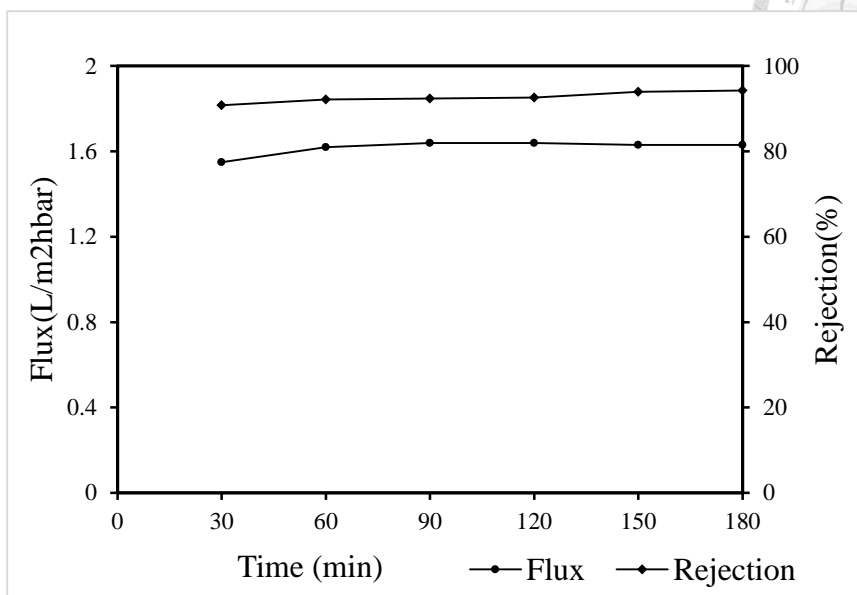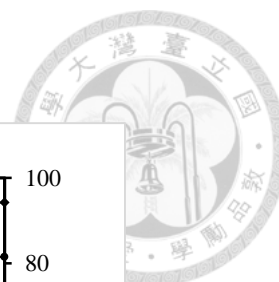
Figure 4. 21 OSN performance of 0.01% BB ethanol solution
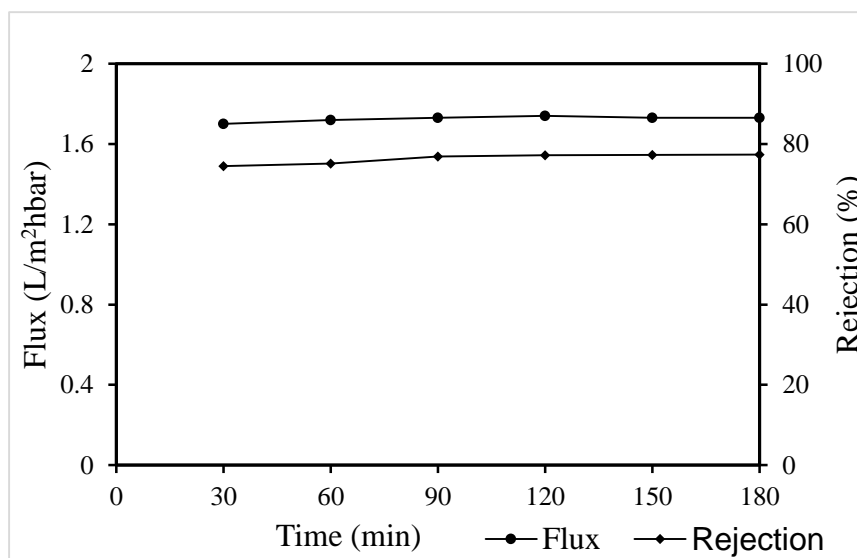
Figure 4. 22 OSN performance of 0.01% ACF ethanol solution

84
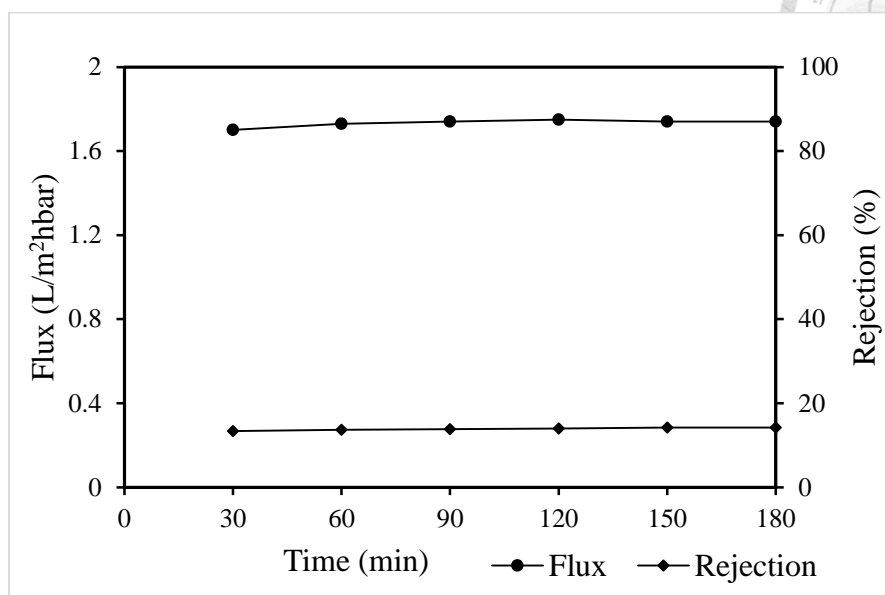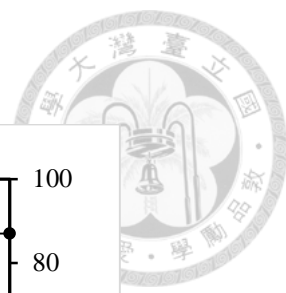
Figure 4. 23 OSN performance of 0.01% SO ethanol solution
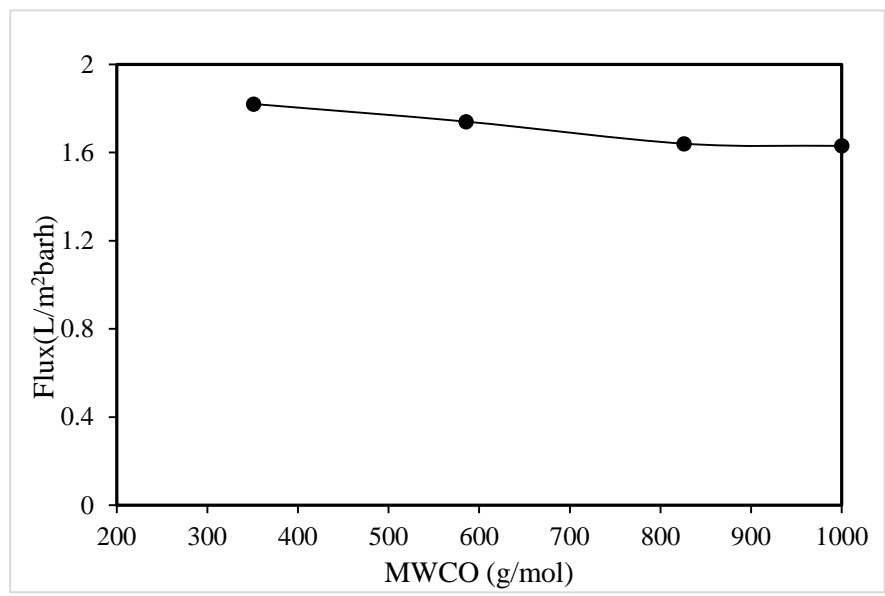
Figure 4. 24 Flux of ethanol solutions with various dyes

85
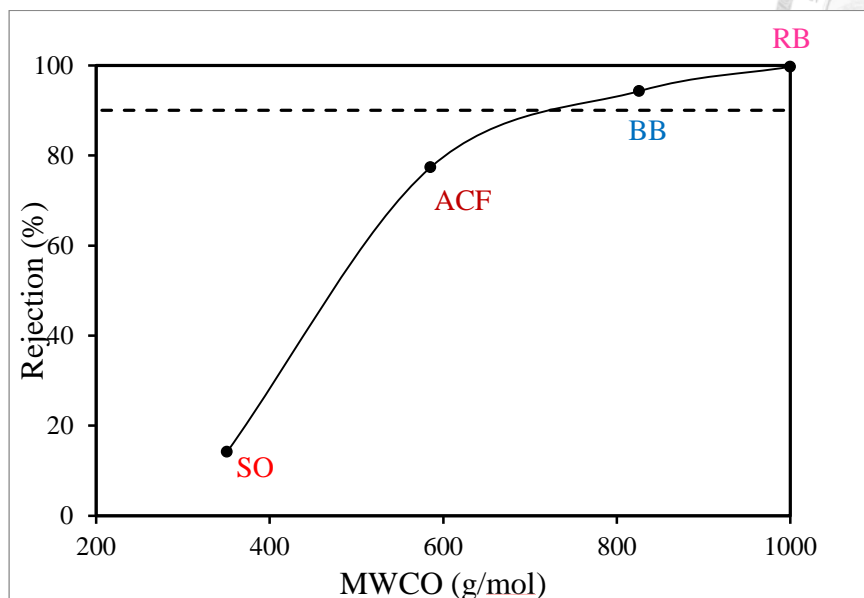
Figure 4. 25 MWCO curve

Rose Bengal dye is used as the markers for stability testing of MIL-101 membrane in harsh solvent like DMSO, DMF, DMAc for OSN. MIL-101 membranes exhibit very good rejections (over 95%) of this dye in the three solvents DMSO, DMF and DMAc as shown in Figure 4.26. Permiabilities of three solvents are around 1.4-1.7 $Lm^{-2}h^{-1}bar^{-1}$ and the small variation in flux may be attributed to the difference of viscosity of these solvents. Stability test demonstrates that MIL-101 membrane can withstand in most of the solvents, that usually dissolve the polymeric membrane, without swelling phenomena. This shows the huge potential of nanosized, highly porousMIL-101 and ceramic substrates to improve the chemical stability of membranes for OSN through provision of inorganic material. Nanofiltration membranes designed for organic solvent applications succeed to maintain their separation performance when exposed to harsh organic solvents. This successful may be observed through high rejection and good flux due to no swelling or dissolution of membrane. Besides, MIL-101 membranes could be a promising material with a simple synthesis method and high performance for OSN.

However, the flux of MIL-101 membrane still low compared to polymeric membrane and need to further study.
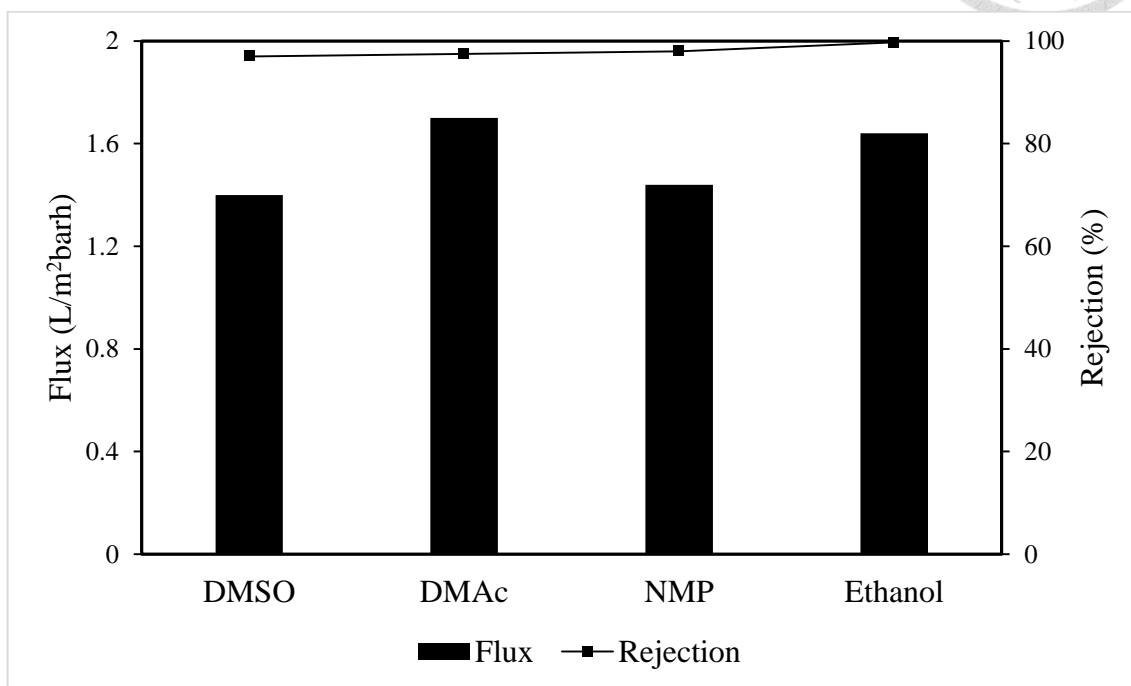
Figure 4. 26 OSN performance with various solvents

Chapter 5 Conclusions
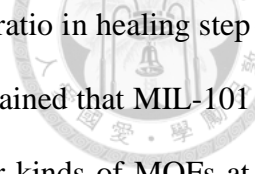
In summary, a MIL-101 membrane applied for organic solvent nanofiltration is successfully synthesized by in-situ assisted acetic acid method, and it shows good permeate flux and rejection for OSN process. The prepared MIL-101 membrane is derived via in-situ method, and defect healing steps. In order to find out the best synthetic condition for free-defect membranes such as: (1) types of additives, (2) $Cr(NO_3)_3/H_2BDC/H_2O$ molar ratio, (3) amount of additive, and (4) molar ratio of reactants in defect healing step are investigated. The results are listed as follows：

NaOH, HF, acetic acid as additive have a significant influence on formation and distribution of MIL-101 on surface of ceramic membrane. Acetic acid is the best additive for generation of MIL-101 membrane because it promotes the grown of MIL-101 and control the particles size that be suitable for close packing of MIL-101 into 200nm ceramic substrate.

$Cr(NO_3)_3/H_2BDC/H_2O$ molar ratio has a great impact on the preparation of MIL-101 layer on the ceramic substrate. The ratio of $Cr(NO_3)_3/H_2BDC/H_2O$ 1:1:277 is found out as the best result. The higher concentration of reactants leads to higher viscous solution and MIL-101 is easy to deposit on the substrate. Besides, nanoparticles size of MIL-101 could be achieved in higher concentration due to the aid of acetic acid.

Amount of acetic acid is a key factor to decide the yield of Cr-BDC and density of MIL-101 in top layer. Increase amount of acetic acid from 0.1-0.8 could reduce the formation of MIL-53 and raise the yield of MIL-101. MIL-101 particles are distributed evenly in the top side and there is no observation of defect and pin holes on the top view of the substrate at 0.8 ml acetic acid

In the contrast to molar ratio of reactants in situ step, the lower ratio in healing step favors a high yield of MIL-101 compare to MIL-53. It could be explained that MIL-101 is a kinetic product and it is straightforward to transform into other kinds of MOFs at higher concentration in a long time. Furthermore, MIL-101 as kinetic product is also demonstrated by comparing in-situ step with thermal seeding method and layer by layer seeding method. Overall, MIL-101 membrane should be synthesized follow the simple step as in-situ method to suppress the formation of undesired product.

MIL-101 membranes are successfully applied in organic solvent nanofiltration. MWCO of membranes is around 760g/mol that be suitable for NF range (200-1000Da) and average flux is about 1.7 $Lm^{-2}h^{-1}bar^{-1}$. MIL-101 membranes are also stable under harsh solvent as DMSO, NMP and DMAc that usually dissolve almost the polymeric membrane with high rejection of RB and no permeance change compared to ethanol solution. From these successful experiments, it opened up a new path for MOF membrane in liquid separation, especially for organic solvent nanofiltration.

Chapter 6 Reference

1.   Cheng, X.Q., et al., "Recent Advances in Polymeric Solvent-Resistant Nanofiltration Membranes", Advances in Polymer Technology, 33, 21455, 2014

2.   Mohammad, A.W., et al., "Nanofiltration membranes review: Recent advances and future prospects", Desalination, 356, 226-254, 2015

3.   Marchetti, P., et al., "Molecular Separation with Organic Solvent Nanofiltration: A Critical Review", Chemical Reviews, 114, 10735-10806, 2014

4.   Mulder, M., "Basic Principles of Membrane Technology, 2nd ed.", Kluwer Academic Publisher: Dordrecht, 2004

5.   Koros, W.J.M., Y. H.; Shimidzu, "Terminology for membranes and membrane process (IUPAC Recommmendations 1996)", Pure and Applied Chemistry, 68, 1479-1489, 1996

6.   Rahimpour, A., et al., "Preparation and characterization of asymmetric polyethersulfone and thin-film composite polyamide nanofiltration membranes for water softening", Applied Surface Science, 256, 1657-1663, 2010

7.   D.R. MacHado, D.H., R. Semiat, "Effect of solvent properties on permeate flow through nanofiltration membranes. Part I: Investigation of parameters affecting solvent flux", Journal of Membrane Science, 163, 93-102, 1999

8.   H.J. Zwijnenberg, A.M.K., K. Ebert, K.V. Peinemann, F.P. Cuperus, "Acetone-stable nanofiltration membranes in deacidifying vegetable oil", Journal of the American Oil Chemists' Society, 76, 83-87, 1999

9.   K. Ebert, P.C., "Solvent resistant nanofiltration membranes in edible oil processing", Membrane Technology, 107, 5-8, 1999

10.   D.R. Machado, D.H., R. Semiat, "Effect of solvent properties on permeate flow through nanofiltration membranes. Part II: Transport model", Journal of Membrane Science, 166, 63-69, 2000

11.   A.W. Mohammad , Y.H.T., W.L. Ang, Y.T. Chung, D.L. Oatley-Radcliffe, N. Hilal, "Nanofiltration membranes review: Recent advances and future prospects", Desalination, 356, 226-254, 2015

12.   Vandezande, P., L.E.M. Gevers, and I.F.J. Vankelecom, "Solvent resistant nanofiltration: separating on a molecular level", Chemical Society Reviews, 37, 365-405, 2008

13.   White, L.S., "Transport properties of a polyimide solvent resistant nanofiltration membrane", Journal of Membrane Science, 205, 191-202, 2002
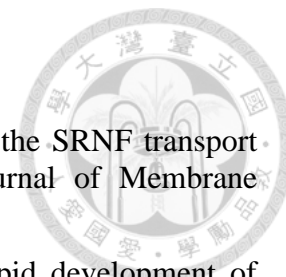
14. Gevers, L.E.M., et al., "Physico-chemical interpretation of the SRNF transport mechanism for solutes through dense silicone membranes", Journal of Membrane Science, 274, 173-182, 2006

15. Vandezande, P., et al., "High throughput screening for rapid development of membranes and membrane processes", Journal of Membrane Science, 250, 305-310, 2005

16. Bhanushali, D., et al., "Performance of solvent-resistant membranes for non-aqueous systems: solvent permeation results and modeling", Journal of Membrane Science, 189, 1-21, 2001

17. Bhanushali, D., S. Kloos, and D. Bhattacharyya, "Solute transport in solvent-resistant nanofiltration membranes for non-aqueous systems: experimental results and the role of solute–solvent coupling", Journal of Membrane Science, 208, 343-359, 2002

18. Fritsch, D., et al., "High performance organic solvent nanofiltration membranes: Development and thorough testing of thin film composite membranes made of polymers of intrinsic microporosity (PIMs)", Journal of Membrane Science, 401–402, 222-231, 2012

19. Rohani, R., M. Hyland, and D. Patterson, "A refined one-filtration method for aqueous based nanofiltration and ultrafiltration membrane molecular weight cut-off determination using polyethylene glycols", Journal of Membrane Science, 382, 278-290, 2011

20. Tsuru, T., et al., "Nanofiltration in non-aqueous solutions by porous silica–zirconia membranes", Journal of Membrane Science, 185, 253-261, 2001

21. Kwiatkowski, J. and M. Cheryan, "Performance of Nanofiltration Membranes in Ethanol", Separation Science and Technology, 40, 2651-2662, 2005

22. Dutczak, S.M., et al., "Composite capillary membrane for solvent resistant nanofiltration", Journal of Membrane Science, 372, 182-190, 2011

23. See Toh, Y.H., et al., "In search of a standard method for the characterisation of organic solvent nanofiltration membranes", Journal of Membrane Science, 291, 120-125, 2007

24. Van der Bruggen, B., et al., "Influence of molecular size, polarity and charge on the retention of organic molecules by nanofiltration", Journal of Membrane Science, 156, 29-41, 1999

25. Stafie, N., D.F. Stamatialis, and M. Wessling, "Effect of PDMS cross-linking degree on the permeation performance of PAN/PDMS composite nanofiltration membranes", Separation and Purification Technology, 45, 220-231, 2005

26. http://www.hussgroup.com/cdc-liquid/en/infocenter/Dead-End.php

27. Mulder, M., "Basic Principles of Membrane Technology, 2nd edition", Kluwer Academic Publishers: Dordretcht, 2004
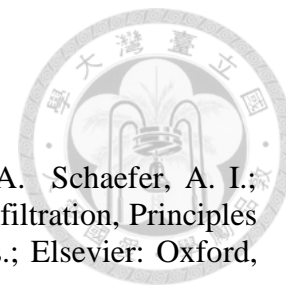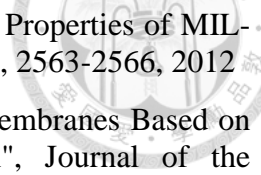
28.   Vankelecom, I.F.J.D.S., K.; Gevers, L. E. M.; Jacobs, P. A. Schaefer, A. I.; Fane, A. G.; Waite, T. D., Eds.; Elsevier: Oxford, UK, 2005, "Nanofiltration, Principles and Applications", Schaefer, A. I.; Fane, A. G.; Waite, T. D., Eds.; Elsevier: Oxford, UK, 2005

29.   Vankelecom, I.F.J.G., L. E. M, "Green Separation Processes: Fundamentals and Applications", Alfonso, C. A. M.; Crespo, J. G., Eds.; Wiley-VCH: Weinheim, Germany, 2005

30.   https://www.pall.com/main/food-and-beverage/product.page?lid=gri78l4d

31.   G. Dudziak, T.H., A. Nickel, P. Puhlfuerss and I. Voigt, Eur. Pat., EP1603663, 2004, 2004

32.   Tsuru, T., et al., "Nanoporous titania membranes for permeation and filtration of organic solutions", Desalination, 233, 1-9, 2008

33.   Voigt, I., et al., "Integrated cleaning of coloured waste water by ceramic NF membranes", Separation and Purification Technology, 25, 509-512, 2001

34.   Tsuru, T., et al., "Inorganic porous membranes for nanofiltration of nonaqueous solutions", Separation and Purification Technology, 32, 105-109, 2003

35.   Van Gestel, T., et al., "Surface modification of γ-Al2O3/TiO2 multilayer membranes for applications in non-polar organic solvents", Journal of Membrane Science, 224, 3-10, 2003

36.   Tsuru, T., et al., "Permeation of nonaqueous solution through organic/inorganic hybrid nanoporous membranes", AIChE Journal, 50, 1080-1087, 2004

37.   Dudziak, G.H., T.; Nickel, A.; Puhlfuerss, P.; Voigt, I., Eur. Patent 1,603,663, 2004

38.   Tsuru, T., et al., "Preparation of hydrophobic nanoporous methylated SiO2 membranes and application to nanofiltration of hexane solutions", Journal of Membrane Science, 384, 149-156, 2011

39.   Rezaei Hosseinabadi, S., et al., "Organic solvent nanofiltration with Grignard functionalised ceramic nanofiltration membranes", Journal of Membrane Science, 454, 496-504, 2014

40.   Chen, H.Z. and T.-S. Chung, "CO2-selective membranes for hydrogen purification and the effect of carbon monoxide (CO) on its gas separation performance", International Journal of Hydrogen Energy, 37, 6001-6011, 2012

41.   Das, J.K., N. Das, and S. Bandyopadhyay, "Highly selective SAPO 34 membrane on surface modified clay–alumina tubular support for H2/CO2 separation", International Journal of Hydrogen Energy, 37, 10354-10364, 2012
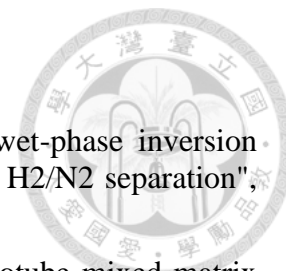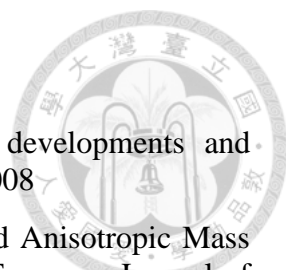
42.   Itta, A.K., H.-H. Tseng, and M.-Y. Wey, "Effect of dry/wet-phase inversion method on fabricating polyetherimide-derived CMS membrane for H2/N2 separation", International Journal of Hydrogen Energy, 35, 1650-1658, 2010

43.   Kim, S., et al., "Polysulfone and functionalized carbon nanotube mixed matrix membranes for gas separation: Theory and experiment", Journal of Membrane Science, 294, 147-158, 2007

44.   Kong, C., et al., "Controlled synthesis of high performance polyamide membrane with thin dense layer for water desalination", Journal of Membrane Science, 362, 76-80, 2010

45.   Kong, C., et al., "Thin carbon-zeolite composite membrane prepared on ceramic tube filter by vacuum slip casting for oxygen/nitrogen separation", Carbon, 45, 2848-2850, 2007

46.   Tseng, H.-H., P.-T. Shiu, and Y.-S. Lin, "Effect of mesoporous silica modification on the structure of hybrid carbon membrane for hydrogen separation", International Journal of Hydrogen Energy, 36, 15352-15363, 2011

47.   Weng, T.-H., H.-H. Tseng, and M.-Y. Wey, "Fabrication and characterization of poly(phenylene oxide)/SBA-15/carbon molecule sieve multilayer mixed matrix membrane for gas separation", International Journal of Hydrogen Energy, 35, 6971-6983, 2010

48.   Yaghi, O.M., et al., "Reticular synthesis and the design of new materials", Nature, 423, 705-714, 2003

49.   Xu, Z., "A selective review on the making of coordination networks with potential semiconductive properties", Coordination Chemistry Reviews, 250, 2745-2757, 2006

50.   McGuire, C.V. and R.S. Forgan, "The surface chemistry of metal-organic frameworks", Chemical Communications, 51, 5199-5217, 2015

51.   Kuppler, R.J., et al., "Potential applications of metal-organic frameworks", Coordination Chemistry Reviews, 253, 3042-3066, 2009

52.   Zhang, S.-Y., Z. Zhang, and M.J. Zaworotko, "Topology, chirality and interpenetration in coordination polymers", Chemical Communications, 49, 9700-9703, 2013

53.   Shah, M., et al., "Current Status of Metal–Organic Framework Membranes for Gas Separations: Promises and Challenges", Industrial & Engineering Chemistry Research, 51, 2179-2199, 2012

54.   Férey, G., et al., "A Chromium Terephthalate-Based Solid with Unusually Large Pore Volumes and Surface Area", Science, 309, 2040-2042, 2005
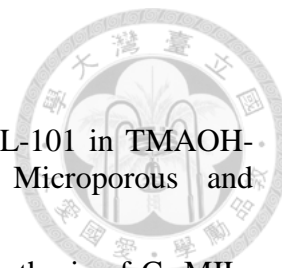
55.   Yang, J., et al., "Synthesis of metal–organic framework MIL-101 in TMAOH-Cr(NO3)3-H2BDC-H2O and its hydrogen-storage behavior", Microporous and Mesoporous Materials, 130, 174-179, 2010

56.   Kim, J., Y.-R. Lee, and W.-S. Ahn, "Dry-gel conversion synthesis of Cr-MIL-101 aided by grinding: high surface area and high yield synthesis with minimum purification", Chemical Communications, 49, 7647-7649, 2013

57.   Liang, Z., et al., "Comparison of Conventional and HF-Free-Synthesized MIL-101 for CO2 Adsorption Separation and Their Water Stabilities", Energy & Fuels, 27, 7612-7618, 2013

58.   Khan, N.A., et al., "Facile synthesis of nano-sized metal-organic frameworks, chromium-benzenedicarboxylate, MIL-101", Chemical Engineering Journal, 166, 1152-1157, 2011

59.   Zhou, J.-J.L., Kai-Yu; Kong, Chun-Long; Chen, Liang;, "Acetate-assisted Synthesis of Chromium(III) Terephthalate and Its Gas Adsorption Properties", Bulletin of the Korean Chemical Society, 34, 1625-1631, 2013

60.   Yang, L.-T., et al., "Rapid hydrothermal synthesis of MIL-101(Cr) metal–organic framework nanocrystals using expanded graphite as a structure-directing template", Inorganic Chemistry Communications, 35, 265-267, 2013

61.   Zhao, T., et al., "High-yield, fluoride-free and large-scale synthesis of MIL-101(Cr)", Dalton Transactions, 44, 16791-16801, 2015

62.   Song, L., et al., "Mesoporous metal-organic frameworks: design and applications", Energy & Environmental Science, 5, 7508-7520, 2012

63.   Bhattacharjee, S., C. Chen, and W.-S. Ahn, "Chromium terephthalate metal-organic framework MIL-101: synthesis, functionalization, and applications for adsorption and catalysis", RSC Advances, 4, 52500-52525, 2014

64.   Pan, Y., et al., "Multifunctional catalysis by Pd@MIL-101: one-step synthesis of methyl isobutyl ketone over palladium nanoparticles deposited on a metal-organic framework", Chemical Communications, 46, 2280-2282, 2010

65.   Yang, C.-X., et al., "High-Performance Separation of Fullerenes on Metal–Organic Framework MIL-101(Cr)", Chemistry – A European Journal, 17, 11734-11737, 2011

66.   Ramos-Fernandez, E.V., et al., "MOFs meet monoliths: Hierarchical structuring metal organic framework catalysts", Applied Catalysis A: General, 391, 261-267, 2011

67.   Anbia, M. and V. Hoseini, "Development of MWCNT@MIL-101 hybrid composite with enhanced adsorption capacity for carbon dioxide", Chemical Engineering Journal, 191, 326-330, 2012

68.   Jiang, D., et al., "Facile synthesis of metal-organic framework films via in situ seeding of nanoparticles", Chemical Communications, 48, 4965-4967, 2012

94

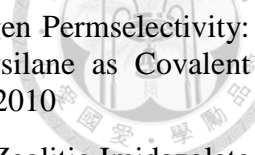69.   Liu, X., et al., "Syntheses, Characterizations and Adsorption Properties of MIL-101/Graphene Oxide Composites", Chinese Journal of Chemistry, 30, 2563-2566, 2012

70.   Sorribas, S., et al., "High Flux Thin Film Nanocomposite Membranes Based on Metal–Organic Frameworks for Organic Solvent Nanofiltration", Journal of the American Chemical Society, 135, 15201-15208, 2013

71.   Somayajulu Rallapalli, P.B., et al., "Activated carbon @ MIL-101(Cr): a potential metal-organic framework composite material for hydrogen storage", International Journal of Energy Research, 37, 746-753, 2013

72.   Ahmed, I., N.A. Khan, and S.H. Jhung, "Graphite Oxide/Metal–Organic Framework (MIL-101): Remarkable Performance in the Adsorptive Denitrogenation of Model Fuels", Inorganic Chemistry, 52, 14155-14161, 2013

73.   Sun, X., et al., "Adsorption performance of a MIL-101(Cr)/graphite oxide composite for a series of n-alkanes", RSC Advances, 4, 56216-56223, 2014

74.   Zhou, X., et al., "A novel MOF/graphene oxide composite GrO@MIL-101 with high adsorption capacity for acetone", Journal of Materials Chemistry A, 2, 4722-4730, 2014

75.   Xin, Q., et al., "Enhanced Interfacial Interaction and CO2 Separation Performance of Mixed Matrix Membrane by Incorporating Polyethylenimine-Decorated Metal–Organic Frameworks", ACS Applied Materials & Interfaces, 7, 1065-1077, 2015

76.   Lin, Y., et al., "Enhanced selective CO2 adsorption on polyamine/MIL-101(Cr) composites", Journal of Materials Chemistry A, 2, 14658-14665, 2014

77.   A. Yu. Alentiev , G.N.B., Yu. V. Kostina, V. P. Shantarovich, S. N. Klyamkin, V. P. Fedin, K. A. Kovalenko, Yu. P. Yampolskii, "PIM-1/MIL-101 hybrid composite membrane material: Transport properties and free volume", Petroleum Chemistry 54, 477-481, 2014

78.   Lin, R., et al., "Mixed-Matrix Membranes with Metal–Organic Framework-Decorated CNT Fillers for Efficient CO2 Separation", ACS Applied Materials & Interfaces, 7, 14750-14757, 2015

79.   Naseri, M., et al., "Synthesis and gas transport performance of MIL-101/Matrimid mixed matrix membranes", Journal of Industrial and Engineering Chemistry, 29, 249-256, 2015

80.   de la Iglesia, Ó., et al., "Metal-organic framework MIL-101(Cr) based mixed matrix membranes for esterification of ethanol and acetic acid in a membrane reactor", Renewable Energy, 88, 12-19, 2016

81.   Hermes, S., et al., "Selective Nucleation and Growth of Metal−Organic Open Framework Thin Films on Patterned COOH/CF3-Terminated Self-Assembled Monolayers on Au(111)", Journal of the American Chemical Society, 127, 13744-13745, 2005

82.   Kepert, C.J., "Advanced functional properties in nanoporous coordination framework materials", Chemical Communications, 695-700, 2006

83.   Biemmi, E., C. Scherb, and T. Bein, "Oriented Growth of the Metal Organic Framework Cu3(BTC)2(H2O)3·xH2O Tunable with Functionalized Self-Assembled Monolayers", Journal of the American Chemical Society, 129, 8054-8055, 2007

84.   Hermes, S., et al., "Selective Growth and MOCVD Loading of Small Single Crystals of MOF-5 at Alumina and Silica Surfaces Modified with Organic Self-Assembled Monolayers", Chemistry of Materials, 19, 2168-2173, 2007

85.   Zacher, D., et al., "Deposition of microcrystalline [Cu3(btc)2] and [Zn2(bdc)2(dabco)] at alumina and silica surfaces modified with patterned self assembled organic monolayers: evidence of surface selective and oriented growth", Journal of Materials Chemistry, 17, 2785-2792, 2007

86.   Qiu, S., M. Xue, and G. Zhu, "Metal-organic framework membranes: from synthesis to separation application", Chemical Society Reviews, 43, 6116-6140, 2014

87.   Li, W., et al., "Metal−organic framework composite membranes: Synthesis and separation applications", Chemical Engineering Science, 135, 232-257, 2015

88.   Liu, Y., et al., "Synthesis of continuous MOF-5 membranes on porous α-alumina substrates", Microporous and Mesoporous Materials, 118, 296-301, 2009

89.   Aceituno Melgar, V.M., H.T. Kwon, and J. Kim, "Direct spraying approach for synthesis of ZIF-7 membranes by electrospray deposition", Journal of Membrane Science, 459, 190-196, 2014

90.   Hara, N., et al., "Metal-organic framework membranes with layered structure prepared within the porous support", RSC Advances, 3, 14233-14236, 2013

91.   Yoo, Y., Z. Lai, and H.-K. Jeong, "Fabrication of MOF-5 membranes using microwave-induced rapid seeding and solvothermal secondary growth", Microporous and Mesoporous Materials, 123, 100-106, 2009

92.   Xomeritakis, G., Z. Lai, and M. Tsapatsis, "Separation of Xylene Isomer Vapors with Oriented MFI Membranes Made by Seeded Growth", Industrial & Engineering Chemistry Research, 40, 544-552, 2001

93.   Lai, Z., et al., "Microstructural Optimization of a Zeolite Membrane for Organic Vapor Separation", Science, 300, 456-460, 2003

94.   Lai, Z., M. Tsapatsis, and J.P. Nicolich, "Siliceous ZSM-5 Membranes by Secondary Growth of b-Oriented Seed Layers", Advanced Functional Materials, 14, 716-729, 2004

95.   Choi, J., et al., "Uniformly a-Oriented MFI Zeolite Films by Secondary Growth", Angewandte Chemie International Edition, 45, 1154-1158, 2006

96.   Caro, J. and M. Noack, "Zeolite membranes – Recent developments and progress", Microporous and Mesoporous Materials, 115, 215-233, 2008

97.   Arnold, M., et al., "Oriented Crystallisation on Supports and Anisotropic Mass Transport of the Metal-Organic Framework Manganese Formate", European Journal of Inorganic Chemistry, 2007, 60-64, 2007

98.   Gascon, J., S. Aguado, and F. Kapteijn, "Manufacture of dense coatings of Cu3(BTC)2 (HKUST-1) on α-alumina", Microporous and Mesoporous Materials, 113, 132-138, 2008

99.   Bux, H., et al., "Zeolitic Imidazolate Framework Membrane with Molecular Sieving Properties by Microwave-Assisted Solvothermal Synthesis", Journal of the American Chemical Society, 131, 16000-16001, 2009

100.   Shah, M.N., et al., "An Unconventional Rapid Synthesis of High Performance Metal–Organic Framework Membranes", Langmuir, 29, 7896-7902, 2013

101.   Shekhah, O., et al., "The liquid phase epitaxy approach for the successful construction of ultra-thin and defect-free ZIF-8 membranes: pure and mixed gas transport study", Chemical Communications, 50, 2089-2092, 2014

102.   Ameloot, R., et al., "Interfacial synthesis of hollow metal–organic framework capsules demonstrating selective permeability", Nat Chem, 3, 382-387, 2011

103.   Kwon, H.T. and H.-K. Jeong, "In Situ Synthesis of Thin Zeolitic–Imidazolate Framework ZIF-8 Membranes Exhibiting Exceptionally High Propylene/Propane Separation", Journal of the American Chemical Society, 135, 10763-10768, 2013

104.   Sun, Y., et al., "Self-modified fabrication of inner skin ZIF-8 tubular membranes by a counter diffusion assisted secondary growth method", RSC Advances, 4, 33007-33012, 2014

105.   Huang, K., et al., "A ZIF-71 Hollow Fiber Membrane Fabricated by Contra-Diffusion", ACS Applied Materials & Interfaces, 7, 16157-16160, 2015

106.   Hara, N., et al., "ZIF-8 membranes prepared at miscible and immiscible liquid–liquid interfaces", Microporous and Mesoporous Materials, 206, 75-80, 2015

107.   Ranjan, R. and M. Tsapatsis, "Microporous Metal Organic Framework Membrane on Porous Support Using the Seeded Growth Method", Chemistry of Materials, 21, 4920-4924, 2009

108.   Zhou, S., et al., "Challenging fabrication of hollow ceramic fiber supported Cu3(BTC)2 membrane for hydrogen separation", Journal of Materials Chemistry, 22, 10322-10328, 2012

109.   Li, Y.-S., et al., "Molecular Sieve Membrane: Supported Metal–Organic Framework with High Hydrogen Selectivity", Angewandte Chemie International Edition, 49, 548-551, 2010
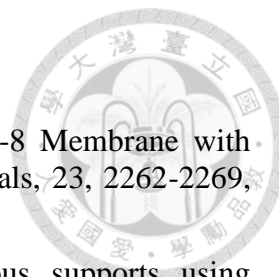
110.   Bux, H., et al., "Oriented Zeolitic Imidazolate Framework-8 Membrane with Sharp H2/C3H8 Molecular Sieve Separation", Chemistry of Materials, 23, 2262-2269, 2011

111.   Guerrero, V.V., et al., "HKUST-1 membranes on porous supports using secondary growth", Journal of Materials Chemistry, 20, 3938-3943, 2010

112.   Tao, K., C. Kong, and L. Chen, "High performance ZIF-8 molecular sieve membrane on hollow ceramic fiber via crystallizing-rubbing seed deposition", Chemical Engineering Journal, 220, 1-5, 2013

113.   Nan, J., et al., "Step-by-Step Seeding Procedure for Preparing HKUST-1 Membrane on Porous α-Alumina Support", Langmuir, 27, 4309-4312, 2011

114.   Liu, Y., et al., "Synthesis of highly c-oriented ZIF-69 membranes by secondary growth and their gas permeation properties", Journal of Membrane Science, 379, 46-51, 2011

115.   Pan, Y., et al., "Effective separation of propylene/propane binary mixtures by ZIF-8 membranes", Journal of Membrane Science, 390–391, 93-98, 2012

116.   Guo, H., et al., ""Twin Copper Source" Growth of Metal−Organic Framework Membrane: Cu3(BTC)2 with High Permeability and Selectivity for Recycling H2", Journal of the American Chemical Society, 131, 1646-1647, 2009

117.   McCarthy, M.C., et al., "Synthesis of Zeolitic Imidazolate Framework Films and Membranes with Controlled Microstructures", Langmuir, 26, 14636-14641, 2010

118.   Zhang, X., et al., "A simple and scalable method for preparing low-defect ZIF-8 tubular membranes", Journal of Materials Chemistry A, 1, 10635-10638, 2013

119.   Zhang, X., et al., "New Membrane Architecture with High Performance: ZIF-8 Membrane Supported on Vertically Aligned ZnO Nanorods for Gas Permeation and Separation", Chemistry of Materials, 26, 1975-1981, 2014

120.   Hu, Y., et al., "Metal-organic framework membranes fabricated via reactive seeding", Chemical Communications, 47, 737-739, 2011

121.   Dong, X., et al., "Synthesis of zeolitic imidazolate framework-78 molecular-sieve membrane: defect formation and elimination", Journal of Materials Chemistry, 22, 19222-19227, 2012

122.   Dong, X. and Y.S. Lin, "Synthesis of an organophilic ZIF-71 membrane for pervaporation solvent separation", Chemical Communications, 49, 1196-1198, 2013

123.   Huang, A., W. Dou, and J. Caro, "Steam-Stable Zeolitic Imidazolate Framework ZIF-90 Membrane with Hydrogen Selectivity through Covalent Functionalization", Journal of the American Chemical Society, 132, 15562-15564, 2010

124.   Huang, A., et al., "Molecular-Sieve Membrane with Hydrogen Permselectivity: ZIF-22 in LTA Topology Prepared with 3-Aminopropyltriethoxysilane as Covalent Linker", Angewandte Chemie International Edition, 49, 4958-4961, 2010

125.   Huang, A. and J. Caro, "Covalent Post-Functionalization of Zeolitic Imidazolate Framework ZIF-90 Membrane for Enhanced Hydrogen Selectivity", Angewandte Chemie International Edition, 50, 4979-4982, 2011

126.   Huang, A., et al., "A highly permeable and selective zeolitic imidazolate framework ZIF-95 membrane for H2/CO2 separation", Chemical Communications, 48, 10981-10983, 2012

127.   Huang, A., et al., "Highly hydrogen permselective ZIF-8 membranes supported on polydopamine functionalized macroporous stainless-steel-nets", Journal of Materials Chemistry A, 2, 8246-8251, 2014

128.   Li, Y.-S., et al., "Controllable Synthesis of Metal–Organic Frameworks: From MOF Nanorods to Oriented MOF Membranes", Advanced Materials, 22, 3322-3326, 2010

129.   Li, Y., et al., "Zeolitic imidazolate framework ZIF-7 based molecular sieve membrane for hydrogen separation", Journal of Membrane Science, 354, 48-54, 2010

130.   Xie, Z., et al., "Deposition of chemically modified [small alpha]-Al2O3 particles for high performance ZIF-8 membrane on a macroporous tube", Chemical Communications, 48, 5977-5979, 2012

131.   Liu, Q., et al., "Bio-Inspired Polydopamine: A Versatile and Powerful Platform for Covalent Synthesis of Molecular Sieve Membranes", Journal of the American Chemical Society, 135, 17679-17682, 2013

132.   Bux, H., et al., "Novel MOF-Membrane for Molecular Sieving Predicted by IR-Diffusion Studies and Molecular Modeling", Advanced Materials, 22, 4741-4743, 2010

133.   Bux, H., et al., "Ethene/ethane separation by the MOF membrane ZIF-8: Molecular correlation of permeation, adsorption, diffusion", Journal of Membrane Science, 369, 284-289, 2011

134.   Hara, N., et al., "Diffusive separation of propylene/propane with ZIF-8 membranes", Journal of Membrane Science, 450, 215-223, 2014

135.   Huang, A., et al., "Organosilica-Functionalized Zeolitic Imidazolate Framework ZIF-90 Membrane with High Gas-Separation Performance", Angewandte Chemie International Edition, 51, 10551-10555, 2012

136.   Zhang, F., et al., "Hydrogen Selective NH2-MIL-53(Al) MOF Membranes with High Permeability", Advanced Functional Materials, 22, 3583-3590, 2012

137.   Zhao, Z., et al., "Gas Separation Properties of Metal Organic Framework (MOF-5) Membranes", Industrial & Engineering Chemistry Research, 52, 1102-1108, 2013

138. Mao, Y., et al., "Enhanced gas separation through well-intergrown MOF membranes: seed morphology and crystal growth effects", Journal of Materials Chemistry A, 1, 11711-11716, 2013

139. Mao, Y., et al., "HKUST-1 Membranes Anchored on Porous Substrate by Hetero MIL-110 Nanorod Array Seeds", Chemistry – A European Journal, 19, 11883-11886, 2013

140. Liu, Y., et al., "Synthesis and characterization of ZIF-69 membranes and separation for CO2/CO mixture", Journal of Membrane Science, 353, 36-40, 2010

141. Aguado, S., et al., "Facile synthesis of an ultramicroporous MOF tubular membrane with selectivity towards CO2", New Journal of Chemistry, 35, 41-44, 2011

142. Zhang, C., et al., "A hybrid zeolitic imidazolate framework membrane by mixed-linker synthesis for efficient CO2 capture", Chemical Communications, 49, 600-602, 2013

143. Xie, Z., et al., "Alumina-supported cobalt-adeninate MOF membranes for CO2/CH4 separation", Journal of Materials Chemistry A, 2, 1239-1241, 2014

144. Zou, X., et al., "Co3(HCOO)6 Microporous Metal–Organic Framework Membrane for Separation of CO2/CH4 Mixtures", Chemistry – A European Journal, 17, 12076-12083, 2011

145. Yin, H., et al., "A highly permeable and selective amino-functionalized MOF CAU-1 membrane for CO2-N2 separation", Chemical Communications, 50, 3699-3701, 2014

146. Diestel, L., et al., "Pervaporation studies of n-hexane, benzene, mesitylene and their mixtures on zeolitic imidazolate framework-8 membranes", Microporous and Mesoporous Materials, 164, 288-293, 2012

147. Fan, L., et al., "ZIF-78 membrane derived from amorphous precursors with permselectivity for cyclohexanone/cyclohexanol mixture", Microporous and Mesoporous Materials, 192, 29-34, 2014

148. Wang, W., et al., "A homochiral metal-organic framework membrane for enantioselective separation", Chemical Communications, 48, 7022-7024, 2012

149. Khan, N.A., J.W. Jun, and S.H. Jhung, "Effect of Water Concentration and Acidity on the Synthesis of Porous Chromium Benzenedicarboxylates", European Journal of Inorganic Chemistry, 2010, 1043-1048, 2010

150. Jiang, D., A.D. Burrows, and K.J. Edler, "Size-controlled synthesis of MIL-101(Cr) nanoparticles with enhanced selectivity for CO2 over N2", CrystEngComm, 13, 6916-6919, 2011

151. Xu, G., et al., "Preparation of ZIF-8 membranes supported on ceramic hollow fibers from a concentrated synthesis gel", Journal of Membrane Science, 385–386, 187-193, 2011

152.   Jiang, D., et al., "Polymer-assisted synthesis of nanocrystalline copper-based metal–organic framework for amine oxidation", Catalysis Communications, 12, 602-605, 2011

153.   Bauer, S., et al., "High-Throughput Assisted Rationalization of the Formation of Metal Organic Frameworks in the Iron(III) Aminoterephthalate Solvothermal System", Inorganic Chemistry, 47, 7568-7576, 2008

154.   Car, A., C. Stropnik, and K.-V. Peinemann, "Euromembrane 2006Hybrid membrane materials with different metal–organic frameworks (MOFs) for gas separation", Desalination, 200, 424-426, 2006

155.   Zornoza, B., et al., "Metal organic framework based mixed matrix membranes: An increasingly important field of research with a large application potential", Microporous and Mesoporous Materials, 166, 67-78, 2013

156.   Bowen, W.R. and J.S. Welfoot, "Modelling of membrane nanofiltration—pore size distribution effects", Chemical Engineering Science, 57, 1393-1407, 2002